Design and synthesis of putative anti-cancer agents using hybrid molecular approach

A Thesis submitted to the Central University of Punjab

For the Award of

Master of Pharmacy

in

Medicinal Chemistry

by

Vijayinder Saini

Research Supervisor: Dr. Vinod Kumar

Research Co-supervisor: Dr. Sandeep Singh

Centre for Chemical & Pharmaceutical Sciences

School of Basic & Applied Sciences

Central University of Punjab, Bathinda

October, 2014

DECLARATION

I declare that the thesis entitled "**Design and synthesis of putative anti-cancer agents using hybrid molecular approach"** has been prepared by me under the guidance of Dr. Vinod Kumar, Assistant Professor, Centre for Chemical and Pharmaceutical Sciences, School of Basic and Applied Sciences, Central University of Punjab and Dr. Sandeep Singh, Assistant Professor, Centre for Genetic Diseases and Molecular Medicine, Central University of Punjab. No part of this dissertation has formed the basis for the award of any degree or fellowship previously.

Vijayinder Saini

Centre for Chemical and Pharmaceutical Sciences
School of Basic and Applied Sciences,
Central University of Punjab,
Bathinda, India - 151001

Date:

CERTIFICATE

We certify that Vijayinder Saini has prepared his thesis entitled "**Design and synthesis of putative anti-cancer agents using hybrid molecular approach**", for the award of M. Pharm. degree in Medicinal Chemistry under our guidance. He has carried out this work at the Centre for Chemical and Pharmaceutical Sciences, School of Basic and Applied Sciences, Central University of Punjab.

Dr. Vinod Kumar
(Supervisor)
Assistant Professor
Centre for Chemical & Pharmaceutical Sciences,
Central University of Punjab,
Bathinda-151001

Dr. Sandeep Singh
(Co-supervisor)
Assistant Professor
Centre for Genetics diseases & Molecular Medicine
Central University of Punjab,
Bathinda-151001

Date:

ABSTRACT

Design and synthesis of putative anti-cancer agents using hybrid molecular approach

Name of student	:	Vijayinder Saini
Registration Number	:	CUPB/MPHARM-MC/SBAS/CPS/2012- 13/01
Degree for which submitted	:	M.Pharm. (Medicinal Chemistry)
Name of supervisor	:	Dr. Vinod Kumar
Name of co-supervisor	:	Dr. Sandeep Singh
Centre	:	Chemical and Pharmaceutical Sciences
School of Studies	:	School of Basic and Applied Science

Key words: MDR, MetAP-2.

A Hybrid drug involves the unification of two drug pharmacophores in one single molecule. The hybrid drugs are designed to interact with multiple targets or to intensify its effect through action on another bio target as one single molecule or to counterbalance the known side effects associated with the other hybrid part. One of the important role of hybrid drugs is to counter multidrug resistance. Muti-drug resistance observed during the treatment for cancer. Target therapy for various cancer are developed and successfully used to treat cancer patient. But treatment can be further strengthen by concurrent administration of single drug by combining two different drugs from different origin act at different receptor to cope MDR. It is also said as to load a multi-target drug in a single drug. In the current research proposal, we have designed and synthesized molecules which affect tubulin polymerization as well as MetAP-2 receptor. Both play vital role in tumor progression by strengthening the cell cytoskeleton and angiogenesis process respectively. The hybrids of chalcone (antitubulin) and arylazole (anti MetAP-2) were synthesized and molecular docking studies were performed. The compounds were synthesized by three step reaction and synthesized compounds were analyzed and confirmed by FTIR, NMR and mass spectrometry. The activity of synthesized compound was evaluated against HCT-116 (wild & null type) colon cancer cell lines at a concentration of 5 µM, 25 µM and 50 µM. Compounds were equally active in wild type and null type HTC-116 cell lines with slight less inhibition in null type. Lastly, the information on inhibitory potential of compounds

were obtained from MTT assay wherein VJ-4, VJ-2PP2 & VJ-4PP1 were found to be active anticancer agents.

Vijayinder Saini Dr. Vinod Kumar Dr. Sandeep Singh

DEDICATED TO MY BELOVED

GRANDFATHER

AND PARENTS

ACKNOWLEDGEMENTS

Life is not as simple and unique as it looks without the relation bound with my parents. The support, patience, strength, courage all I got from them. I wouldn't see the whole world until they carry me on their shoulder and lift me up so that the world can see me. I don't have words to express my heartiest thanks to my parents which mentor me to be a good person.

I also express my deepest thanks to all my close relatives who always encourage me and provide all the necessary care to make my life easy.

I consider myself to be extremely blessed to obtain an opportunity to work under the guidance of Dr. Vinod Kumar and Dr. Harish Holla, Assistant Professor, Centre for Chemical and Pharmaceutical Sciences and have him as the guru of my master's dissertation I wish to express my sincere gratitude to him for his deep vision, in depth knowledge and enormous experience in the field of pharmaceutical chemistry and his selfless guidance for my research work. Sir, you help and taught me a lot and always guided me for every single step during my dissertation Thank you again sir, for everything.

I gratefully acknowledge my Co-Supervisor Dr. Sandeep Singh, Assistant Professor, Centre for Genetic disease and Molecular Medicine for his advice, supervision, and vital contribution in biological activity of compounds and encouragement and support throughout my dissertation work.

I wish to express my warm and sincere thanks to Prof. (Dr.) P. Ramarao, Acting Vice Chancellor and DAA, Central University of Punjab, Bathinda and Prof. (Dr.) Jairup Singh, Ex. Vice Chancellor, Central University of Punjab, Bathinda for their cooperation, loving

support and allowing me to avail the essential infrastructure, library facilities and providing me the opportunity and all the necessary facilities for carrying out the research work.

I would like to express my deepest gratitude to Prof. (Dr.) R.G Saini and Prof. (Dr.) R.C. Sharma, Professor in-charge and controller, Examinations for their valuable guidance and generous advice.

I am very grateful to all the faculty members Dr. Vikas Jaitak, Dr. Raj Kumar of Centre for Chemical and Pharmaceutical Sciences for their valuable support and suggestions whenever required.

I also express my sincere thanks to Dr. Bhupesh sir who helped in Molecular docking section and give me a vision to explore the world of computational chemistry.

Further I would also extend my thanks to Dr. Nagendra Babu, Assistant Professor, Centre for Environment and Earth Sciences, for his assiduous work in the Central Instrument Laboratory and for carrying various spectroscopic analysis that help me in characterization of my synthesized compounds.

I also find this opportunity to thanks all my Laboratory assistants and technicians Mr. Rajesh, Mr. Roshan and Mr. Vishal for their continuous support in my research work in laboratory.

I also thank to the staff of computer center, electric substation, security, institute drivers, canteen and all the non-staff members which help me direct and indirect way for their assistance.

I would like to thanks my seniors for praising me up. Thanks to Jimi Marin Alex, Ramit Singla, Arvind Negi, Vinay Kumar, Deependra Kumar, Monika Chauhan, Yashika Bhalla, Rabindra Kumar, Balraj gill, Pushpendra sir, for their encouragement and support during good and bad

times. Sincere acknowledgements to Ramit singla & Jimi Marin Alex who help me a lot in the docking and biological section respectively.

Thanks for the helping hands provided by my all juniors.

A very special thanks goes out to some very special individuals Parminder Badhan, Ashish, Anil, Ankur, Shishir, Mayank, Sheetal, Akansha, Gagandeep, Sheetal dubey for providing me loveliest and memorable moments of my life. Thanks Ashish and Anil for helping me out in laboratory work and spectra interpretation.

-Vijayinder Saini

TABLE OF CONTENTS

LIST OF TABLES

LIST OF FIGURES

LIST OF SCHEMES

LIST OF APPENDICES

LIST OF ABBREVATION

Sr.No	Full Form	Abbrevation
1.	Multi-drug resistance	MDR
2.	World Health Organization	WHO
3.	Histone Deacetylace	HDAC
4.	Food & Drug Administration	FDA
5.	Adenosine Tri-phosphate	ATP
6.	Guanosine Tri-phosphate	GTP
7.	Guanosine Di-phosphate	GDP
8.	Microtubules	MT
9.	Human epidermal growth factor receptor	HER
10.	Hypoxia Inducible Factor	HIF
11.	Anaplastic Thyroid Cancer	ATC
12.	Bleomycin	BLM
13.	Human Methionine Aminopeptidase-2	hMetAP-2
14.	Platelet-derived growth factor	PDGF
15.	Vascular endothelial growth factor	VEGF
16.	Epidermal growth factor	EGF
17.	Protein Kinases	PTKs
18.	Kilo Dalton	KDa
19.	Heat Shock Protein 90	HSP 90
20.	Tyrosine Kinases	TK
21.	Nuclear factor-Kb	NF-kB
22.	Mitogen-activated protein kinase	MAPK
23.	N, N-Dimethyl Formamide	DMF
24.	Non-small cell lung carcinoma	NSCLC
25.	Non-Steroidal Anti-Inflammatory Drugs	NSAIDs
26.	Thin layer chromatography	TLC
27.	Fourier Transform Infrared	FT-IR

28.	Ultraviolet	UV
29.	Time-of-flight mass spectrometry	TOF-MS
30.	Electrospray Ionisation Mass Spectrometry	ESI
31.	Dulbecco's Modified Eagle's medium	DMEM
32.	3-(4, 5-dimethylthiazol-2-yl)-2, 5-diphenyl tetrazolium bromide	MTT
33.	American Type Culture Collection	A.T.C.C
34.	Fetal Bovine Serum	FBS
35.	Dimethyl sulfoxide	DMSO
36.	Micromolar	µM
37.	Standard Deviation	SD
38.	Nuclear Magnetic Resonance	NMR
39.	Gas Chromatography-Mass Spectroscopy	GC-MS
40.	Structure activity relationship	SAR
41.	Molecular Operating Environment	MOE
42.	Multi-drug Resistant associated protein	MRP
43.	Growth factor receptor-bound protein 2	GRB2
44.	Chronic myelogenous (or myeloid or myelocytic) leukemia	CML
45.	Concentration	Conc.
46.	3-dimensional	3-D
47.	2-dimensional	2-D
48.	Protein data bank	PDB
49.	Epidermal growth factor receptor	EGFR
50.	Melting Point	mp
51.	Doublet	D
52.	Singlet	S
53.	Multiplet	M
54.	Triplet	T
55.	Doublets of doublets	dd
56.	Coupling constant	J

57.	Parts per million	ppm
58.	Hertz	Hz
59.	Milliliter	ml
60.	Milligram	mg
61.	Millimole	mmol
62.	Angstrom	A°

CHAPTER 1
INTRODUCTION

1.1 Introduction

Hybrid molecules are defined as chemical entities with two (or more than two) structural domains having different biological functions and dual activity indicates that a hybrid molecule acts as two distinct pharmacophores. Both entities of the hybrid molecule are not necessarily acting on the same biological target.(Meunier, 2007).

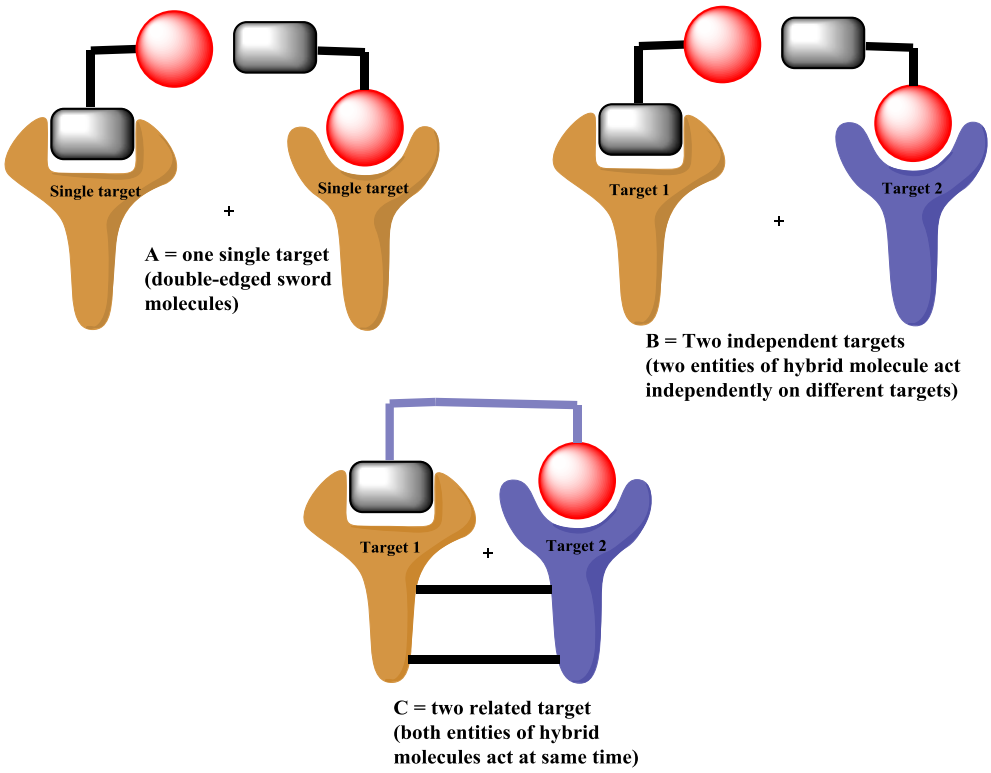

Figure 1.1*:* Schematic representation of three different possible modes of interaction of hybrid molecules: (A) one single target (for double-edged molecules), (B) two independent targets (each entity of the hybrid molecule acts with its target), and (C) two related targets (both entities of the hybrid molecule act at the same time on two connected targets) adapted from (Meunier, 2007)

A Hybrid drug comprises the unification of two drug pharmacophores in one single molecule, designed to interact with multiple targets or to intensify its effect through action on another bio target as one single molecule or to counterbalance the known side effects associated with the other hybrid part. Over the years, scientist & researchers have employed this technique to discover some promising chemical architectures displaying significant anticancer profiles. The microtubule inhibitors such as taxol, colchicine, chalcones, combretastatin,

phenstatins and vinca alkaloids have been utilized as one of the functionality of the hybrids and promising results have been obtained in most of the cases with some of the tubulin based hybrids exhibiting anticancer activity at nanomolar level (Altmann & Gertsch, 2007). Various heteroaryl based hybrids in particular isatin and coumarins have also been designed and reported to possess remarkable inhibitory potential (Amin et al., 2013).

A large number of molecules are being synthesized using the hybrid molecular approach. For example the hybrid molecule (A) is derived from two different scaffolds artemisinin & quinolone and it act as antimalarial agent with improved potency from its parent compounds and comparatively less toxicity (Kaur et al., 2010).

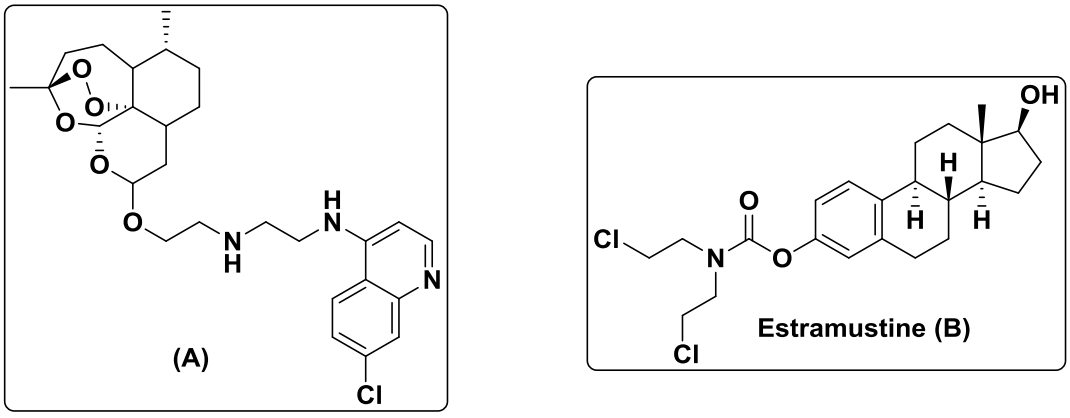

Figure 1.2: Examples of hybrid molecules of artemisinin and quinolone (A), estradiol and nitrogen-mustard carbamate ester (B)

Similarly estramustine, (B) an antimicrotubule agent, was approved by FDA for palliative treatment of metastatic and progressive prostate cancer. It is hybrid of oestrogen (specifically, estradiol) & a nitrogen mustard-carbamate ester moiety (Pienta & Lehr, 1993). (Figure 1.2)

The molecule described in figure 1.3 is developed as anticancer agent inspired form two different molecules. It is a hybrid of 1-deoxynojirimycin (DNJ) and 5-aryl-1, 2, 3-triazole and synthesized as potential bifunctional inhibitors of angiogenesis. The DNJ component inhibits the biosynthesis of cell surface oligosaccharides necessary for angiogenesis, whereas the aryl-1, 2, 3-triazole

inhibits methionine aminopeptidase-2, a target in angiogenesis therapy (Zhou et al., 2008). (Figure 1.3)

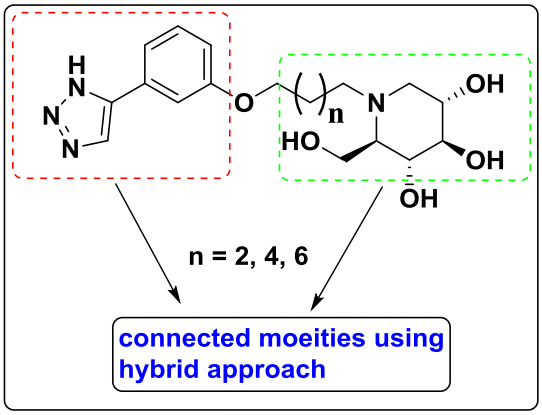

Figure 1.3: Anticancer agent inspired form 1-deoxynojirimycin (DNJ) and 5-aryl-1, 2, 3-triazole.

Molecular hybrids containing pyrazolyl chalcones and p-nitro benzyl functionalities are designed, synthesized and evaluated for cytotoxic studies against three human cancer cell lines (THP, COLO-205, A-549) (Singh et al., 2013). (Figure 1.4)

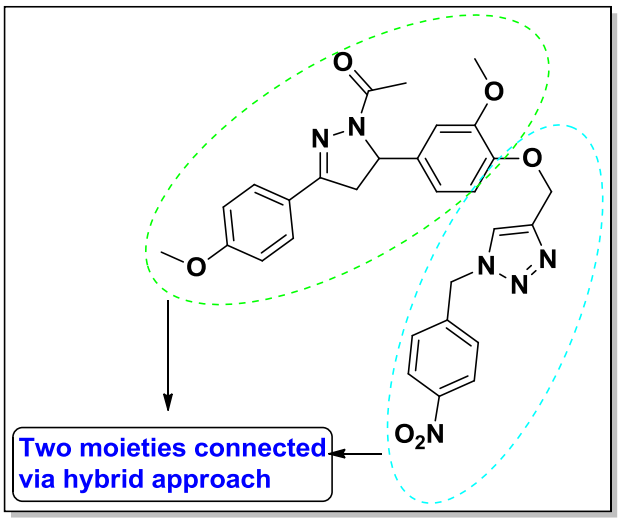

Figure 1.4: Molecular hybrids of pyrazolyl chalcones and p-nitro benzyl functionalities tethered by triazole ring

Herein the pyrazolyl chalcone showed cytotoxic activity by inhibiting Hypoxia Inducible Factor (HIF) which is a transcriptional complex that plays a key role in mammalian oxygen homeostasis. It regulates a host of hypoxic response genes responsible for angiogenic, glycolytic, and erythropoietic activity (Warshakoon et

al., 2006), whereas p-nitro benzyl triazole group is introduced to enhance the cytotoxic activity (Avanzo et al., 2012).

Bleomycin (Figure 1.5) is an excellent example of the design of a hybrid molecule by a microorganism containing three structural entities with three different biological roles. After cell penetration facilitated by the carbohydrate domain, the bithiazole entity and its positively charged terminal chain binds to GC-rich sequences of DNA and an amine-rich domain that strongly chelate redox-active metal ion, such as iron. The BLM–Fe complex is easily reduced inside cells to BLM–Fe, which reacts with molecular oxygen, a second electron, and a proton to generate “activated bleomycin”. The last intermediate that detected prior DNA cleavage is a low-spin BLM–Fe–OOH complex, which can abstract a H atom at the C4' position of deoxyribose units after the homolytic cleavage of the O–O bond or via a high-valent iron– oxo species produced by the heterolysis of the same O–O bond.

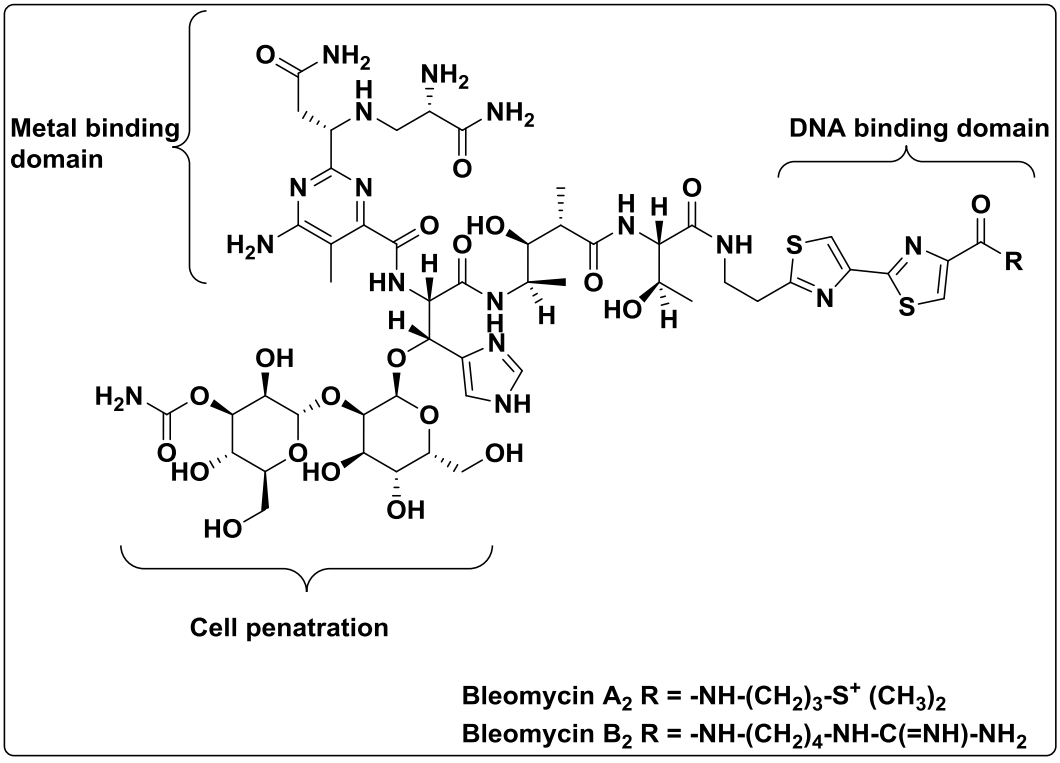

Figure 1.5: Representation of bleomycin with its three different structural domains.

1.2 Anti-cancer drugs & their action

Drugs which are available to cure cancer are divided into various category according to their mode of action. These drugs are summarized in figure 1.6.

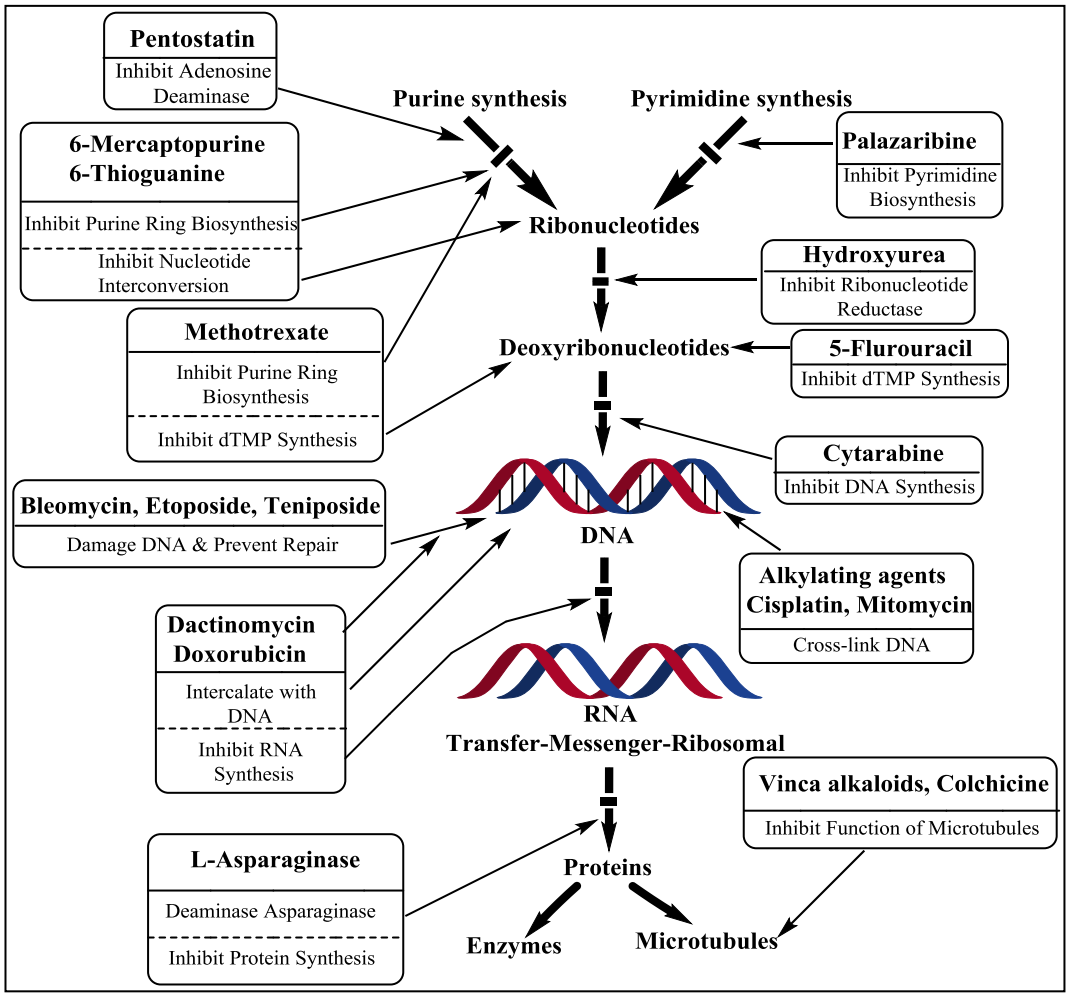

Figure 1.6: Summary of mechanism of action of anticancer drugs (Sirajuddin et al., 2013).

1.3 Approaches to target cancer

Main therapies used to treat cancer are radiation therapy, chemotherapy and surgery. However, these therapies have various side-effects which include neurotoxicity, anemia, impaired wound healing, bleeding, hair loss, sterility, nausea, kidney damage etc. Most traditional anticancer drugs act by disrupting the functioning of DNA and are referred to as cytotoxic. Some anticancer drugs act on DNA directly, while others act indirectly by inhibiting the enzymes involved

in DNA synthesis. These drugs produce cytotoxicity in both, the normal cells and the cancer cells. To overcome the side-effects caused by traditional anticancer drugs, a more selective approach described as molecular targeted therapeutics has been developed; in which highly selective agents target specific molecular targets that are abnormal or over-expressed in the cancer cell (Patrick, 2013).

Some of the approaches involving a particular target for the treatment of cancer have been described below:

1.3.1 Tubulin binding agents

Microtubules represent the best known cancer target and the compounds acting on tubulin are found to be highly successful in the treatment of cancer. Drugs acting on microtubules bind to several sites of tubulin and at different positions of the microtubules, where they suppress microtubule dynamics, thereby blocking mitosis at the metaphase/anaphase transition and induce cell death. Compounds acting on microtubules have been classified into: microtubule-destabilizing agents and microtubule-stabilizing agents. Compounds binding to a vinca binding site (vinblastine, vincristine) and colchicine binding site (colchicine, combretastatin) inhibit tubulin assembly i.e. they are microtubule-destabilizing agents (Figure 1.7). While, compounds binding to the Taxol binding site (paclitaxel) prevent microtubule disassembly i.e. they are microtubule-stabilizing agents (Dumontet & Jordan, 2010).

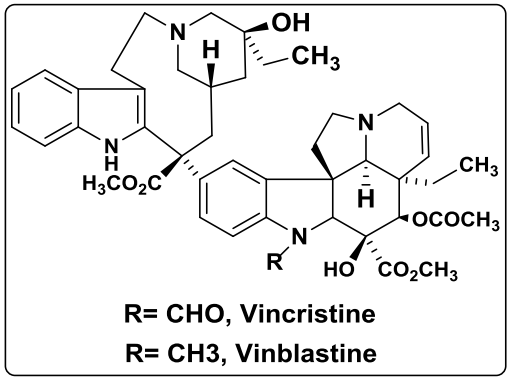

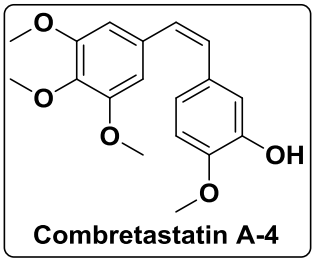

Figure 1.7: Examples Drugs which act as tubulin-stabilizing and tubulin de-stabilizing.

1.3.2 Inhibition of methionine aminopeptidase-2 (*MetAP-2*)

MetAP-2 is the class of aminopeptidase which is responsible for removal of amino acids from unblock terminal of peptide or its modification, which occur during translational phase of cell cycle. It is the key enzyme responsible for the angeogenesis. Removal or absence of this enzyme leads to decrease in cell growth and it is also reported from the study that it is required for germ-cell proliferation (Boxem et al., 2004). Inhibtion of MetAP-2 activity leads to improper biological activity of proteins, their degradation and impairment in normal cell function. Overactivity and elevated level of this enzyme is observed in malignant cell than normal, indicates that the enzyme is important for cancer cell growth (Catalano et al., 2001). Elevated level is observed in colorectal adenocarcinoma, advanced squamous cell cancer of cervix, metastatic renal carcinoma etc (Catalano et al., 2001). Recently a drug, TNP-470 entered human clinical trial targeting MetAP-2. The mechanism of action of MetAP-2 is still not very clear and it is required to conduct more vast study to open the cancer treatment gateway without compromising the MDR and relapse of disease (Selvakumar et al., 2006).

Inhibition of angiogenesis is considered a desirable pathway for stopping tumor growth & metastasis primarily because of the low potential for toxicity or resistance, as well as the promise of treating a broad spectrum of tumor types (Kallander et al., 2005). Fumagillin, a natural product that exerts its anti-angiogenic effects through the inhibition of endothelial cell proliferation, was discovered to be an irreversible inhibitor of methionine aminopeptidase-2 (MetAP-2) by covalently binding to His231 (Selvakumar et al., 2006). It was found that the MetAP-2 inhibition by fumagillin (and analogues Figure 1.8) is responsible for the observed antiangiogenic activity. A reversible bestatin-based MetAP-2 inhibitor was shown to inhibit angiogenesis & suppress tumor growth (Kallander et al., 2005). Human MetAP-2 is one of two enzymes that catalyze the removal of N-terminal methionine residues from intracellular protein. The enzyme is characterized by a bimetallic center activated by either cobalt or manganese,

which is supported by residues that form a pita-bread shaped fold (Hu et al., 2007).

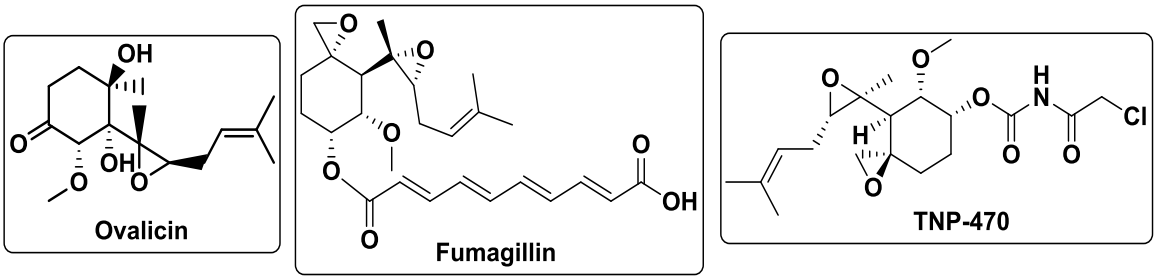

Figure 1.8: Drugs inhibit MetAP-2 enzyme. TNP-470, a MetAP-2 inhibitor which is under clinical trial.

Elevated level of MetAP-2 enzyme is observed in malignant lymphomas of B-cell and in colorectal cancer which attracted the attention of the researcher more towards the MetAP-2 enzyme. Inhibition of MetAP-2 enzyme by fumagillin leads to more down regulation of MetAP-2 enzyme which ultimately leads to more inhibition of endothelial cell proliferation. One more calcium-binding protein S100A4 is directly related with MetAP-2 which is responsible for metastasis regulation (Selvakumar et al., 2006). (Figure 1.9)

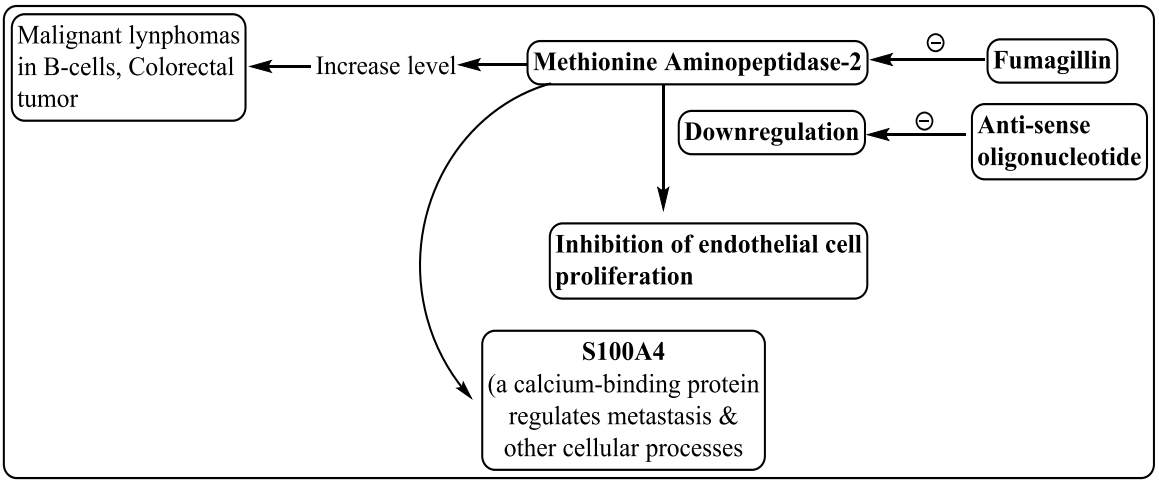

Figure 1.9: Mode of action of fumagillin drug inhibiting MetAP-2 enzyme (Selvakumar et al., 2006).

1.4.3 Inhibition of protein kinases

Protein kinases (PTKs) are enzymes that regulate the biological activity of proteins by phosphorylation of specific amino acids with ATP as the source of phosphate, thereby inducing a conformational change from an inactive to an active form of the protein. PTKs have been classified into the three main types: tyrosine kinases (TKs) that phosphorylate the Tyrosine phenolic hydroxyl, Serine-threonine kinases that phosphorylate the hydroxyl group of these two amino acids and Histidine kinases, recently discovered, that phosphorylate the nitrogen of Histidine residues. Protein phosphorylation is one of the most significant signal transduction mechanisms involved in regulation of crucial intra-cellular processes such as ion transport, cellular proliferation and differentiation, and hormone responses. PTKs have been found to be over-expressed in many cancer cells, so PTK inhibitors can act as anticancer agents. Some of the PTK inhibitors are undergoing clinical trials and some are under clinical use. For example, Erlotinib (Figure 1.10) is an approved drug for the treatment of non-small cell lung cancer (FDA) and semaxanib (Figure 1.10) is a drug that has completed phase II clinical trials for the treatment of cervical cancer (clinicaltrials.gov).

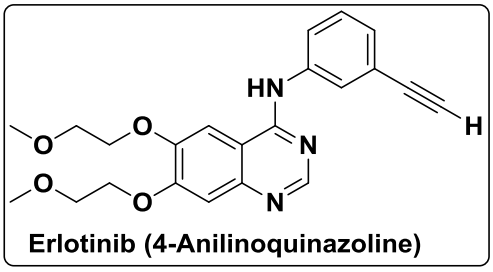

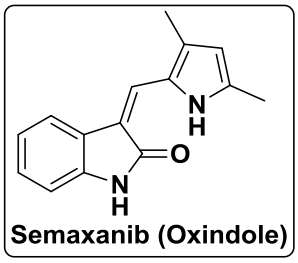

Figure 1.10: Drug inhibit protein kinases.

1.4.4 Inhibition of heat shock protein 90

HSP 90 inhibitors act by locking multi chaperone complex in the open state, leading to proteasomal degradation of client proteins (Bremer et al., 2006). HSP 90 has gained interest as a promising anticancer drug target, due to its importance in maintaining the stability, integrity, conformation and function of key oncogenic proteins. These HSP 90 “client proteins” have been demonstrated to

play fundamental roles in the processes of signal transduction, cell proliferation and survival, cell cycle progression and apoptosis, as well as other features of malignant cells, such as invasion, tumor angiogenesis and metastasis. The cancer selectivity and anti-tumoral effects of Hsp90 inhibitors are mediated by simultaneous and combined actions, in terms of directly affecting multiple cancer targets and pathways (Moser, Lang, & Stoeltzing, 2009). Drug IPI-504 (Figure 1.11) has completed phase II clinical trials for activity in patients with hormone-resistant prostate cancer (clinicaltrials.gov).

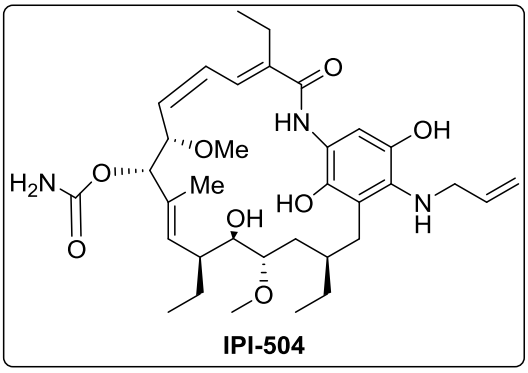

Figure 1.11: Drug affecting heat shock protein 90.

1.4.5 Proteasome inhibition

Proteasome degrades the endogenous proteins that are damaged or are not required. Hence, proteasome controls the levels of several proteins that are essential for the progression of the cell cycle and apoptosis, including cyclins, caspases, Bcl-2, the tumor-suppressing factor p53, and nuclear factor-kB (NF-kB). Accumulation of various other regulatory proteins of cell cycle can be achieved by blocking the proteasome, which leads to cell death by a variety of mechanisms. So, proteasome inhibitors may act as anticancer agents. Bortezomib (Figure 1.12) was approved in 2003 for the treatment of multiple myeloma, the second most common hematological cancer, and is currently being clinically evaluated for various other malignancies (Avendano & Menendez, 2008).

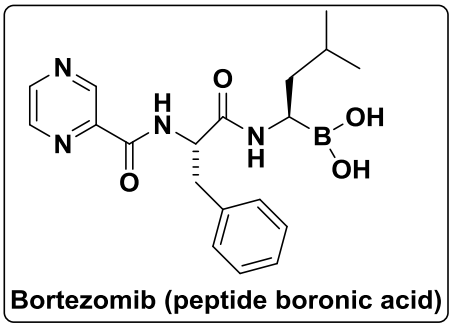

Figure 1.12: Drug inhibit proteosomes.

1.4.6 Inhibition of histone deacetylases

Histone acetylase is an enzyme that adds acetyl groups to the lysine residues of histones associated with the DNA chromatins leading to a less compact structure, while histone deacetylase removes the acetyl groups leading to a more compact structure. The less compact structure due to histone acetylation allows transcription factors to access promoter regions of various genes. On the other hand, the more compact structure due to histone deacetylation prevents transcription factors to access the promoter regions (Patrick, 2013).Thus, histone acetylation is being associated with transcriptionally active genes and deacetylation with transcriptionally inactive genes (Bremer et al., 2006). HDACs cause gene silencing, may also lead to decreased DNA repair, thus resulting into an increased chance of cancer (Patrick, 2013). In cancer, there is overexpression of histone deacetylases (HDACs). Inhibitors of HDACs induce growth arrest, differentiation and apoptosis in various cancer cells (Bremer et al., 2006). Vorinostat (Figure 1.13), a HDAC inhibitor was approved in 2006 by the US FDA for the treatment of cutaneous T-cell lymphoma (Patrick, 2013).

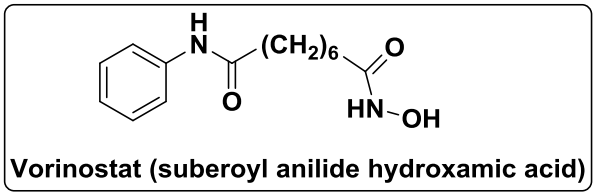

Figure 1.13: Histone deacetylases inhibitor.

1.4.7 DNA alkylating agents

Alkylating agents are a class of antineoplastic or anticancer drugs which act by inhibiting the transcription of DNA into RNA and thereby stopping the protein synthesis. Alkylating agents substitute alkyl groups for hydrogen atoms on DNA, resulting in the formation of cross links within the DNA chain and thereby resulting in cytotoxic, mutagenic, and carcinogenic effects. This action occurs in all cells, but alkylating agents have their primary effect on rapidly dividing cells which do not have time for DNA repair. Cancer cells are among the most affected because they are among the most rapidly dividing cells. The end result of the alkylation process results in the misreading of the DNA code and the inhibition of DNA, RNA, and protein synthesis and the triggering of programmed cell death (apoptosis) in rapidly proliferating tumor cells (Patrick, 2013).

1.5 Mechanism of drug resistance

Multidrug resistance (MDR) is a phenomenon in which cancer cells exhibit a cross-resistant phenotype against multiple unrelated drugs that are structurally and/or functionally different and may also have different molecular targets. Cancer cells may exhibit intrinsic MDR or they may acquire MDR during chemotherapy. For intrinsic MDR, cancer cells exhibit resistance to chemotherapy at their initial exposure to the anticancer drug. However, in acquired MDR, resistance to chemotherapy occurs during the course of the treatment or upon recurrence of the disease after successful chemotherapy. Several host factors are involved in the development of both intrinsic and acquired MDR including those that impair the delivery of anticancer drugs to the cancer cells and nullify their cytotoxic effects, and those that alter the genetic or epigenetic factors of cancer cells, which leads to drug insensitivity (Nieth et al., 2003). As evident from clinical practice, two or more MDR mechanisms often act simultaneously in each cancer type thereby making treatment more challenging (Saraswathy & Gong, 2013). Some of the factors which cause MDR are described in figure 1.14.

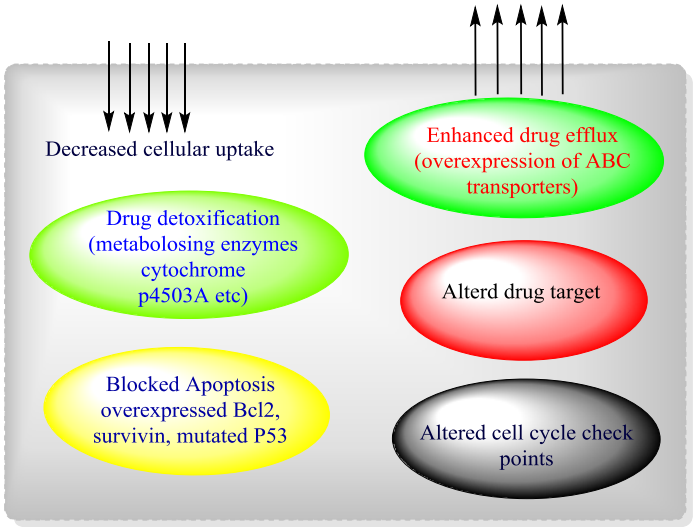

Figure1.14: Various mechanisms of MDR (Saraswathy & Gong, 2013).

In clinical practice, MDR becomes a crucial problem when an effective dose of anticancer drug increases to a non-manageable level. Since several factors are involved in the development of both intrinsic and acquired MDR, a clear understanding of these molecular mechanisms is necessary to develop effective treatment modalities. For instance, vascular networks induced by tumor angiogenesis are structurally and functionally abnormal due to the imbalance of angiogenic regulators, such as vascular endothelial growth factor (VEGF) and angiopoietins. Consequently, tumor blood flow is hectic, which can lead to hypoxic and acidic regions in tumors. Hypoxia in cancer might lead to multidrug resistance via different cellular pathways such as lost sensitivity to p53-mediated apoptosis, and enhanced p-glycoprotein expression.

The occurrence of multi-drug resistant (MDR) leads to the failure of therapy and increase in the morbidity rate of the patient (Krishna & Mayer, 2000). The best approach to cope MDR is to design pharmacophores on the basis of hybrid molecular approach targeting two different receptors at the same time which will surely improve the treatment progression. The effect may be synergistic when two pharmacophores are given in a single molecule targeting different cycles of cancer progression. This will leads to decrease in therapeutic dose of drug administered and hence decrease the treatment duration with less chance of resistance. In synergism the drug efficacy increase and dose decrease i.e.

pharmacological effect observed with the less dose compared to the individual drug administered. The drug achieve the therapeutic window but remain nontoxic. Duffy et al. evaluated the activity of combination of NSAIDs ((indomethacin, sulindac, tolmetin, acemetacin, zomepirac and mefenamic acid) and cytotoxic drugs (doxorubicin, daunorubicin and epirubicin) against multi-drug resistant lung & human leukemia cancer cell line (A-549 & HL-60/ADR respectively). There is no significant activity observed against lung cancer cell line but in the HL-60/ADR and COR-L23R cell lines, in which multidrug resistance is due to overexpression of the multidrug resistance-associated protein MRP, a significant increase in cytotoxicity was observed in the presence of the active NSAIDs (Duffy et al., 1998). Xiao et al. synthesized series of novel stilbene-coumarin based hybrid which showed more potent inhibitory effects against MCF-7/ADR cell lines (IC_{50}= 11.94, 11.11mmol/L, respectively) than normal MCF-7 cell lines (IC50= 21.43, 22.94mmol/L, respectively), point toward a remarkable anti-MDR properties associated with these compounds (Xiao et al., 2010).

CHAPTER 2
LITERATURE REVIEW

2.1 Chalcones and its derivatives

Chalcones occur abundantly in nature, and these can be synthesized in the laboratory via very simple and efficient synthetic routes. Cytotoxic activities of both naturally-occurring and synthetic chalcones have been reported in the literature (Avanzo et al., 2012). Depending upon the structure, different chalcone derivatives activate different pathways to exhibit anticancer activities.

2.2 Chalcones interfering with tubulin polymerization

Compounds that inhibit tubulin polymerization act on vinca and colchicine binding site of tubulin. Several chalcones that act as cytotoxic agents or as microtubule-destabilizing agents have been reported in the literature (Dyrager et al., 2011). Most of these chalcones have structural similarity to the combretastatin A-4 (CA4) such as compound **(1)** (Ducki et al., 2009). Other chalcone derivatives acting as microtubule-destabilizing agents are coumarin-chalcone hybrids **(2)** (Sashidhara et al., 2010), resveratrol derivative possessing chalcone moiety **(3)** (Ruan et al., 2011). (Figure 2.1)

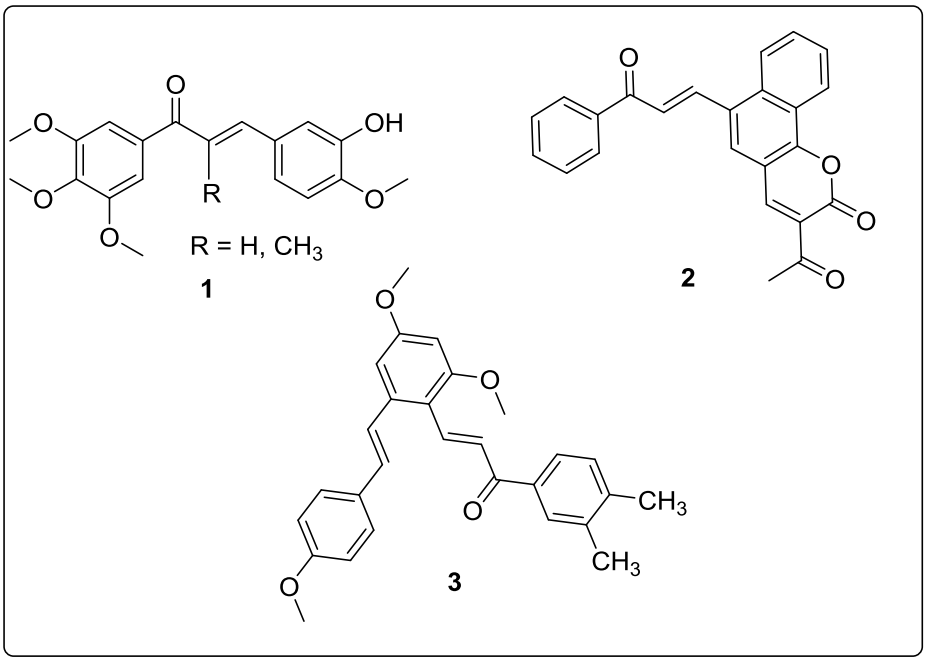

Figure 2.1: Chalcones derived from combretastatins and resveratrol.

Microtubules are the important targets for the binding of anticancer drugs, as these are involved in the spindle formation during the cell-division. Spindle formation is necessary for the segregation of chromosomes to ensure the transfer of chromosomes from parent to the daughter cells. Microtubules are hollow structures formed by 13 parallel proto filaments that grow and shorten by the reversible, non-covalent addition of tubulin dimers at their ends. Tubulin is a protein that contains two subunits called α and β in a head to tail arrangement. Microtubules and free tubulin dimers are involved in a highly dynamic equilibrium (Avendaño & Menendez, 2008). The α-tubulin subunit is always bound to GTP, acquiring a conformation suitable for MT polymerization, whereas the β-tubulin subunit can be bound either to GTP or GDP, favorable for MT polymerization or depolymerization, respectively (Pasquier & Kavallaris, 2008). During cell division, microtubules in the cytoplasmic network depolymerize, and the tubulin, thus liberated is again polymerized to give the mitotic spindle. (Figure 2.2)

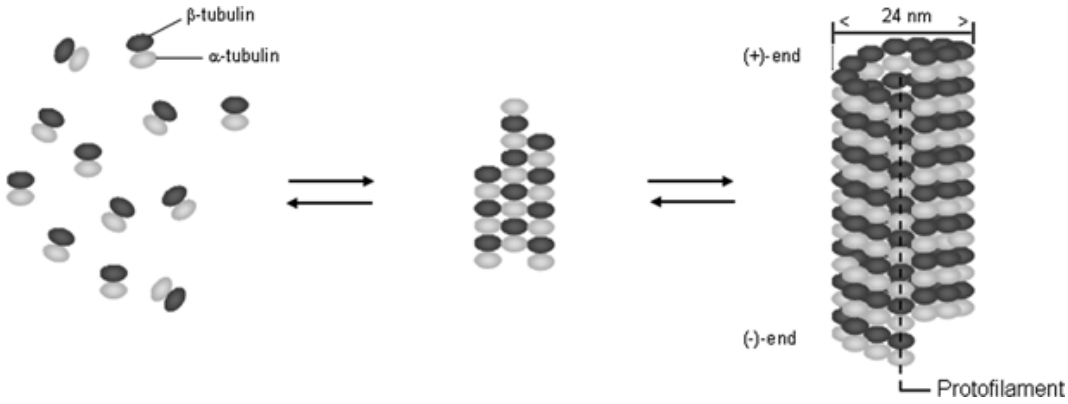

Figure 2.2: Dynamic equilibrium between microtubules and tubulin dimers (Altmann & Gertsch, 2007).

Microtubule-destabilizing agents inhibit microtubule polymerization when present at high concentrations, and at low concentration they disturb the dynamic stability of microtubules (Dumontet & Jordan, 2010). Most of them strongly bind to the colchicine binding site of β-tubulin and interfere with the polymerization of tubulin, thus preventing the formation of mitotic spindle.

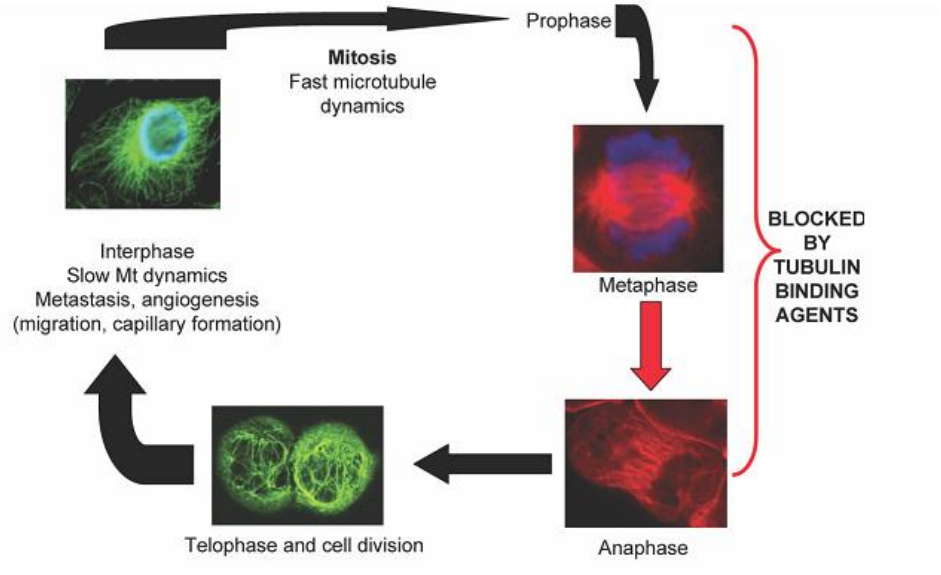

Figure 2.3: Microtubule structures through the cell cycle (Pasquier & Kavallaris, 2008)

This results in the slowing down of the metaphase–anaphase transition, impaired chromosomal segregation, mitotic block, and subsequent induction of the mitochondrial apoptotic pathway (Pasquier & Kavallaris, 2008). (Figure 2.3)

2.3 Chalcones acting on apoptotic signaling pathways

Apoptosis is normally defined as programmed cell death (Avendaño & Menendez, 2008). It is a built-in cellular destruction process, in which the body protects itself against abnormal or faulty cells (Patrick, 2013). Apoptosis occurs during development and ageing and as a homeostatic mechanism to maintain cell populations in tissues (Elmore, 2007). Several genes like the Bcl2 and caspase-family genes involved in the apoptosis process have been found to be defective in cancer cells. Apoptosis is caused by a group of cysteine aspartyl specific proteases called caspases, which cleave their substrates at aspartic acid residues. Caspases are produced as inactive zymogens, which are activated by a hydrolysis reaction at aspartic acid sites. Because, both the activation of caspases and the cleavage of their substrates take place at aspartic acid sites, they can act in proteolytic cascade processes (Patrick, 2013). In most of the cases chalcones act as the inducers of apoptosis (Batovski & Parushev, 2010).

Some of the chalcones that act in the apoptotic pathways are described in figure 2.4.

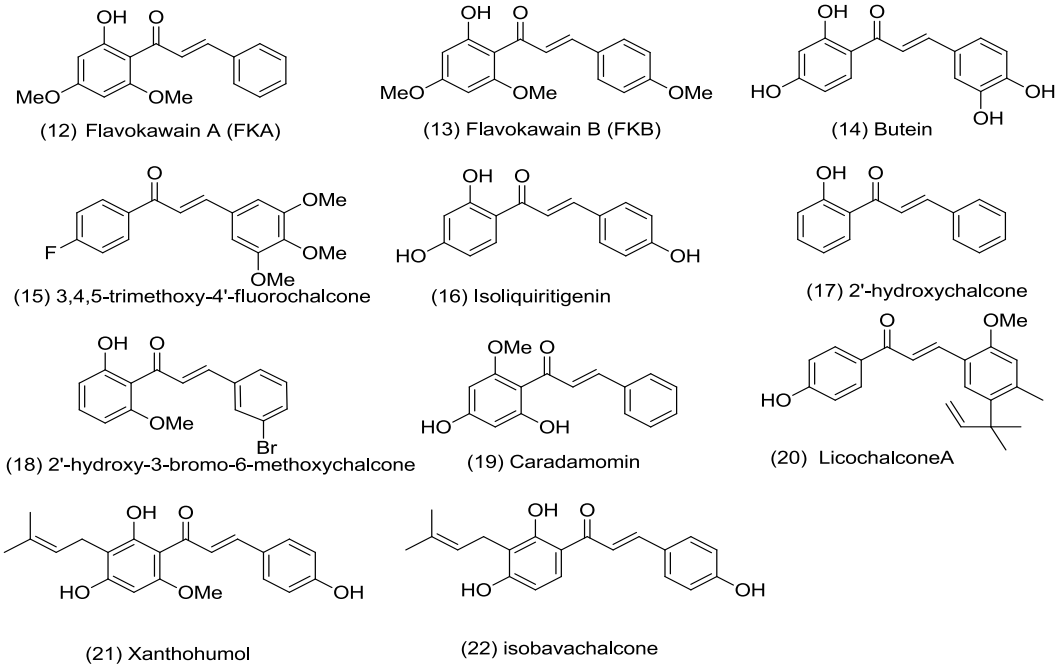

Figure 2.4: Chalcones that act at specific targets in the apoptotic pathways.

2.4 Methionine aminopeptidase-2 inhibition

It was reported that various compounds containing a aryl triazoles scaffold showed good inhibitory action on cobalt-activated hMetAP-2 (Kallander et al.). Specially 3-methylphenyl-1, 2, 3-triazole has shown it's binding in the active site of hMetAP-2. The key binding interaction between triazole nitrogen N-1 and N-2 and the active site cobalt atoms were found to be similar to as noticed in the crystal structure of a 1, 2, 4-triazole bound to cobalt activated bacterial MetAP-2. This tight coordination may account for much of the strong binding of these small molecules. The third triazole nitrogen appears not to be directly involved in binding to the metals but engages in hydrogen bonding to His339. Replacing N-1 with carbon significantly reduced the MetAP-2 potency. It was concluded that N-1 and N-2 in the heteroaryl ring are responsible for maintaining direct coordination with the active site metals and are thus important for inhibition. The orientation of the aromatic ring relative to the triazole ring is important for binding; the coplanar orientation observed

in the X-ray crystal structure may be preferred because it avoids steric crowding between the aromatic ring and His231. Further modification are done at the aryl part which showed different activity even the aryl part was also replaced with the heteroatoms to obtain good activity in triazole compounds. On the basis of this interpretation, it was proposed that other form of triazole like 5-aryl triazole and 3-aryl triazole may show such activity (Kallander et al., 2005). (Figure 2.5)

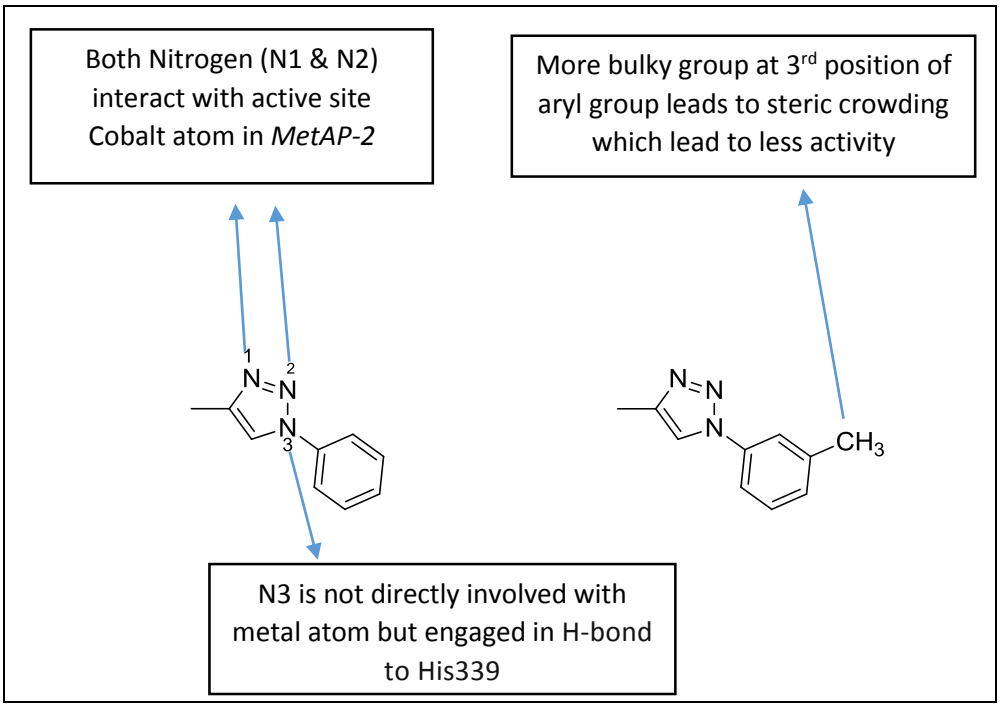

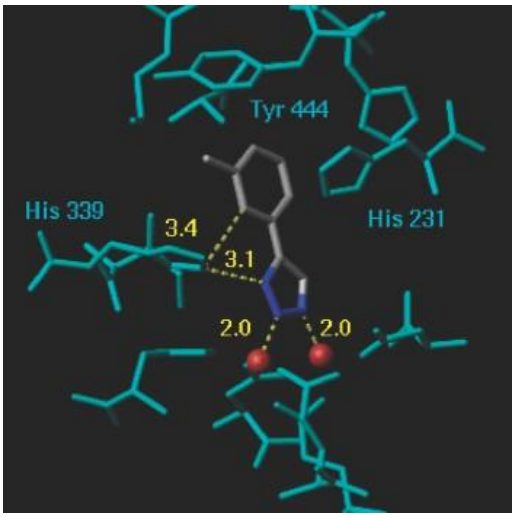

Figure 2.5: X-ray crystal structure of compound 3-Methylaryl triazole (grey and blue) bound to hMetAP-2. Cobalts are given in red. The atomic coordinates and structure factors (code 2ADU) have been deposited in the Protein Data Bank. (http://www.rcsb.org/). This figure was generated using the program MolMol.(Koradi et al., 1996)

Marino et al. designed and synthesize various compound based on 1, 2, 4-triazole nucleus and evaluated their inhibitory activity on MetAP-2 enzyme. A total of 96 compounds were screened and 5-(benzylthio)-N-phenyl-4H-1,2,4-triazol-3-aminetriazole (Figure 2.6) was reported as most potent in the series (Marino et al., 2007).

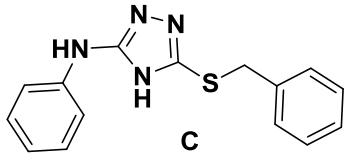

C

5-(benzylthio)-*N*-phenyl-4*H*-1,2,4-triazol-3-amine

Figure 2.6: Potent MetAP-2 enzyme inhibitor.

Hou et al. synthesized a class of potent MetAP-2 inhibitors having 1, 4-benzodioxane fragment. The compounds were evaluated for their antitumor activities. The compound, shown in figure 2.7 exhibited most potent inhibitory

activity that inhibited the growth of HEPG2 cells with IC_{50} of 0.81 µM and inhibited the activity of MetAP-2 with IC_{50} of 0.93 µM, which was comparable to the positive control TNP-470 (Hou et al., 2011).

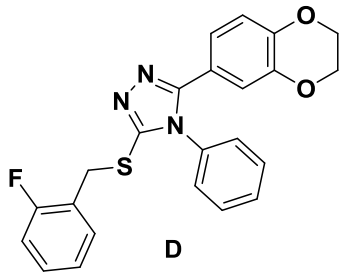

D

3-(2,3-dihydrobenzo[*b*][1,4]dioxin-6-yl)-5-((2-fluorobenzyl)thio)-4-phenyl-4*H*-1,2,4-triazole

Figure 2.7: MetAP-2 enzyme inhibitor showed a good activity compared to TNP-470 (Standard drug).

CHAPTER 3

RATIONALE

&

OBJECTIVES

3.1 Rationale of proposal

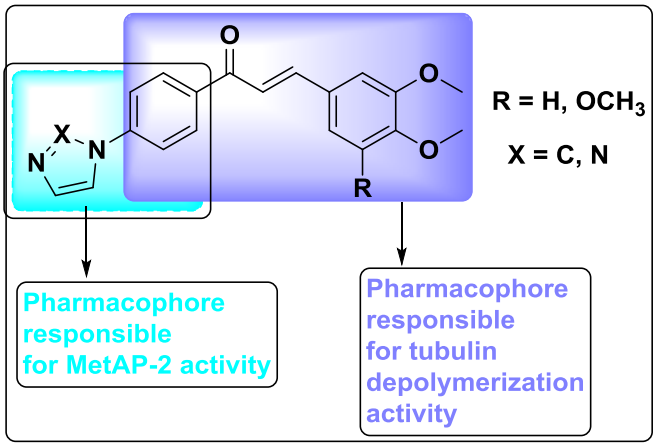

Figure 3.1: Rational behind the design of molecule been synthesized in laboratory.

From literature review tubulin receptor comprises of two subunits i.e. α & β-subunits in alternate fashion. The most important region for tubulin de-polymerization agents like colchicine, podophyllotoxin is confined in β-subunit. The amino acid AsnD249 present in β-chain of tubulin receptor play vital role in tubulin polymerization inhibition mechanism. It comprises the T7 loop which flips when colchicine binds with the receptor. Apart from that CysC241 present in α-chain of tubulin receptor is also important as it is part of extra exploration site in the receptor. Compound like ABT751 (Figure 3.2) show interaction with S9 & T7, the border where the colchicine binds on β-chain of tubulin (Ravelli et al., (2004)).

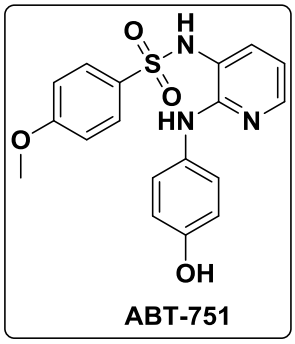

Figure 3.2: *ABT751 show interaction with S9 & T7, the border where the colchicine binds on β-*chain of tubulin.

The trimethoxy group present in A-ring is the necessity, which interact in β-chain and show a relation with CysD241, LeuD255, LeuD252 amino acids. The

combretastatin molecule also contains trimethoxy group in A-ring and one olefinic linker along with B-ring. The A-ring is necessary for binding with colchicine site so it remains intact, we planned to introduce pyrazole ring at α, β-unsaturated carbonyl system of chalcones. The introduction of pyrazole ring at α, β-unsaturated ketone site may increases the number of hydrogen bond acceptor in molecule which may exploit some unexplored hydrophilic pockets in colchicine binding site. Similarly the introduction of optionally substituted B-ring which contains different polar substitutions may also increases the polar interaction with deeply buried hydrophilic pockets which get opens due to change in confirmation of proteins on binding of ligand with colchicine binding site.

In addition using hybrid approach the molecule which show as anti-angiogenic activity by inhibiting Methionine Aminopeptidase-2 which is important enzyme for tissue repairing is 1, 2, 3-aryl triazole is made by researcher after studying the pure inhibitors of MetAP-2 enzyme like fumagillin, ovalicin, TNP-470 (Kallander et al.). It is proven as effective moiety when they check the activity of compound. 1, 2, 3-aryl triazole molecule show a pi-pi stacking with two main amino acids which is Tyr444 and Phe219 which is must hydrophobic interaction in any other compound. His339 amino acid involve in the hydrogen bond with nitrogen of triazole ring and one nitrogen engaged in metal binding with cobalt atom which is co-factor in MetAP-2 enzyme.

In reference to these literature reports we proposed some molecules as described in figure 3.3 which can mimics tubulin binding chalcones and azoles based ligands acting as MetAP-2 inhibitors. In Figure 3.3 four different types

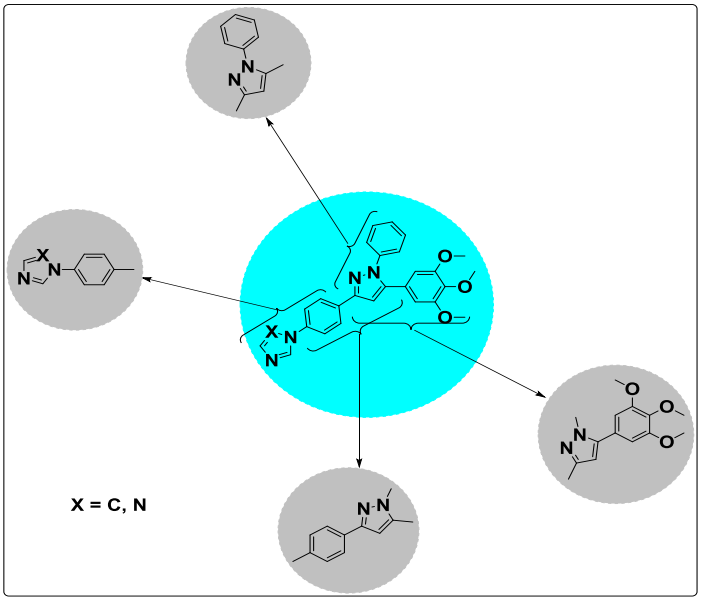

Figure 3.3: Different types of aryl azole moiety in single synthesized structure.

of aryl azoles are described which are proposed as potential pharmacophores for active site of MetAP-2. Three of aryl azole pharmacophores are present as a rigid structure but one aryl azole with B-ring of compound is of main focus which is enough flexible to explore the MetAP-2 receptor cavity.

For tubulin activity the compound itself act as hybrid of two pharmacophores which is combretastatin and chalcone as shown in Figure 3.4. Due to this it is expected that the compound might show potent anti-tubulin activity by interacting at colchicine binding domain.

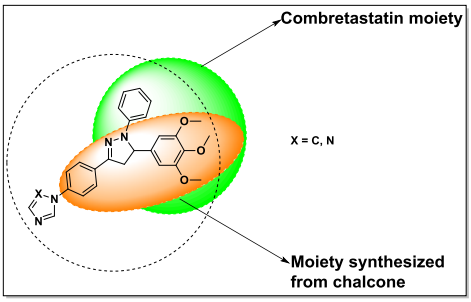

Figure 3.4: Synthesized compound showing two different active structural moieties.

Objectives

- To design the chalcone derivatives through hybrid molecular approach
- Molecular docking of designed compounds at the tubulin & MetAP-2 receptor
- To synthesized the chalcone derivatives in laboratory
- The screening of synthesized compound against Cancer cell-lines

CHAPTER 4

MOLECULAR DOCKING

4.1 Molecular docking (*in silico* drug design)

In past years lots of money have been spent to investigate the activity of new compounds which ultimately increase the cost of drug. From screening of drug to the 1st clinical trial phase, 5 to 10 years is the period to get the molecule which may or may not be active. Screening of compounds is the core area which required most of attention. But now using Molecular docking it is easy to screen millions of drug molecule.

Before all above, there are some definition which clarify what Molecular Docking is?

- **Receptor** or **host** or **lock** – The "receiving" molecule, most commonly a protein or other biopolymer.
- **Ligand** or **guest** or **key** – The complementary partner molecule which binds to the receptor. Ligands are most often small molecules but could also be another biopolymer.
- **Docking** – Computational simulation of a candidate ligand binding to a receptor.
- **Binding mode** – The orientation of the ligand relative to the receptor as well as the conformation of the ligand and receptor when bound to each other.
- **Pose** – A candidate binding mode.
- **Scoring** – The process of evaluating a particular pose by counting the number of favorable intermolecular interactions such as hydrogen bonds and hydrophobic contacts.
- **Ranking** – The process of classifying which ligands are most likely to interact favorably to a particular receptor based on the predicted free-energy of binding.

Various software are available in market which helps to predict the binding mode either using static docking (receptor is rigid) or dynamic docking (receptor is

dynamic). Among these some software are Autodock, Chimera, MOE, Accelrys Discovery studio, Schrodinger Maestro.

Static molecular docking was performed using Autodock, Autodock vina, Discovery studio (as a visualizer) and Schrodinger Maestro which helps me to tell whether these synthesized compounds show better activity comparison to the standard drugs.

4.2 In-silico study of the proposed compounds

The molecular docking studies of proposed compounds were performed on two receptors which are tubulin and MetAP-2. Tubulin is responsible to maintain cell cytoskeleton and maintain integrity and shape of cell whereas MetAP-2 is present in cytoskeleton and it is metallo-enzyme responsible for tissue repairing and angiogenesis.

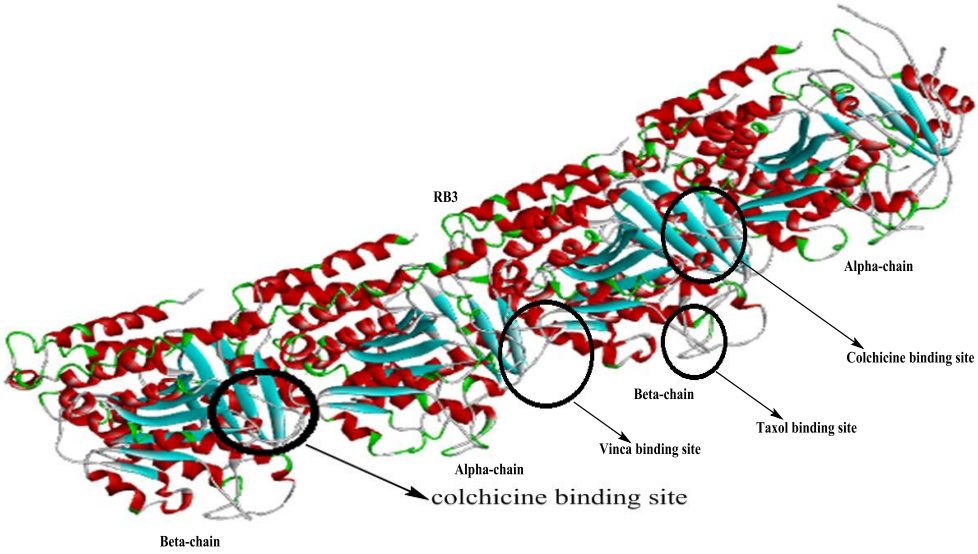

Figure 4.1*: Different binding sites for anti-tubulin drug on tubulin receptor (PDB ID- 1SA0). (Cao, et al., 2012)*

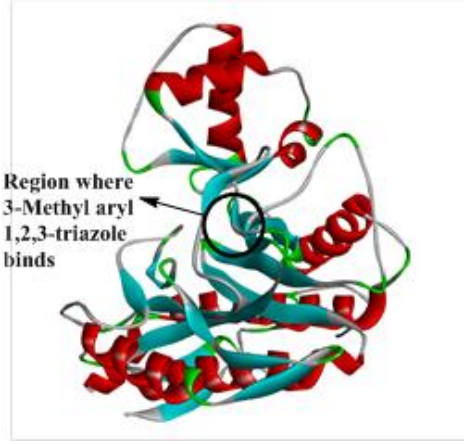

Figure 4.2*: Sites for MetAP-2 inhibitor drug on Methionine aminopeptidase-2 receptor (PDB ID-2ADU).*

4.3 Molecular docking using autodock 4.2

The molecule synthesized was docked over Beta-tubulin receptor (1SA0) and Methionine Aminopeptidase-2 receptor (2ADU) taking colchicine and 3-Methylaryl triazole as standard drug respectively, using Autodock 4.2 (Goodsell et al., 1996).

4.3.1 Protein preparation

The PDB for the crystal structure of beta-tubulin receptor ligand binding domain (1SA0) and methionine aminopeptidase-2 receptor (2ADU) ligand-binding domain were retrieved from protein data bank. During the protein preparation only polar hydrogens and kollman charges were added. The atoms in the protein were assigned for Autodock 4.2 type. Now the PDBQT file of the protein was saved in which its different pdb records from “ATOM” select till **“**END” were added.

4.3.2 Ligand preparation

The 3D structure of the ligand was created using ChemBio Draw 3D, and saved in .mol2 (SYBYL2) format. The ligand energy is minimized through MMFF94 parameter displayed in ChemBio Draw 3D. The ligand was selected from the ligand menu of autodock and from the torsion tree, its roots were first detected

and then selected. Now it will show number of rotatable bonds in the ligand. The resultant ligand file is saved in standard autodock .pdbqt file format.

4.3.3 Grid generation

From the GRID menu of autodock, the macromolecule (targeting protein) was selected and the protein is initialized in the autodock for the grid generation. Herein this step additional charges and bond orders are assigned. The PDBQT file generated in this step overwrites the previously created PDBQT file. The Grid was generated by taking the bound ligand as the center of grid. The grid maps representing the proteins will be calculated using auto grid and grid size was set to 40x40x40 points with grid spacing of 0.375 Å.

4.3.4 Docking

Docking of protein to ligands were carried out using LGA (Lamarckian Genetic Algorithm) with standard docking protocol on the basis a population size of 150 randomly placed individuals; a maximum number of 2.5 x107 energy evaluations, a mutation rate of 0.02, a crossover rate of 0.80 and an elitism value of 1. Ten independent docking runs will be carried out for each ligand and results will be clustered according to the 2.0 Å rmsd criteria.

4.4 Molecular docking using autodock vina

Autodock Vina is a new generation of docking software from the Molecular Graphics Lab. It achieves significant improvements in the average accuracy of the binding mode predictions, while also being up to two orders of magnitude faster than Autodock 4. Autodock Vina does not require choosing atom types and pre-calculating grid maps for them. Instead, it calculates the grids internally, for the atom types that are needed, and it does this virtually instantly.

Because the scoring functions used by Autodock 4.2 and Autodock Vina are different and inexact, on any given problem, either program may provide a better result.

Autodock vina needs file in .pdbqt format both for receptor and ligand which is prepared in Autodock 4.2.

4.5 Molecular docking using schrodinger

Schrodinger maestro is a powerful software tool for molecular docking. This software comes with graphical user interface for windows and through this software I have performed static docking, where the maximum glide score is considered compared with standard to check whether the synthesized molecule shows valid interaction or not (Release, Schrodinger, 2013).

4.5.1 Protein preparation

In Schrodinger maestro software where the protein preparation wizard is there where complete protein preparation is done.

4.5.2 Ligand & grid preparation

Ligand is prepared by selecting the ligand in required receptor and then there is automatically grid and co-ordinates selection around the particular area.

4.5.3 Docking

Docking is performed using XP (Extra precision) method to calculate the exact interaction compared to standard. The glide score comes for each ligand and hence compared with standard molecule.

4.6 *In silico* study of proposed compounds

In-silico study of compound synthesized was done on Tubulin (1SA0) and MetAP-2 receptor (2ADU) (Figure 3.1 & 3.2 respectively). The docking score obtained for the respective receptor along with the score of their standard are given in Table 3.1. Result indicated that synthesized compound has a strong binding affinity for the Tubulin receptor as well as MetAP-2 receptor when compared with its standard molecule which is combretastatin & 3-methylaryl triazole respectively. It has been evidently found that, in majority of cancer there

is rapid progression of growth signals and in that cases drugs like vincristine, vinblastine has proven for treatment with noticeable success. Similar kind of drug Zybrestat completed Phase II clinical trial in combination therapy with carboplatin /paclitaxel in anaplastic thyroid cancer (ATC) and in clinical trial phase II for Neuroendocrine Tumors with Carcinoid syndrome as a single agent therapy. Zybrestat is the phosphate analogue of combretastatin which is inspired from colchicine. Combining anti-tubulin drugs with a pharmacophores which inhibit tumor growth by affecting angiogenesis is not yet reported but drugs which inhibit angiogenesis by inhibiting MetAP-2 enzymes are fumagillin, ovalicin, TNP-450. From these molecules a pharmacophore was designed by Kallander et al. group with a good anti-angiogenic activity.

The amino acid AsnD249 present in β-chain of tubulin receptor play vital role in tubulin polymerization inhibition mechanism. It comprises the T7 loop which flips when colchicine binds with the receptor (Ravelli et al., 2004). Apart from that CysC241 present in α-chain of tubulin receptor is also important as it is part of extra exploration site in the receptor. Compound like ABT751 show interaction with S9 & T7, the border where the colchicine binds on β-chain of tubulin.

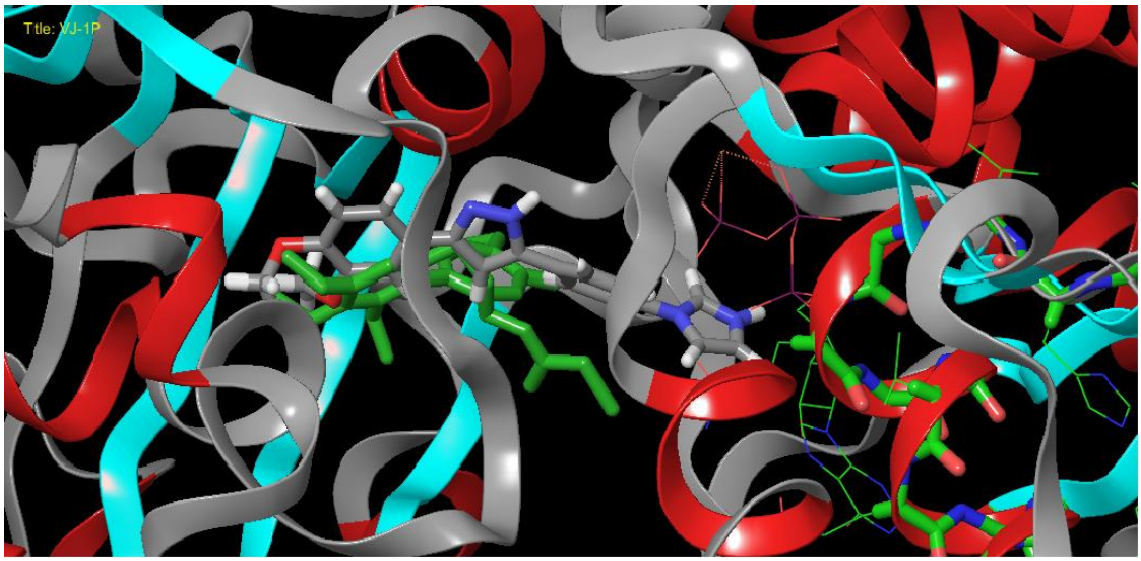

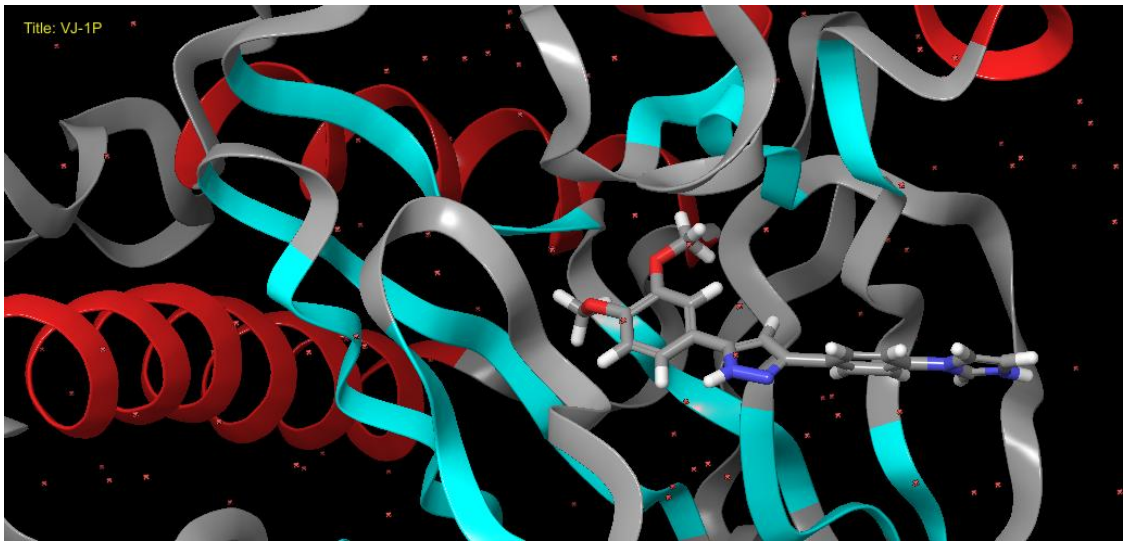

Figure 4.3: Docking pose of synthesized compound VJ-1P on (A) tubulin receptor (1SA0) (top), (B) Methionine aminopeptidase-2 receptor (2ADU) (bottom)

Table 4.1: Docking energy of VJ-1P and standard with their respective receptor in schrodinger

S.No	Receptor	Ligand	Binding Energy (kcal/mol)
1	Tubulin Receptor	VJ-1P Colchicine	-6.438 -5.284
2	Methionine Aminopeptidase-2 Receptor	VJ-1P 3-Methylaryl triazole	-4.446 -3.828

Compounds that are designed other than VJ-1P are VJ-1, VJ-2, VJ-3, VJ-4, VJ-5, VJ-2P, VJ-3P, VJ-4P, VJ-6P, VJ-1PP1, VJ-1PP2, VJ-2PP1, VJ-2PP2, VJ-3PP1, VJ-3PP2, VJ-4PP1, VJ-4PP2, VJ-6PP2.

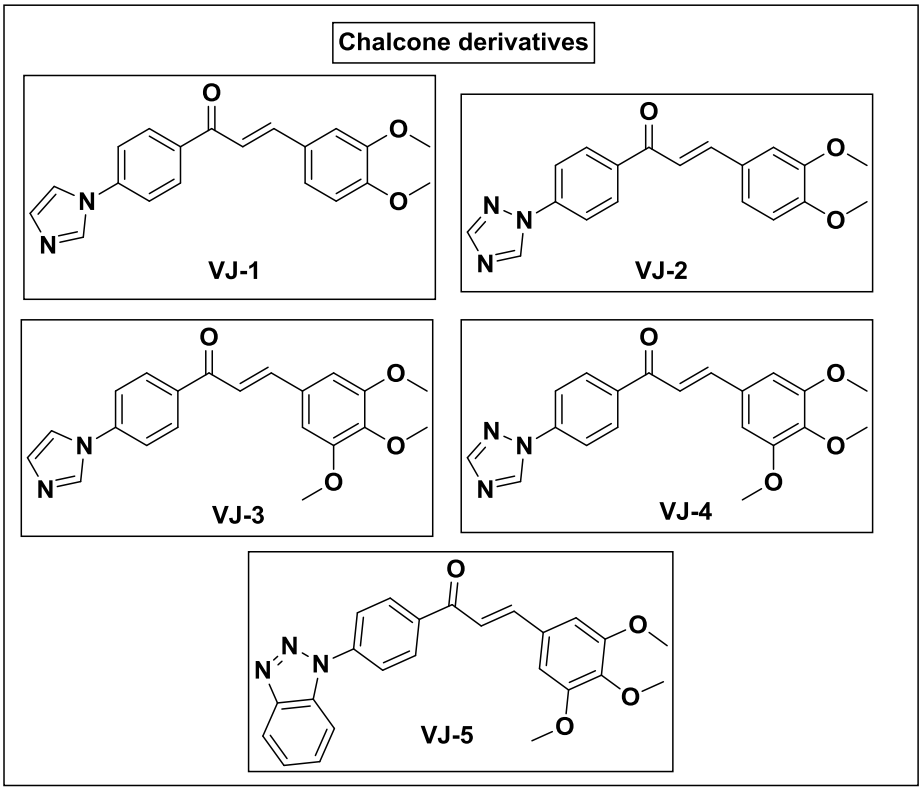
Chalcone derivatives
VJ-1
VJ-2
VJ-3
VJ-4
VJ-5

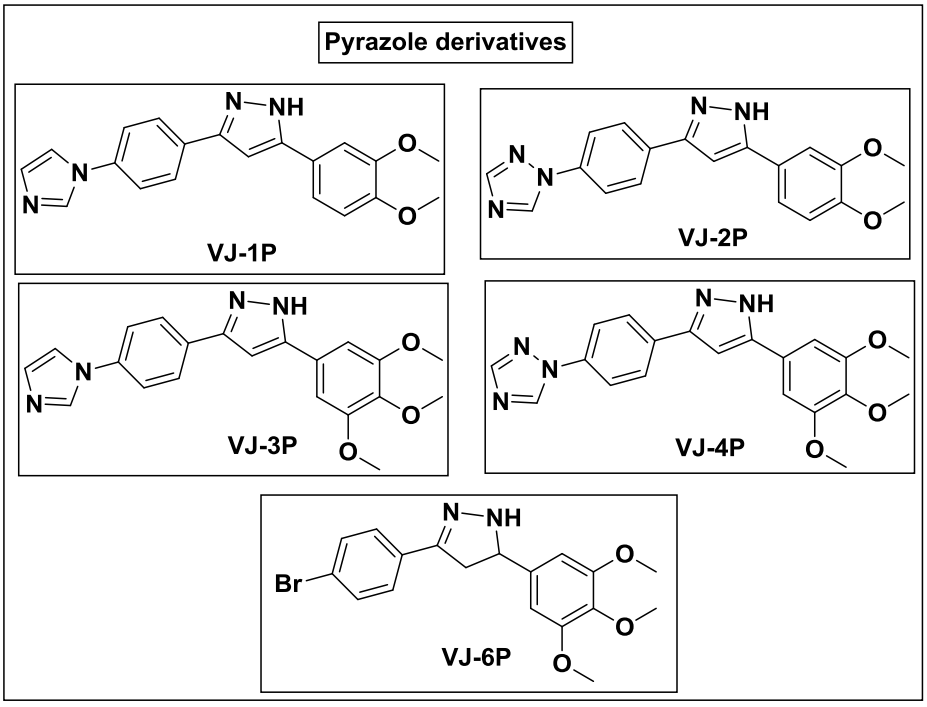
Pyrazole derivatives
VJ-1P
VJ-2P
VJ-3P
VJ-4P
VJ-6P

Phenyl Pyrazole derivatives

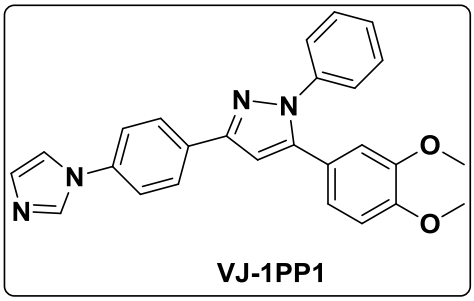

VJ-1PP1

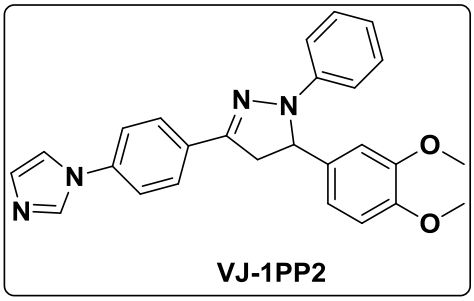

VJ-1PP2

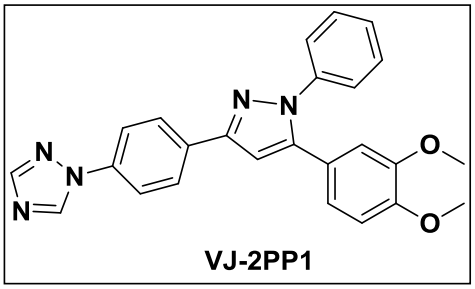

VJ-2PP1

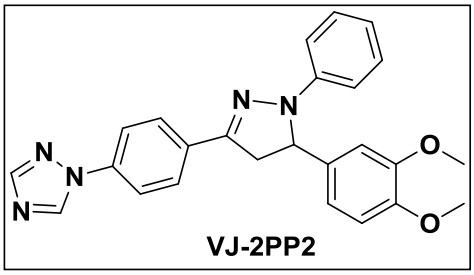

VJ-2PP2

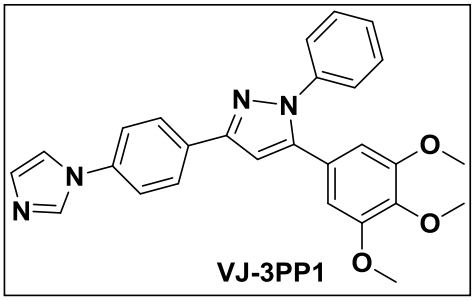

VJ-3PP1

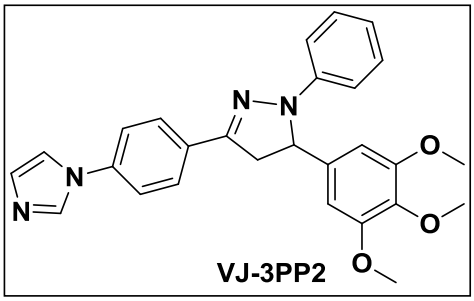

VJ-3PP2

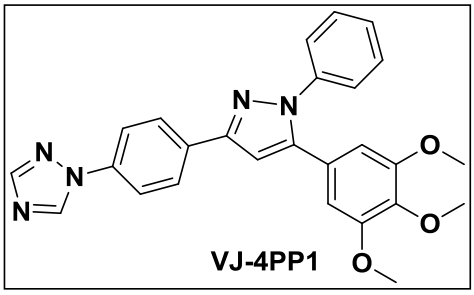

VJ-4PP1

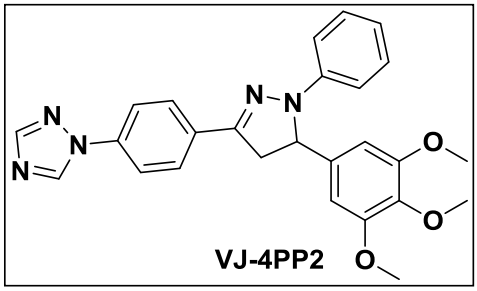

VJ-4PP2

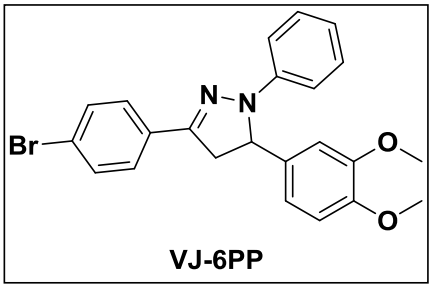

VJ-6PP

Table 4.2: Docking energy of VJ compound series in Schrodinger, Autodock 4.2 & Autodock vina

S. No.	Receptor	COUMPOUNDS	Schrodinger docking score Binding Energy (kcal/mol)	Autodock 4.2 Binding Energy (kcal/mol)	Inhibition Constant*	Autodock Vina scores Binding Energy (kcal/mol)
1	Tubulin/*MetAP-2* Receptor	VJ-1	-5.350/-5.609	-7.72/-8.29	9.51 µM/ 844.28 Nm	-8.2/-6.2
2	Tubulin/*MetAP-2* Receptor	VJ-2	-4.783/-4.133	-7.7/-8.30	2.27 µM/ 818.78 nM	-8.2/-6.1
3	Tubulin/*MetAP-2* Receptor	VJ-3	-5.043/-5.404	-7.68/-7.04	2.36 µM/ 6.89 µM	-8.0/-6.1
4	Tubulin/*MetAP-2* Receptor	VJ-4	-4.990/-5.307	-7.69/-7.25	2.3 µM/ 4.81 µM	-8.3/-5.9
5	Tubulin/*MetAP-2* Receptor	VJ-5	-5.429/-3.572	-8.03/-8.10	1.30 µM/ 1.16 µM	-9.2/-6.8
6	Tubulin/*MetAP-2* Receptor	VJ-1P	-6.438/-4.446	-7.48/-4.58	3.28 µM/ 440.04 µM	-8.4/-6.0
7	Tubulin/*MetAP-2* Receptor	VJ-2P	-5.539/-2.565	-7.45/-4.68	3.49 µM/ 374.0 µM	-8.3/6.0
8	Tubulin/*MetAP-2* Receptor	VJ-3P	-5.497/-2.520	-7.34/3.53	4.2 µM/ 2.6 mM	-8.3/-6.0
9	Tubulin/*MetAP-2* Receptor	VJ-4P	-5.315/-2.708	-7.40/-4.05	3.74 µM/ 1.08 mM	-8.4/-5.8
10	Tubulin/*MetAP-2* Receptor	VJ-6P	-4.723/-1.902	-7.35/-4.28	4.6 µM/ 2.6 mM	-7.4/-5.4
11	Tubulin/*MetAP-2* Receptor	VJ-1PP1	-5.854/-4.457	-8.69/-3.28	426.06 nM/ 3.93 mM	-9.0/-6.1
12	Tubulin/*MetAP-2* Receptor	VJ-1PP2	-5.342/-3.987	-6.45/-4.08	5.1 µM/ 3.6 mM	-7.2/-5.1
13	Tubulin/*MetAP-2* Receptor	VJ-2PP1	-5.247/-2.748	-8.33/-1.42	785.11 nM/ 91.4 mM	-9.8/-6.0
14	Tubulin/*MetAP-2* Receptor	VJ-2PP2	-5.345/-2.321	-7.00/-3.68	4.0 µM/ 2.1 mM	-7.1/-5.6
15	Tubulin/*MetAP-2* Receptor	VJ-3PP1	-5.988/-4.049	-5.6/-1.71	78.52 µM/ 55.69 mM	-8.7-6.2
16	Tubulin/*MetAP-2* Receptor	VJ-3PP2	-5.971/-2.320	-5.45/-4.68	10.2 µM/ 8.6 mM	-6.2/-5.7
17	Tubulin/*MetAP-2* Receptor	VJ-4PP1	-5.174/-1.753	-8.58/-1.97	511.85 nM/ 35.96 mM	-9.5/-6.0
18	Tubulin/*MetAP-2* Receptor	VJ-4PP2	-5.300/-2.548	-6.45/-4.22	4.8 µM/ 2.9 mM	-7.1/-5.3
19	Tubulin/*MetAP-2* Receptor	VJ-6PP2	-5.265/-1.694	-7.96/-4.53	3.0 µM/ 2.3 mM	-7.9/-5.9

Some of the best docking poses for compounds which are synthesized are given below:

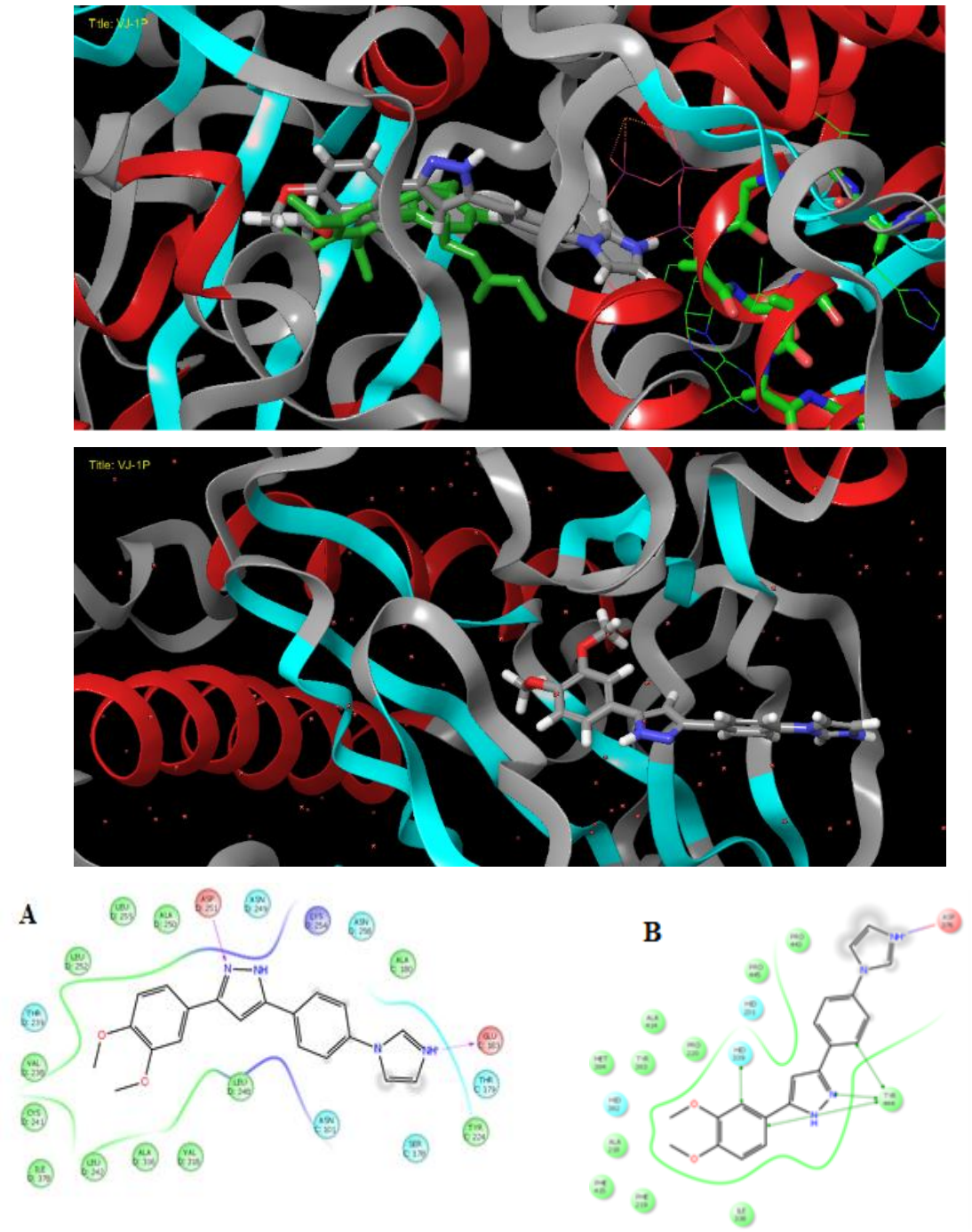

Figure 4.4: Ligand interaction diagram of VJ-1P with the colchicine binding site of tubulin receptor showing additional H-bond interaction with AspD251 and GluC183 (PDB Id- 1SA0) (A) & with MetAP-2 receptor showing pi-pi stacking of Tyr444 with aromatic as well as heterocyclic rings and dimethoxy benzene ring show one moe pi-pi stacking with His339 which is hydrophobic interaction in nature (PDB Id- 2ADU)

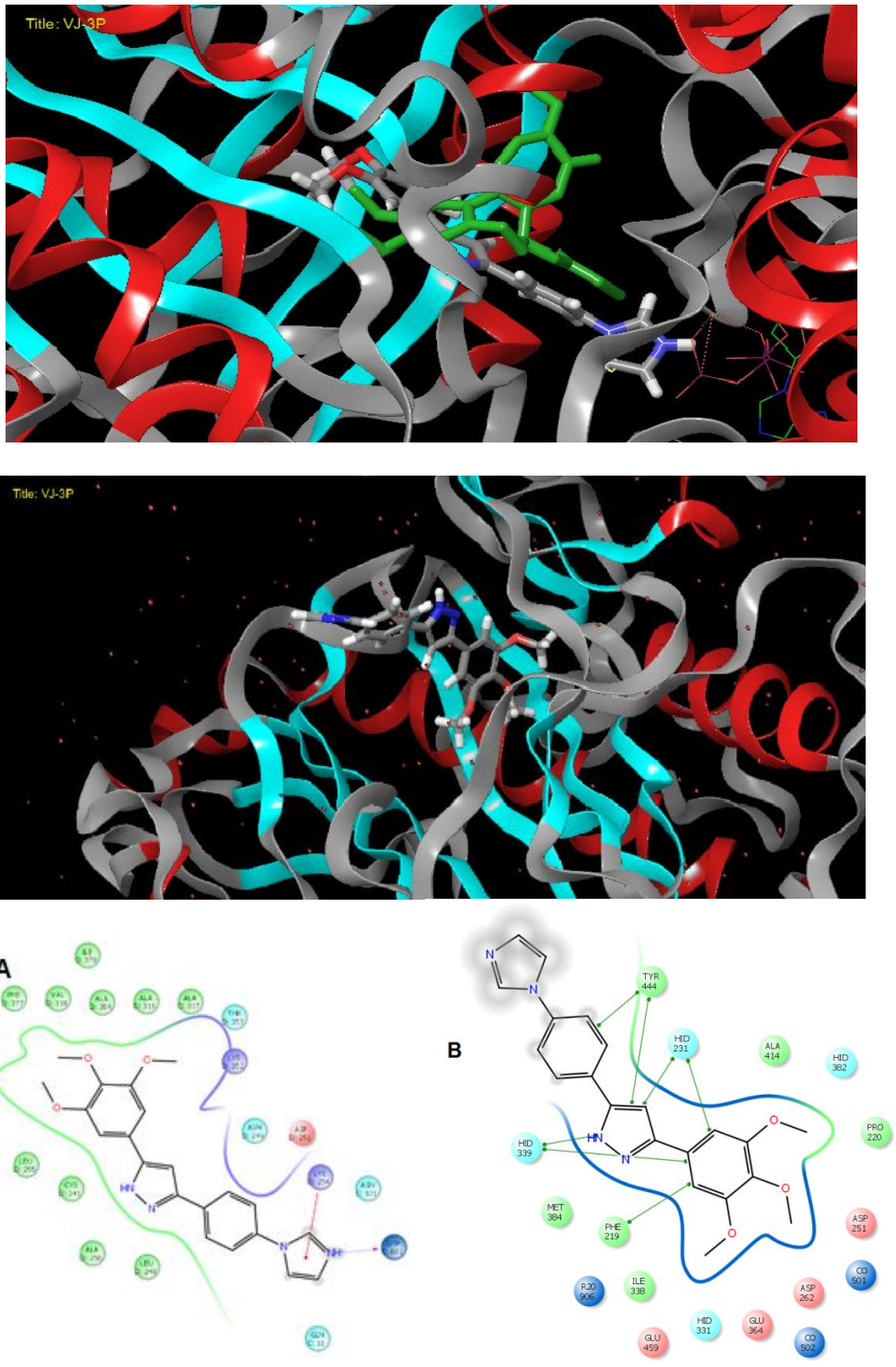

Figure 4.5: Ligand interaction diagram of VJ-3P with the colchicine binding site of tubulin receptor showing H-bonding with GTP present in C-chain of tubulin (PDB Id- 1SA0) (A) & with MetAP-2 receptor showing very strong pi-pi interaction with His339, His231, Tyr444 & Phe219 which is very strong hydrophobic interaction (PDB Id- 2ADU)

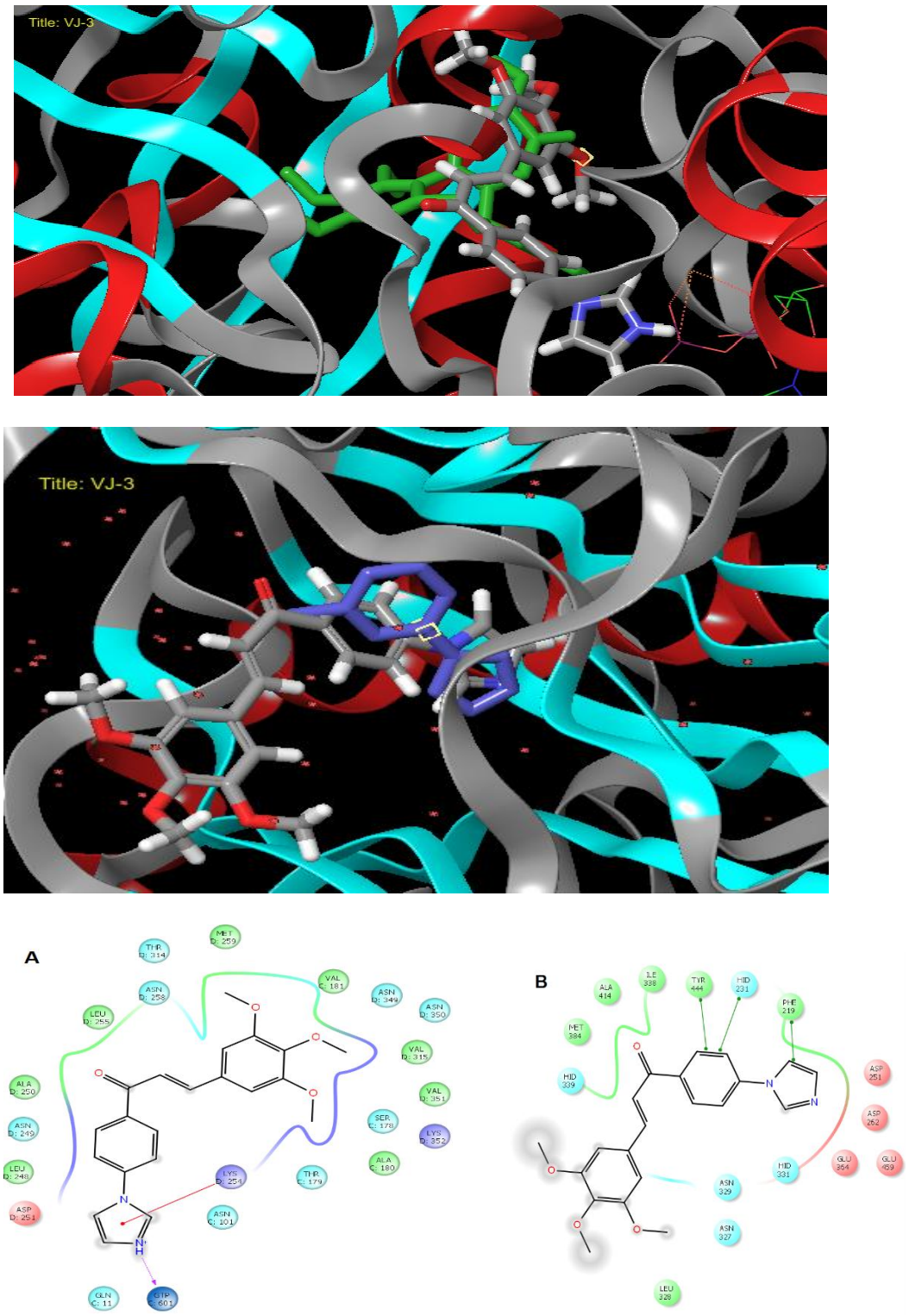

Figure 4.6: Ligand interaction diagram of VJ-3 with the colchicine binding site of tubulin receptor showing the ligand explore the cavity (PDB Id- 1SA0) (A) & with MetAP-2 receptor showing pi-pi stacking with three main amino acids i.e. Hid231, Tyr444 & Phe219 (PDB Id- 2ADU)

From all these docking studies, it is concluded that the molecule, which are proposed explore the same binding sites where colchicine and 3-methylaryl triazole explore in tubulin and MetAP-2 receptor respectively. The important amino acid that allow the hydrophobic pharmacophores to interact in tubulin are CysD241, LeuD255, LeuD252 whereas additional interaction is observed in C-chain (α-chain) of tubulin is GluC183 with imidazole moiety attached with B-ring at para-position, whereas the pyrazoline bridge connecting two rings showing H-bond interaction with AspD251 which reveals that it explore extra binding sites which are being untouched by colchicine. The important amino acid involve in flipping of T7 loop which is AsnD249 is also present near the ligand and making a pocket to allow the ligand which I have synthesized but the flipping is only confirmed via dynamic docking studies.

In case of MetAP-2 receptor the ligand binding area is very small, so only those molecules can easily explore the receptor cavity which is flexible enough to reach there and this was observed when I docked one of my final compound that contain four different types of aryl azole moieties. The structure was very rigid, which cannot explore the cavity, but on the other hand compound having chalcone structure show good binding interaction with all the amino acids which are involved in standard drug like Tyr444, Hid231, Phe219.

A molecule with a side with flexible aryl azole moiety is must need for MetAP-2 receptor, but on the other hand a rigid structure connecting two rings of chalcone is to maintain the configuration of the structure.

CHAPTER 5

SYNTHESIS

OF

COMPOUNDS

5.1 General

1. All the reagents were of AR/GR quality and was purchased from Sigma-Aldrich, Loba-Chemie Pt. Ltd., S.D. Fine Chemicals, Spectrochem, Sisco Research Laboratory and Avra Synthesis Ltd. and was used without further purification.
2. Sartorius analytical balance (BSA224S-CW) was used for the weighing purposes. JSGW heating mantle, Tarson spinot digital, ILMVAC RO dist digital rota vapour, digital hop top and NSW oven/vacuum oven were used during the course of the reaction.
3. The progress of the reaction was monitored by TLC, using Petroleum ether/ethyl acetate and chloroform or DCM/methanol as the mobile phase on pre-coated Merck TLC plates & glass plates made of F_{254} UV grade silica in JSGW UV/fluorescent analysis cabinet and/or iodine chamber.
4. Melting points were recorded on the Stuart melting point apparatus (SMP-30) with open glass capillary tubed and was uncorrected.
5. Infrared (IR) spectra of compounds were recorded with KBr on a Bruker FT-IR spectrophotometer.
6. ^{1}H and ^{13}C Nuclear magnetic resonance (NMR) spectra was obtained in $CDCl_3$/d_6-DMSO on a Bruker Avance II (400 MHz) NMR spectrometer using TMS ($\delta = 0$) as internal standard.
7. Mass spectra were recorded in GC-MS (ESI), Central University of Punjab, Bathinda.

5.2 Synthesis of target molecules

5.2.1 Synthetic scheme

The reaction is performed by using two schemes: scheme 5.1 & scheme 5.2

Formation of chalcone intermediate by reacting aryl aldehyde and aryl ketone, then C-N bond formation reaction of chalcone and finally heterocyclic ring formation reaction at α, β-unsaturated ketone site (Scheme 5.1).

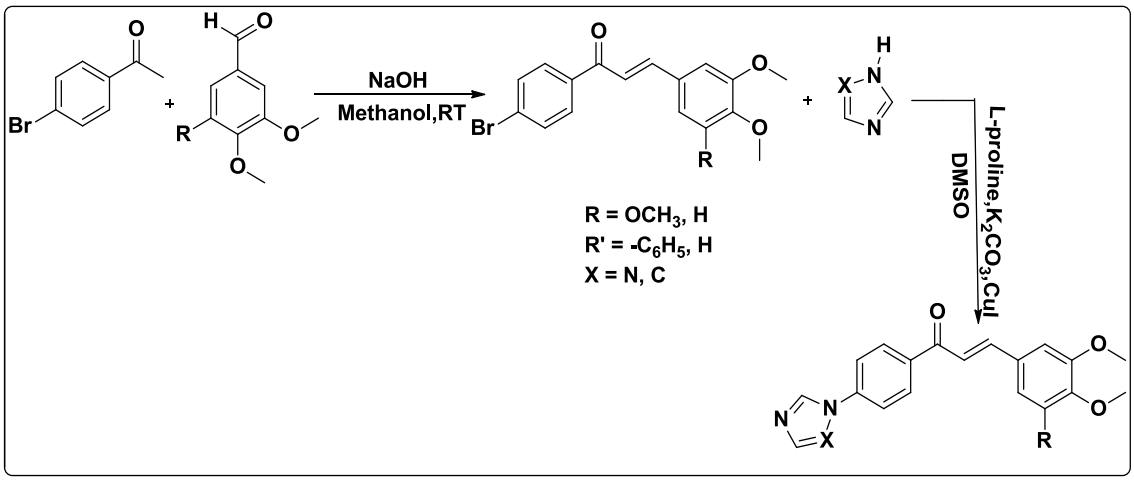

Scheme 5.1: Route for the synthesis of target compounds

5.2.2 Synthesis of proposed compound using scheme 5.1

Formation of chalcone via claisen-Schmidt condensation is a well-known method. The reaction for the synthesis of chalcone was tried via three possible ways. 1st with potassium hydroxide in the presence of methanol as solvent wherein equimolar mixture of benzaldehyde and acetophenone is reacted with two equivalent base (KOH). The reaction was kept for stirring at room temperature for overnight but did not complete as analyzed by TLC. Thereafter reaction was performed in the presence of excess of base (NaOH) which result in the completion of reaction (Nepali et al., 2011). This reaction can also be performed in acidic condition by using sulfuric acid as catalyst. The product is precipitated and recrystallized in methanol and confirmed by GCMS. (Scheme 5.1.1)

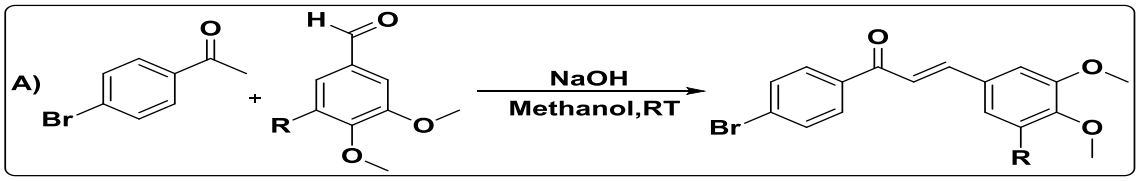

Scheme 5.1.1: Synthesis of chalcone intermediate.

After obtaining chalcone (dimethoxy and trimehoxy chalcone) intermediate, C-N bond forming reaction is performed with heterocyclic ring system (imidazole and 1, 2, 4-triazole). Reaction is performed in the presence of L-proline, potassium carbonate, copper iodide in DMSO and in N, N-dimethylformamide (DMF) (Moustafa & Ahmad, 2003, Chen et al., 2014).

Various reaction conditions were tried in order to optimize the product yield. For example the reaction was performed with (1H)-1, 2, 4-triazole and (1H)-1, 3-imidazole and palladium acetate as catalyst was tried in DMF as a solvent. Reaction were also performed by using CuI as catalyst however a number of spots were observed on TLC and none of the reaction was found clean (Bellina et al., 2007).

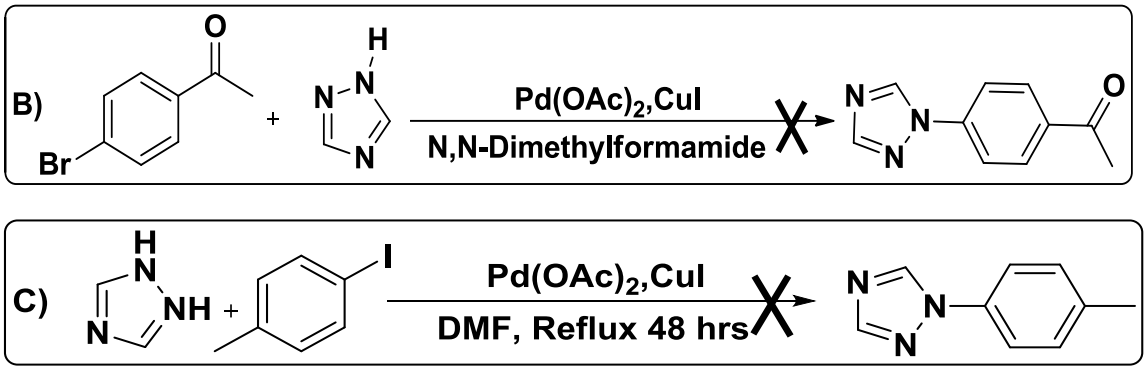

Thereafter another reactions were tried by reacting the chalcone ((E)-1-(4-bromophenyl)-3-(3,4,5-trimethoxyphenyl)prop-2-en-1-one) (Scheme 5.1.2) and ((E)-1-(4-bromophenyl)-3-(3,4-dimethoxyphenyl)prop-2-en-1-one) (Scheme 5.1.3) with heterocyclic compounds (with triazole and imidazole respectively) in the presence of L-proline, cesium carbonate, copper iodide in DMSO and DMF but the product yield was very low.

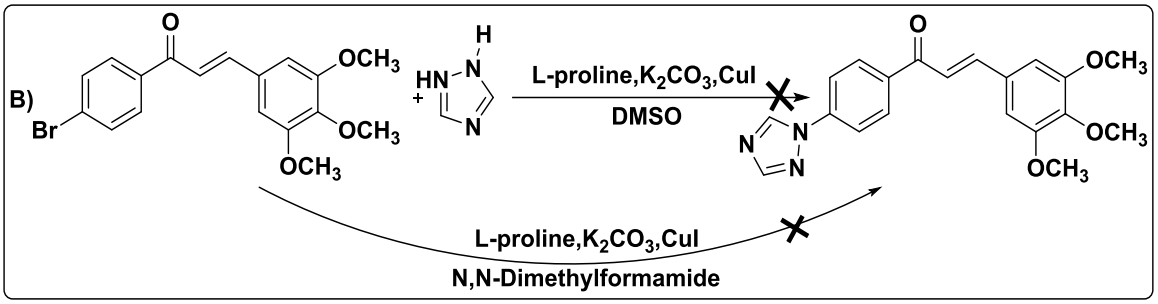

Scheme 5.1.2: C-N bond formation with triazole.

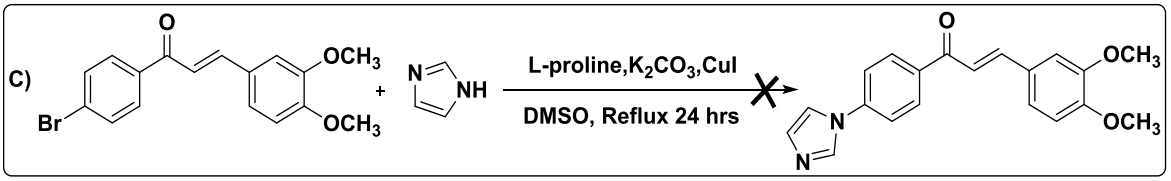

Scheme 5.1.3: C-N bond formation reaction of bromo substituted chalcone with imidazole.

After failure of first scheme 5.1, it was planned to explore the second route for the synthesis of target molecule. To optimize the reaction conditions for the synthesis of proposed compound, scheme 5.2 was introduced.

It was decided to first perform C-N coupling of acetophenone with imidazole/triazole and then do the chalcone formation reaction.

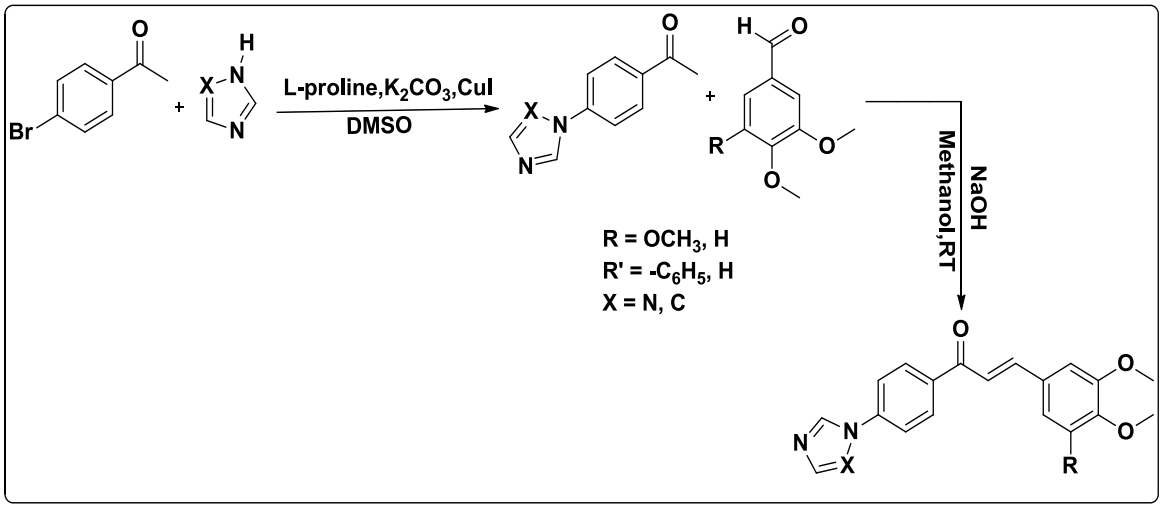

Scheme 5.2: Route for the synthesis of compounds

5.2.3 Synthesis of pyrazole ring

Synthesis of pyrazole ring was performed using imidazole or triazole substituted chalcones and hydrazine hydrate in sonicator with methanol as a solvent at 60^{o}C. The reaction mixture was work up which provided mixture of pyrazole and pyrazoline derivatives of chalcones. The impure mixture was purified by column chromatography and two products were isolated where in pyrazoline derivative was obtained as major while pyrazole was obtained in low in yield. The synthesized and isolated compounds were confirmed by GCMS and NMR.

Compound i.e 1-(4-(5-(3,4-dimethoxyphenyl)-1-phenyl-1H-pyrazol-3-yl)phenyl)-1H-1,2,4-triazole is synthesized by reacting (E)-1-(4-(1H-1,2,4-triazol-1-yl)phenyl)-3-(3,4-dimethoxyphenyl)prop-2-en-1-one with phenylhydrazine in methanol as a solvent in a sonicator at 60^{o}C. Formation of two product in which the major is pyrazoline derivative and the other product which is pyrazole is very low in yield (Scheme 5.2.1).

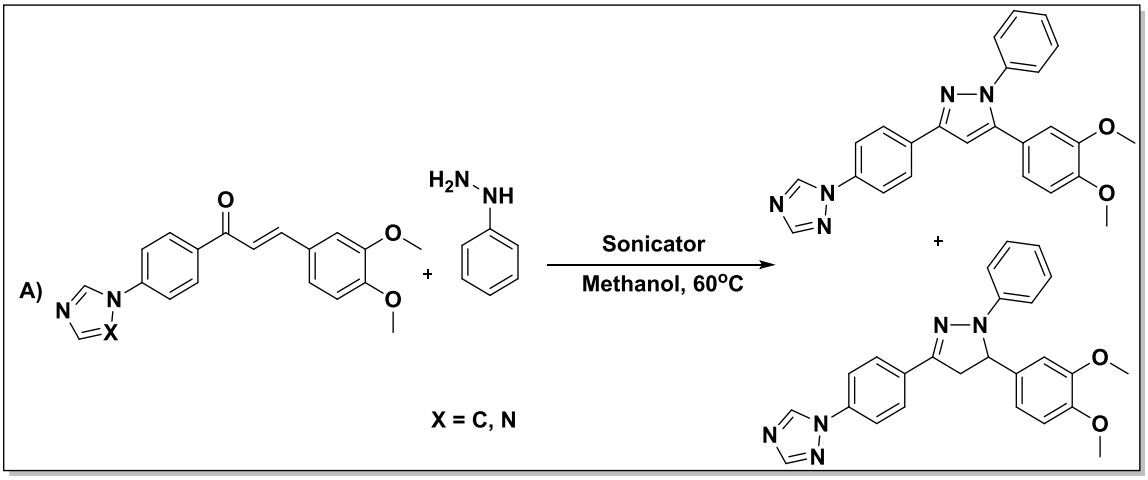

Scheme 5.2.1: Synthesis of pyrazole derivative from phenyl hydrazine

The reaction was also tried with imidazole & triazole substituted trimethoxy chalcone but there is formation of one product with good yield (pyrazoline) compared to other (pyrole). (Scheme 5.2.2)

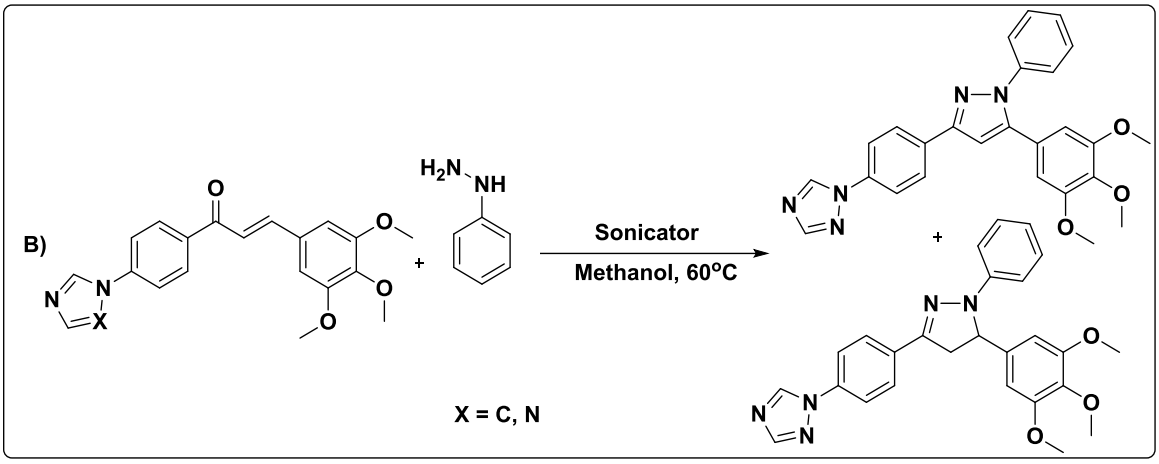

Scheme 5.2.2: Synthesis of pyrazole derivative from phenyl hydrazine.

5.2.4 Synthesis of pyrazole/pyrazoline from hydrazine hydrate

Reaction of 1, 2, 4-triazole substituted tri-methoxy and di-methoxy chalcone was performed (Scheme 5.2.3) in the presence of hydrazine hydrate under sonication for 1-2 hours at 60°C temperature in methanol as a solvent (Johnson et al., 2007). Reaction was monitored via TLC. Multi-spot was observed after which the reaction was workout and finally analyzed by GC-MS which clarify that the product was not formed.

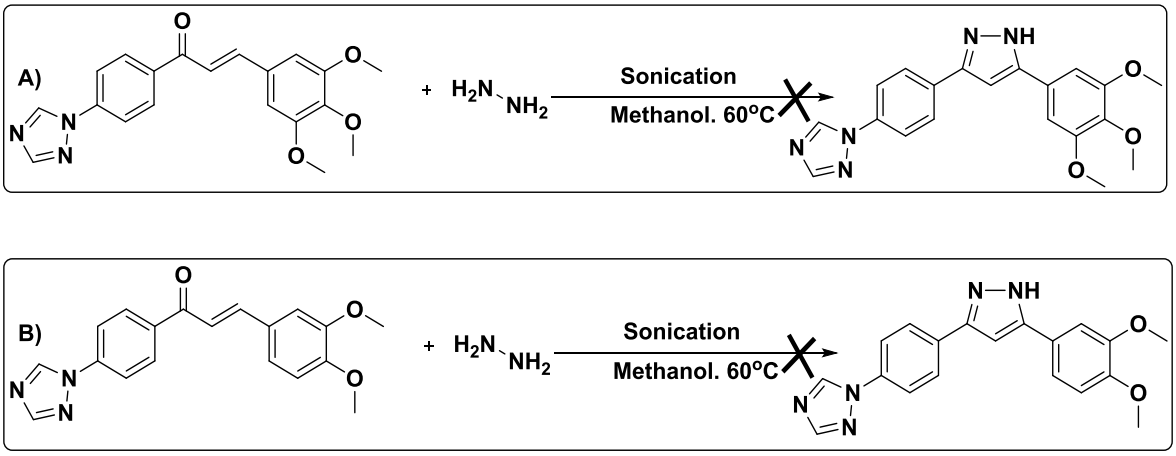

Scheme 5.2.3: Synthesis of pyrazole derivative from hydrazine hydrate.

5.3 General procedure for synthesis of proposed compound

5.3.1 Synthesis of VJ-3

Synthesis of compound **VJ-3** was carried out by taking mixture of imidazole (1g), p-bromo acetophenone (1.05 eq.), copper iodide (0.1 eq.), potassium carbonate (2 eq.), L-proline (0.2 eq.) in 100 ml RBF containing 5-7 ml DMSO. The reaction is kept under reflux condition for 24 hours at 60^{o}C. After completion of reaction monitored by TLC, add 2-5 ml of saturated solution of ammonium chloride under stirring condition for half hour. Then extract the reaction mixture with ethyl acetate (2-3 times), then with brine solution and finally pass through sodium sulphate. Dry the under low pressure to get brown solid which further washed with diethyl ether to obtain pure product (p-imidazo acetophenone). To this intermediate compound add trimethoxy or dimethoxy benzaldehyde (1 eq.) in presence of methanol under stirred condition at room temperature for half hour. Add drop wise solution of 10% sodium hydroxide (2 eq.) to the reaction mixture and allow it for 1 hour. TLC was checked in 20 % ethyl acetate:petroleum ether and 2% methanol: dichloromethane. Precipitates are formed which is washed with excess of methanol, then with water and finally dried and recrystallize in methanol to obtain pure product.

(*E*)-1-(4-(*1H*-imidazol-1-yl)phenyl)-3-(3,4,5-trimethoxyphenyl)prop-2-en-1-one (VJ-3)

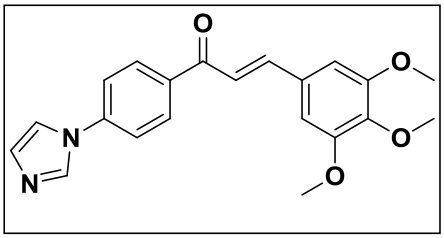

Figure 5.1: Structure of (E)-1-(4-(1H-imidazol-1-yl)phenyl)-3-(3,4,5-trimethoxyphenyl)prop-2-en-1-one

Spectral data: ^{1}H NMR (400MHz, $CDCl_3$, TMS = 0) δ = 3.74 (3H, s), 3.85 (6H, s), 7.06 (2H, s), 7.65-7.72 (2H, m), 7.99 (3H, d. J = 8 Hz), 8.11 (1H, s), 8.23 (2H, d, J = 12 Hz), 9.28 (1H, d, J = 2.4Hz).

^{13}C NMR (100 MHz, $CDCl_3$, TMS = 0) δ = 55.78, 59.99, 105.98, 118.71, 120.60, 129.95, 136.39, 139.55, 139.69, 142.19, 144.63, 152.27, 152.85, 187.60.

5.3.2 Synthesis of VJ-2 & VJ-4

Synthesis of compound **VJ-2** & **VJ-4** was carried out by taking mixture of 1, 2, 4-triazole (1g), p-bromo acetophenone (1.05 eq.), copper iodide (0.1 eq.), potassium carbonate (2 eq.), L-proline (0.2 eq.) in 100 ml RBF containing 5-7 ml DMSO. The reaction is kept under reflux condition for 24 hours at 60^{o}C. After completion of reaction monitored by TLC, add 2-5 ml of saturated solution of ammonium chloride under stirring condition for half hour. Then extract the reaction mixture with ethyl acetate (2-3 times), then with brine solution and finally pass through sodium sulphate. Dry the under low pressure to get brown solid which further washed with diethyl ether to obtain mixture of product in organic layer (p-1, 2, 4-triazo acetophenone). The organic layer is further dried and purified through column chromatography to obtain pure product. To this intermediate compound add trimethoxy or dimethoxy benzaldehyde (1 eq.) in presence of methanol under stirred condition at room temperature for half hour. Add dropwise solution of 10% sodium hydroxide (2 eq.) to the reaction mixture and allow it for 1 hour. TLC was checked in 20 % ethyl acetate:petroleum ether and 2% methanol: dichloromethane. Precipitates are formed which is washed with excess of methanol, then with water and finally dried and recrystallize in methanol to obtain pure product.

_(E)_-1-(4-(_1H_-1,2,4-triazol-1-yl)phenyl)-3-(3,4-dimethoxyphenyl)prop-2-en-1-one (VJ-2)

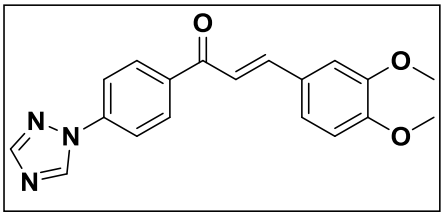

Figure 5.2: Structure of (E)-1-(4-(1H-1,2,4-triazol-1-yl)phenyl)-3-(3,4-dimethoxyphenyl)prop-2-en-1-one

Spectral data: ^{1}H NMR (400MHz, $CDCl_3$, TMS = 0) δ = 3.96 (3H, s), 3.99 (3H, s), 6.90 (1H, d, J = 8 Hz), 7.15 (1H, s), 7.26-7.30 (1H, m), 7.37 (1H, d, J = 16.6 Hz), 7.79 (1H, d, J = 16.6), 7.84 (2H, d, J = 8Hz), 8.15 (1H, s), 8.16 (2H, d, J = 8 Hz), 8.67 (1H, s).

^{13}C NMR (100 MHz, $CDCl_3$, TMS = 0) δ = 56.17, 110.24, 111.26, 119.43, 119.65, 123.58, 127.71, 130.41, 130.83, 137.97, 139.85, 141.84, 146.03, 149.42, 153.17, 189.17

***(E)*-1-(4-(*1H*-1,2,4-triazol-1-yl)phenyl)-3-(3,4,5-trimethoxyphenyl)prop-2-en-1-one (VJ-4)**

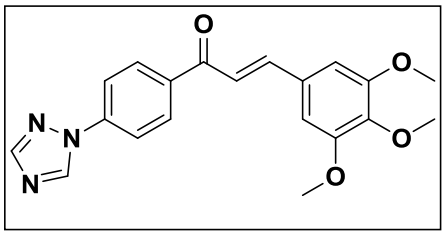

Figure 5.3: Structure of (E)-1-(4-(1H-1,2,4-triazol-1-yl)phenyl)-3-(3,4,5-trimethoxyphenyl)prop-2-en-1-one

Spectral data: ^{1}H NMR (400MHz, $CDCl_3$, TMS = 0) δ = 3.90 (3H, s), 3.92 (6H, s), 6.87 (2H, s), 7.37 (1H, s), 7.42 (1H, s), 7.53 (2H, d, J = 8 Hz), 7.78 (1H, s), 7.97 (1H, s), 8.14 (2H, d, J = 8 Hz).

^{13}C NMR (100 MHz, $CDCl_3$, TMS = 0) δ = 56.36, 61.80, 76.84, 77.16, 77.48, 105.83, 107.28, 117.90, 120.80, 120.94, 130.21, 130.62, 131.01, 131.24, 135.53, 137.06, 140.57, 140.75, 145.87, 188.97

5.3.3 Synthesis of VJ-2PP2

Synthesis of compound **VJ-2PP2** was carried out by taking mixture of **VJ-2** (200 mg) and phenylhydrazine (1.2 eq.) in a 20 ml conical flask containing 3-5 ml of methanol and kept under sonication for 1-2 hours at 60^{o}C temperature. Allow the reaction mixture cool at room temperature and placed in refrigerator for 2 hour to get the precipitates from which remaining methanol is decanted and precipitates

are washed with methanol to obtain pure product **VJ-2PVJVP2**. TLC was checked in 20 % ethyl acetate:petroleum ether and 2% methanol:chloroform.

1-(4-(5-(3,4-dimethoxyphenyl)-1-phenyl-4,5-dihydro-*1H*-pyrazol-3-yl)phenyl)-*1H*-1,2,4-triazole (VJ-2PP2)

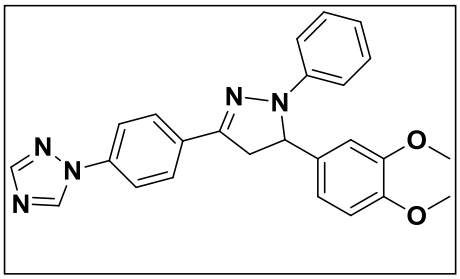

Figure 5.4: Structure of 1-(4-(5-(3,4-dimethoxyphenyl)-1-phenyl-4,5-dihydro-1H-pyrazol-3-yl)phenyl)-1H-1,2,4-triazole

Spectral data: ^{1}H NMR (400MHz, $CDCl_3$, TMS = 0) δ = 3.87 (3H, s), 3.89 (3H, s), 5.11 (2H, m), 6.75-6.78 (3H, m), 7.10 (2H, d, J = 8 Hz), 7.20-7.24 (2H, m), 7.62 (2H, d, J = 8 Hz), 7.95 (2H, d, J = 8 Hz), 8.03-8.09 (2H, m), 8.5 (1H, s).

^{13}C NMR (100 MHz, $CDCl_3$, TMS = 0) δ = 31.24, 55.52, 55.71, 60.23, 104.39, 110.95, 111.78, 120.04, 121.29, 122.58, 124.26, 125.32, 126.88, 127.52, 128.22, 128.22, 129.88, 133.18, 136.17, 139.92, 144.56, 148.55, 149.12, 150.25, 152.13

5.3.4 Synthesis of VJ-3PP2

Synthesis of compound **VJ-3PP2** was carried out by taking mixture of **VJ-3** (100 mg) and phenylhydrazine (1.2 eq.) in a 20 ml conical flask containing 3-5 ml of methanol and kept under sonication for 1-2 hours at 60^{o}C temperature. Allow the reaction mixture cool at room temperature and placed in refrigerator for 2 hour to get the precipitates from which remaining methanol is decanted and precipitates are washed with methanol to obtain pure product **VJ-3PP2**. TLC was checked in 20 % ethyl acetate:petroleum ether and 3% methanol:chloroform.

3-(4-(*1H*-imidazol-1-yl)phenyl)-1-phenyl-5-(3,4,5-trimethoxyphenyl)-4,5-dihydro-*1H*-pyrazole (VJ-3PP2)

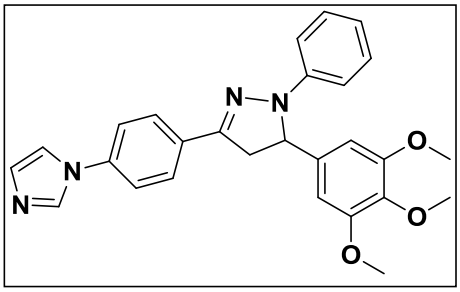

Figure 5.5: Structure of 3-(4-(1H-imidazol-1-yl)phenyl)-1-phenyl-5-(3,4,5-trimethoxyphenyl)-4,5-dihydro-1H-pyrazoline

Spectral data: ^{1}H NMR (400MHz, $CDCl_3$, TMS = 0) δ = 3.8 (3H, s), 3.83 (6H, s), 5.19-5.22 (3H, m), 6.54 (2H, s), 6.84-6.86 (1H, m), 7.11 (2H, d, J = 8 Hz), 7.11 (2H, d, J = 4 Hz), 7.40 (2H, d, J = 8 Hz), 7.81 (2H, d, J = 4 Hz), 7.92 (1H, s).

^{13}C NMR (100 MHz, $CDCl_3$, TMS = 0) δ = 43.70, 56.36, 60.97, 65.52, 102.71, 113.82, 119.94, 121.56, 125.71, 127.30, 129.12, 130.37, 132.34, 137.14, 137.56, 138.21, 145.05, 145.64, 154.10.

5.3.5 Synthesis of VJ-4PP1

Synthesis of compound **VJ-4PP1** was carried out by taking mixture of **VJ-4** (200 mg) and phenylhydrazine (1.2 eq.) in a 20 ml conical flask containing 3-5 ml of methanol and kept under sonication for 1-2 hours at 60^{o}C temperature. Allow the reaction mixture cool at room temperature and placed in refrigerator for 2 hour to get the precipitates from which remaining methanol is decanted and precipitates are washed with methanol to obtain precipitate which was not product. The decanted methanol is evaporated under rotavapour & then purified with column chromatography to obtain **VJ-4PP1.** TLC was checked in 20 % ethyl acetate:petroleum ether and 2% methanol:chloroform.

1-(4-(1-phenyl-5-(3,4,5-trimethoxyphenyl)-*1H*-pyrazol-3-yl)phenyl)-*1H*-1,2,4-triazole (VJ-4PP1)

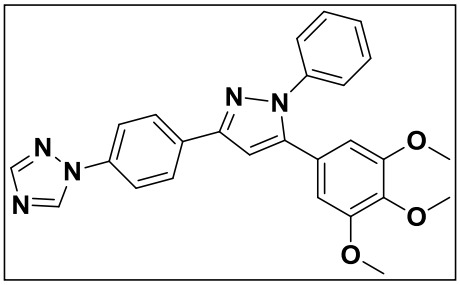

Figure 5.6: Structure of 1-(4-(1-phenyl-5-(3,4,5-trimethoxyphenyl)-1H-pyrazol-3-yl)phenyl)-1H-1,2,4-triazole

Spectral data: ^{1}H NMR (400MHz, $CDCl_3$, TMS = 0) δ = 3.84 (3H, s), 3.86 (6H, s), 6.39 (1H, s), 6.47 (1H, s), 6.79-6.81 (1H, m), 7.33-7.35 (2H, m), 7.77-7.79 (2H, m), 7.79 (1H, s), 8.09 (4H, d, J = 8 Hz), 8.55 (1H, s), 8.62 (1H, s).

^{13}C NMR (100 MHz, $CDCl_3$, TMS = 0) δ = 56.09, 56.38, 61.12, 104.78, 105.87, 106.05, 119.70, 120.36, 120.83, 125.71, 127.18, 128.02, 129.19, 130.19, 130.49, 146.06, 152.30, 153.03, 153.24, 153.64, 190.0

5.4 Structure of compounds with m/z data

Table 5.1: A Lucid summary of the compound synthesized along with their codes, chemical structure, molecular weight & the % yield obtained.

S.No	Code	Name with structure	m/z	%Yield
1	VJ-2	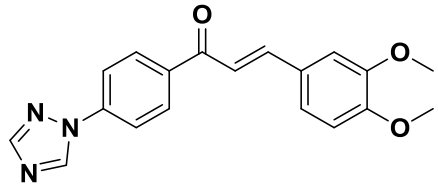 **(*E*)-1-(4-(1*H*-1,2,4-triazol-1-yl)phenyl)-3-(3,4-dimethoxyphenyl)prop-2-en-1-one**	335	95%
2	VJ-3	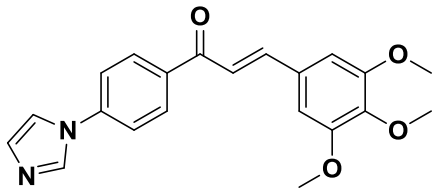 **(*E*)-1-(4-(1*H*-imidazol-1-yl)phenyl)-3-(3,4,5-trimethoxyphenyl)prop-2-en-1-one**	364	94%
3	VJ-4	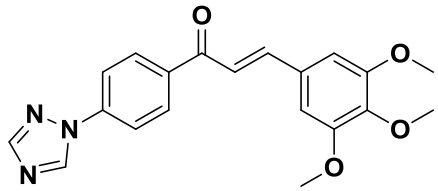 **(*E*)-1-(4-(1*H*-1,2,4-triazol-1-yl)phenyl)-3-(3,4,5-trimethoxyphenyl)prop-2-en-1-one**	365	96%
4	VJ-2PP2	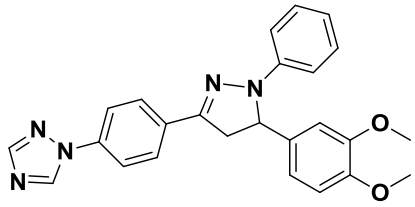 **1-(4-(5-(3,4-dimethoxyphenyl)-1-phenyl-4,5-dihydro-1*H*-pyrazol-3-yl)phenyl)-1*H*-1,2,4-triazole**	425	41%

5	VJ-3PP2	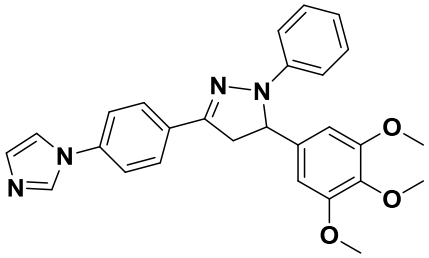 **3-(4-(1*H*-imidazol-1-yl)phenyl)-1-phenyl-5-(3,4,5-trimethoxyphenyl)-4,5-dihydro-1*H*-pyrazole**	454	65%
6	VJ-4PP1	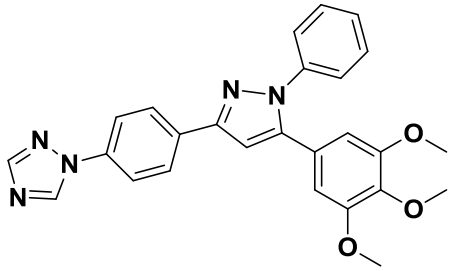 **1-(4-(1-phenyl-5-(3,4,5-trimethoxyphenyl)-1*H*-pyrazol-3-yl)phenyl)-1*H*-1,2,4-triazole**	453	10%

5.4 Synthesis of isoxazole derivative

Apart from above listed compounds the reaction was also performed for the formation of isoxazole ring (Moustafa & Ahmad, 2003) and 1, 2, 3-triazole derivatives. But they were unsuccessful due to difficulties in purification and low % yield. Following reaction conditions were explored for the formation of isoxazole:

1) Reaction with hydroxylamine HCl in ethanol as a solvent in reflux condition for 18-20 Hrs.

2) Reaction with hydroxylamine HCl & sodium acetate in methanol as a solvent in reflux condition for 8-12 Hrs.

3) Reaction with hydroxylamine HCl & water in pyridine as a solvent in reflux condition for 8 Hrs.

Among these the 2nd and 3rd method goes successfully, but due to ill effects of pyridine I switch to the 2nd method but the problem was its purification is very difficult as no. of products are formed. Also the % yield of product is very less.

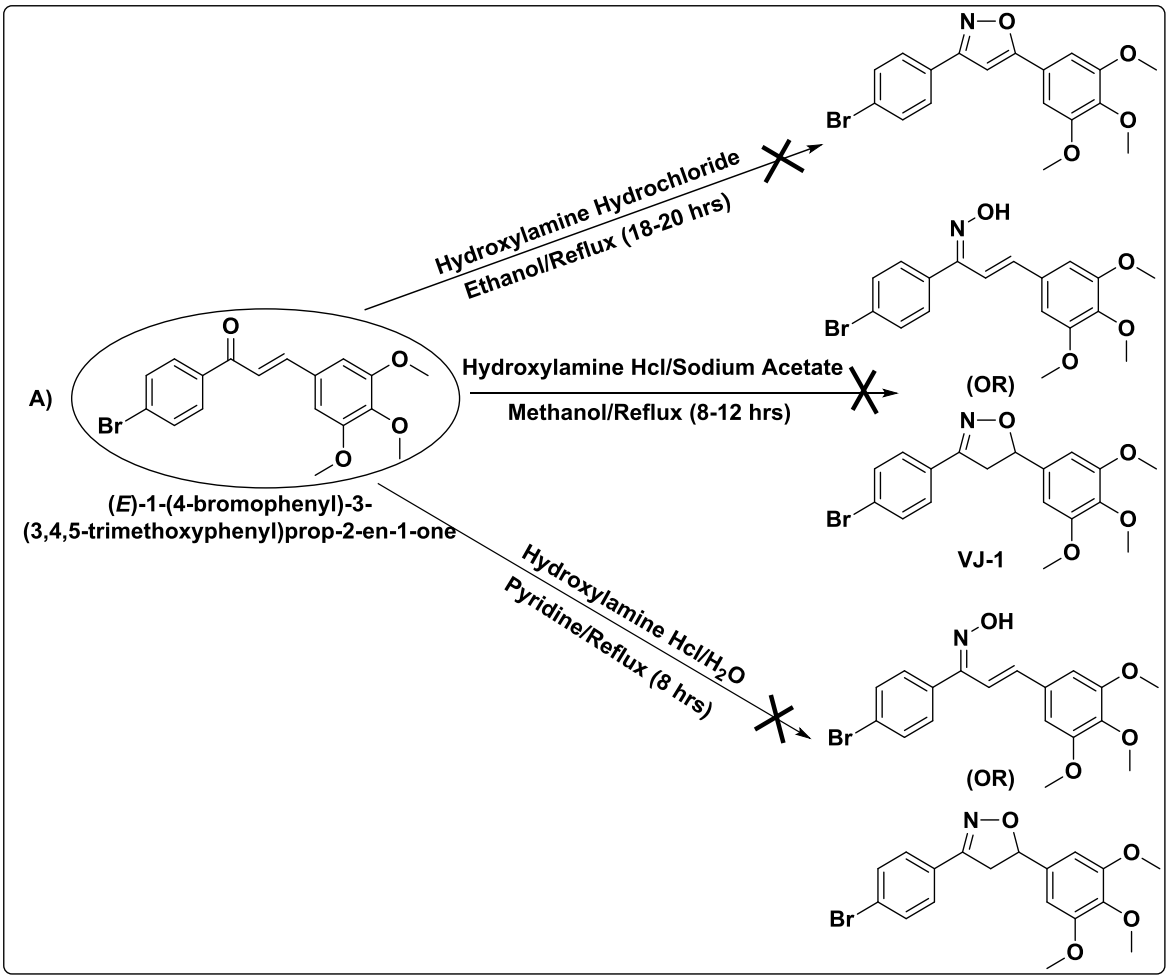

Figure 5.7: *Synthesis of isoxazole from bromo substituted chalcone.*

The reaction was also tried with imidazole derivative of chalcone with hydroxylamine hydrochloride and sodium acetate in ethanol at reflux condition for 10-12 hours but the reaction was unsuccessful as confirmed by GC-MS.

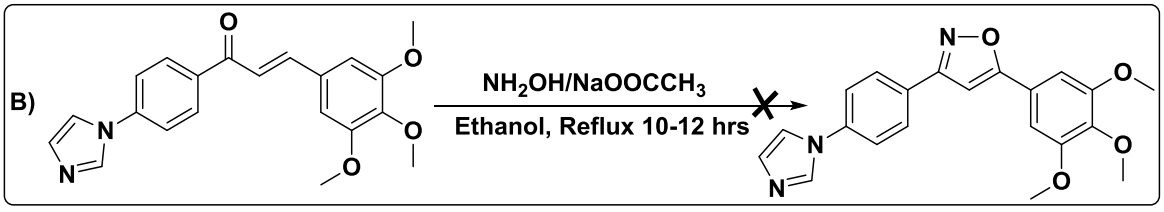

Figure 5.8: *Synthesis of isoxazole from imidazole substituted chalcone.*

5.5 Synthesis of 1, 2, 3-triazole derivatives

Azidation of p-bromoacetophenone with sodium azide is performed by reacting p-bromo acetophenone with sodium azide, L-proline, potassium carbonate, copper iodide in DMSO as a solvent (Chen et al., 2014). The reaction is performed under reflux condition for 24 Hrs at 80-90^{o}C temperature. Further addition of phenylacetylene was done and the reaction mixture was heated at same temperature for 48-72 Hrs. Reaction was monitored continuously via TLC and there is unreacted product left after 72 hours. The product after work up analysed by GC-MS which showed that the desired product was not formed.

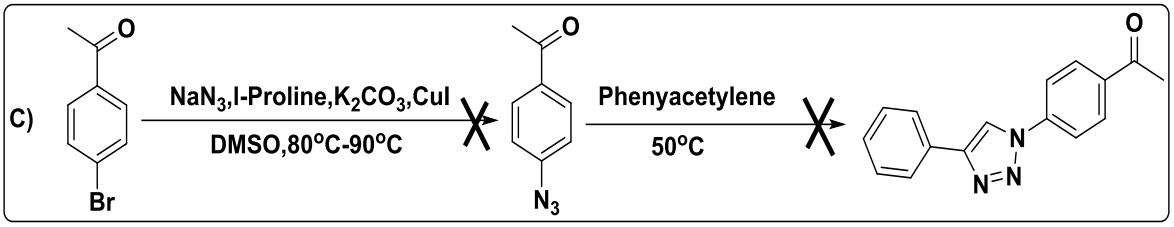

Figure 5.9: *Synthesis of 1, 2, 3-triazole derivative from p-bromo acetophenone.*

Reaction was also performed by with chalcone in place of p-bromo acetophenone and triethylamine was used as base in place potassium carbonate. However no product could be traced in GCMS analysis.

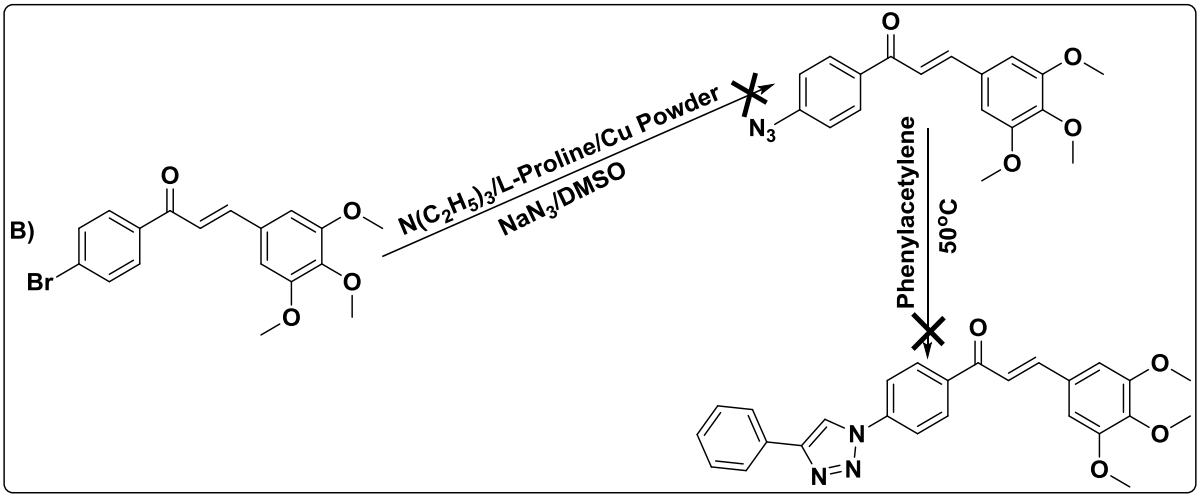

Figure 5.10: *Synthesis of 1, 2, 3-triazole derivative from bromo substituted chalcone.*

CHAPTER 6

BIOLOGICAL STUDIES

Biological studies

6.1 Chemicals

1. Cancer cell lines was cultured with media - RPMI 1640 and DMEM, Penicillin/ Streptomycin antibiotic solution, phosphate buffer saline and fetal bovine serum were purchased from HiMedia.
2. MTT dye used for MTT assay was purchased from HiMedia.
3. DMSO, extra pure AR was purchased from SRL.

6.2 Instruments

All experiments involving cell culture was carried out in aseptic conditions under laminar air flow. Cells were counted on automated cell counter and incubated in the incubator at 37˚C. Finally centrifugation was done and inverted microscope is used for observing the cancer cells. The absorption is measured by spectrophotometer.

Table 6.1: List of Instruments Used in Biological Evaluation.

S.No.	Instruments	Purpose	Company
1	Automatic cell Counter	For counting of cells	Invitrogen
2	Incubator	Incubation	Galaxy
3	Centrifuge 5430 R	Centrifugation	Eppendorf
4	Inverted microscope	Visualization of the cancer cells	Magnus, Olympus
5	Laminar air flow	For aseptic condition	Macro Scientific Works
6	UV-VIS Spectrophotometer	Absorption studies	Shimadzu

6.3 Cell lines under study

Colon cancer cell lines HCT-116 (p53 null and wild type) were used for evaluation of anti-proliferative assay.

HCT-116 – It is morphologically epithelial and has adherent properties. It is obtained from colon tissue of Homo sapiens, human in the disease condition of colorectal carcinoma. This cell line is a suitable transfection host. This line has a mutation in codon 13 of the Ras proto-oncogene, and can be used as a positive control for PCR assays of mutation in this codon **(ATCC®).**

6.4 Routine assay in cell culture laboratory

6.4.1 Culturing of the cell lines

DMEM is used as medium for culturing of the cancer cell lines. As cancer cells are adherent cells, trypsin was added to detach them from the surface (trypsinization). Cells were harvested in 5ml media containing serum which also inactivates trypsin enzyme. Harvested cells were centrifuged at 1200 rpm at 4˚C for 5 minutes and supernatant was removed and pellet was re-suspended in media (2 mL). The cell number was counted using automated cell counter. The cells were transferred to fresh media every three days.

6.4.2 Maintenance and sub-culturing of cell lines

The maintenance and culturing of cancer cell lines was done in 25 cm^2 or 75 cm^2 flasks containing DMEM medium supplemented with 10% fetal bovine serum (FBS), 1X antibiotic solution and then incubated at 37˚C in a humidified atmosphere containing 5% CO_2.

Further sub-culturing of cells was done in 25 cm^2 flasks up to when the cancer cell lines have attained 70-80% growth. The reagents essential for the procedure were placed in water bath maintained at 37˚C for 10-15 minutes and trypsin was added for the detachment of adherent cells. 1 ml of media containing serum was added after 5 minutes, for stopping the action of trypsin. Then, cells were then

transferred to 15 mL centrifuge tubes and centrifuged for 5 mins at 1200 rpm at 4^{o}C. The supernatant was removed and the cell pellet was again resuspended in complete media. The cell lines were transferred to fresh media every three days (cell passaging).

6.5 Evaluation of antiproliferative activity of the synthesized compounds (MTT Assay)

MTT is a colorimetric assay for the measurement of cell proliferation (Mosmann, 1983; Sumantran, 2011). It was specified by Mosmann and is also known as cell viability assay. The tetrazolium yellow compound MTT (3-[4,5-dimethylthiazol-2-yl]-2,5-diphenyl tetrazolium bromide) is reduced to an insoluble purple colored formazan product by mitochondrial reductase or succinate dehydrogenase in metabolically active cells only. When formazan passes to the mitochondria it gets solubilized with DMSO and measured spectrophotometrically.

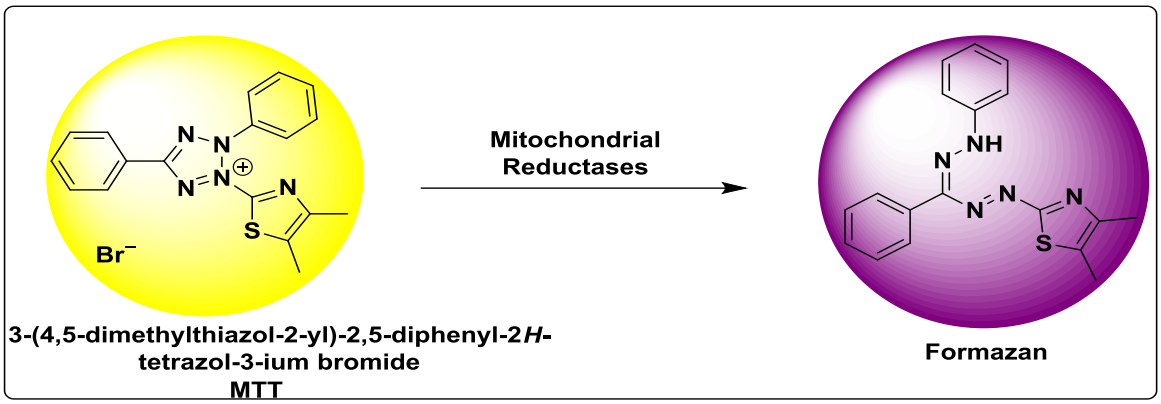

Figure 6.1: Reduction of MTT

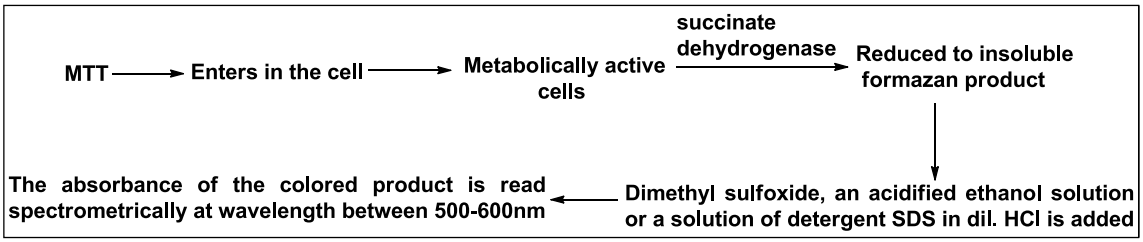

Figure 6.2: Rudimentary Principle of MTT Assay.

Material: MTT (3-[4,5-dimethylthiazol-2-yl]-2,5-diphenyl tetrazolium bromide), Phosphate buffer solution, DMSO (Dimethylsulfoxide).

Procedure: The cell from the cancer cell line – HCT-116 (p53 null and wild type) cells were counted on the automated cell counter. Nearly 8,000-10,000 cells were seeded in each well of the 96 well plates. The plate was incubated at 37˚C with 5% CO_2 for 24 h followed by serum starvation for 8hrs for synchronization and replenishing with complete media. The treatment was given to the cells in triplicate concentrations of 5 µM and 25 µM and incubated for 48 h. MTT solution (5 mg/10mL) was added after removing the media from each well and incubated in the dark for 4 h. At the end of 4 h., the MTT solution was removed from each well and the intracellular precipitate was dissolved in DMSO solution and the absorbance of the violet color formed as consequence of DMSO addition is read spectrometrically at 570 nm which was expressed as % inhibition (Mean ± S.D).

CHAPTER 7

RESULT & DISCUSSION

7.1 Molecular docking studies

After analyzing the crystal structure of tubulin and MetAP-2 receptor the compound was designed and synthesized which were docked using different software to the respective receptor which show positive results compared with their standard drugs. It was studied that the compound which was synthesized explore the same site where the colchicine and 3-methylaryl triazole explore. The important hydrophilic interaction was with the insertion of imidazole/triazole moieties substituted at the para position of B-ring. A-ring is remain intact but methoxy group is important to place the molecule in hydrophobic pocket. The important amino acid that allow the hydrophobic pharmacophores to interact in tubulin are CysD241, LeuD255, LeuD252 whereas additional interaction is observed in C-chain (α-chain) of tubulin is GluC183 with imidazole moiety attached with B-ring at para-position, whereas the pyrazoline bridge connecting two rings showing H-bond interaction with AspD251 which reveals that it explore extra binding sites which are being untouched by colchicine. In MetAP-2 receptor the important residue that hold the compound at the receptor site was Tyr444, His231 and Phe219. These interaction was hydrophobic which fully overlap the 3-methylaryl triazole structure. A molecule with a side with flexible aryl azole moiety is must need for MetAP-2 receptor, but on the other hand a rigid structure connecting two rings of chalcone is to maintain the configuration of the structure.

7.2 Synthesis

Several synthetic routes for the efficient synthesis of C-N bond formation were explored in order to optimize the reaction conditions for the formation of products. The target molecules were synthesized through three step process. First step involve the C-N bond coupling in which CuI was used as catalyst, thereafter in step 2 chalcones were synthesized under basic conditions by reacting the intermediate obtained in step one with benzaldehyde and in step 3 pyrazole/pyrazoline derivatives were synthesized using sonicator. In the third step of the reaction mixture of pyrazole and pyrazoline was obtained and it was observed that pyrazoline was major product in most of the cases.

7.3 Anti-proliferative activity

In order to determine the anti-proliferative activity, the synthesized compounds (chalcones & pyrazole derivatives) were tested on colon carcinoma cell lines (HCT- 116 p53 wild type and null type). Briefly approximately 8,000-10,000 cells were seeded per well of 96 well plate and treatments with the compounds at 5, 25 and 50 µM concentration were given in triplicate for 48h followed by MTT assay and plotted for percentage cell survival. The values obtained were expressed as % inhibition (Mean ± S.D.) and graph was plotted. On the whole, the compounds displayed potent activity against both the cell lines as discussed below.

7.3.1 Anti-proliferative activity against HCT-116 (WILD TYPE): Among the tested compounds, compound VJ-4 showed more than 50% inhibition even at a low concentration of 5 µM. On the other hand, at higher dose of 25 µM, VJ-4 exhibited excellent activity which was comparable to VJ-3. VJ-2PP2, VJ-3PP2 and VJ-4PP1 showed good inhibitory potential, although, lesser than the former two. At 50 µM, all compounds displayed good activity with VJ-3PP2 portraying excellent potency around 60% whereas VJ-2, VJ-3, VJ-2PP2 AND VJ-4PP1 also showed commendable inhibitory potential between 55-60%. (Figure 7.1).

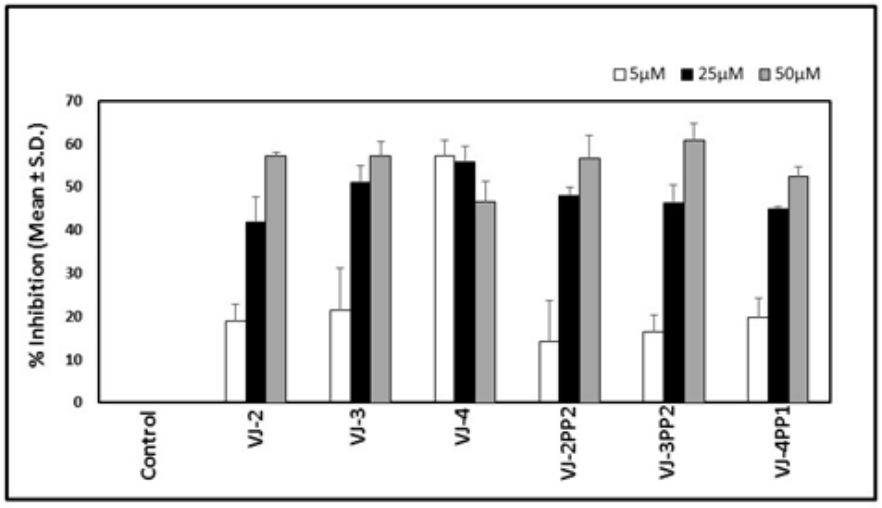

Figure 7.1: Percent inhibition of HCT-116 (WILD TYPE) in response to treatment with synthesized compounds at concentrations of 5 µM, 25 µM and 50 µM for time duration of 48 h. Data is expressed as mean values ± S.D. of three independent experiments

7.3.2 Anti-proliferative activity against HCT-116 (NULL TYPE): It was observed that VJ-3 and VJ-4PP1 of the tested compounds exhibited good inhibitory potential, among the other compounds, which was around 30-35% at 5 µM. At higher concentration of 25 µM, compounds VJ-4PP1 showed significant increase in cytotoxicity while other compounds VJ-2, VJ-3, VJ-4, VJ-2PP2 and VJ-3PP2 showed inhibitory activity to a lesser extent at 20-35% at 25 µM. At 50 µM, three compounds i.e. VJ-2, VJ-2PP2 & VJ-4PP1 showed significant inhibitory activity while VJ-3, VJ-4 and VJ-3PP2 showed equivalent inhibitory but less as compared to VJ-4PP1 (Figure 7.2).

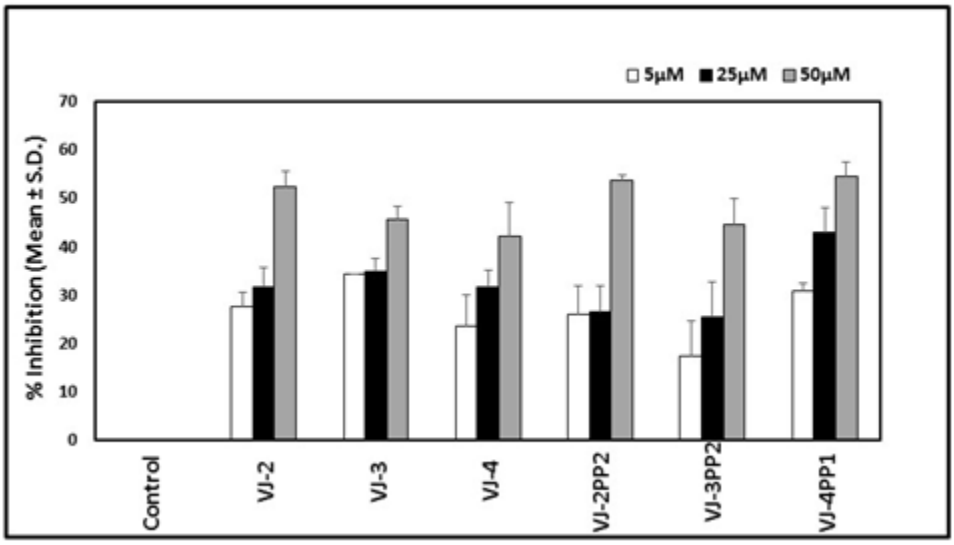

Figure 7.2: Percent inhibition of HCT-116 (NULL TYPE) in response to treatment with synthesized compounds at concentrations of 5 µM, 25 µM and 50 µM for time duration of 48 h. Data is expressed as mean values ± S.D. of three independent experiments

CHAPTER 8
CONCLUSION

A Hybrid drug involves the unification of two drug pharmacophores in one single molecule. The hybrid drugs are designed to interact with multiple targets or to intensify its effect through action on another bio target as one single molecule or to counterbalance the known side effects associated with the other hybrid part. One of the important role of hybrid drugs is to counter multidrug resistance. Muti-drug resistance observed during the treatment for cancer. Target therapy for various cancer are developed and successfully used to treat cancer patient. But treatment can be further strengthen by concurrent administration of single drug by combining two different drugs from different origin act at different receptor to cope MDR. It is also said as to load a multi-target drug in a single drug. In the current research proposal, we have designed and synthesized molecules which affect tubulin polymerization as well as MetAP-2 receptor. Both play vital role in tumor progression by strengthening the cell cytoskeleton and angiogenesis process respectively. The hybrids of chalcone (antitubulin) and arylazole (anti MetAP-2) were synthesized and molecular docking studies were performed. The compounds were synthesized by three step reaction and synthesized compounds were analyzed and confirmed by FTIR, NMR and mass spectrometry. The activity of synthesized compound was evaluated against HCT-116 (wild & null type) colon cancer cell lines at a concentration of 5 µM, 25 µM and 50 µM. Compounds were equally active in wild type and null type HTC-116 cell lines with slight less inhibition in null type. Lastly, the information on inhibitory potential of compounds were obtained from MTT assay wherein VJ-4, VJ-2PP2 & VJ-4PP1 were found to be active anticancer agents.

The active compounds need to be explored for MetAP-2 activity, and homology or protein-protein docking need to be performed to extrapolate the binding studies on tubulin and MetAP-2.

REFERENCES

Altmann, K.-H., & Gertsch, J. (2007). Anticancer drugs from nature—Natural products as a unique source of new microtubule-stabilizing agents. Natural product reports, 24(2), 327-357.

Amin, K. M., Eissa, A. A. M., Abou-Seri, S. M., Awadallah, F. M., & Hassan, G. S. (2013). Synthesis and biological evaluation of novel coumarin–pyrazoline hybrids endowed with phenylsulfonyl moiety as antitumor agents. European Journal of Medicinal Chemistry, 60(0), 187-198.

Avanzo, R. E., Anesini, C., Fascio, M. L., Errea, M. I., & D'Accorso, N. B. (2012). 1, 2, 4-Triazole d-ribose derivatives: Design, synthesis and antitumoral evaluation. European Journal of Medicinal Chemistry, 47, 104-110.

Avendano, C., & Menendez, J. C. (2008). Medicinal Chemistry of Anticancer Drugs: Elsevier.

Batovski, D., & Parushev, S. (2010). An Update on the Anticancer Effects of Chalcones. International Journal of Current Chemistry, 1(4), 217-236.

Bellina, F., Calandri, C., Cauteruccio, S., & Rossi, R. (2007). Efficient and highly regioselective direct C-2 arylation of azoles, including free (NH)-imidazole,-benzimidazole and-indole, with aryl halides. Tetrahedron, 63(9), 1970-1980.

Boxem, M., Tsai, C. W., Zhang, Y., Saito, R. M., & Liu, J. O. (2004). The methionine aminopeptidase 2 analog (map-2) is required for germ cell proliferation. FEBS letters, 576(1), 245-250.

Bremer, E., van Dam, G., Kroesen, B. J., de Leij, L., & Helfrich, W. (2006). Targeted induction of apoptosis for cancer therapy: current progress and prospects. Trends in Molecular Medicine, 12(8), 382-393.

Catalano, A., Romano, M., Robuffo, I., Strizzi, L., & Procopio, A. (2001). Methionine aminopeptidase-2 regulates human mesothelioma cell survival: role of Bcl-2 expression and telomerase activity. The American Journal of Pathology, 159(2), 721-731.

Chen, Y., Zhuo, Z.-J., Cui, D.-M., & Zhang, C. (2014). Copper catalyzed synthesis of 1-aryl-1, 2, 3-triazoles from aryl iodides, alkynes, and sodium azide. Journal of Organometallic Chemistry, 749, 215-218.

Ducki, S., Rennison, D., Woo, M., Kendall, A., Chabert, J. F. D., McGown, A. T., & Lawrence, N. J. (2009). Combretastatin-like chalcones as inhibitors of microtubule polymerization. Part 1: synthesis and biological evaluation of antivascular activity. Bioorganic & Medicinal Chemistry, 17(22), 7698-7710.

Duffy, C. P., Elliott, C. J., O'Connor, R. A., Heenan, M. M., Coyle, S., Cleary, I. M., Clynes, M. (1998). Enhancement of chemotherapeutic drug toxicity to human tumour cells in vitro by a subset of non-steroidal anti-inflammatory drugs (NSAIDs). Europian Journal of Cancer, 34(8), 1250-1259.

Dumontet, C., & Jordan, M. A. (2010). Microtubule-binding agents: a dynamic field of cancer therapeutics. Nature Reviews Drug Discovery, 9(10), 790-803.

Dyrager, C., Wickström, M., Fridén-Saxin, M., Friberg, A., Dahlén, K., Wallén, E. A., Luthman, K. (2011). Inhibitors and promoters of tubulin polymerization: Synthesis and biological evaluation of chalcones and related dienones as potential anticancer agents. Bioorganic & Medicinal Chemistry, 19(8), 2659-2665.

Elmore, S. (2007). Apoptosis: a review of programmed cell death. Toxicologic pathology, 35(4), 495-516.

Goodsell, D. S., Morris, G. M., & Olson, A. J. (1996). Automated docking of flexible ligands: applications of AutoDock. Journal of Molecular Recognition,9(1), 1-5.

Hou, Y. P., Sun, J., Pang, Z. H., Lv, P. C., Li, D. D., Yan, L., Zhu, H. L. (2011). Synthesis and antitumor activity of 1, 2, 4-triazoles having 1, 4-benzodioxan fragment as a novel class of potent methionine aminopeptidase type II inhibitors. Bioorganic & Medicinal Chemistry, 19(20), 5948-5954.

Hu, X., Dang, Y., Tenney, K., Crews, P., Tsai, C. W., Sixt, K. M., Liu, J. O. (2007). Regulation of c-Src Nonreceptor Tyrosine Kinase Activity by Bengamide A through Inhibition of Methionine Aminopeptidases. Chemical Biology, 14(7), 764-774.

Johnson, M., Younglove, B., Lee, L., LeBlanc, R., Holt Jr, H., Hills, P., Lee, M. (2007). Design, synthesis, and biological testing of pyrazoline derivatives of combretastatin-A4. Bioorganic & Medicinal chemistry letters, 17(21), 5897-5901.

Kallander, L. S., Lu, Q., Chen, W., Tomaszek, T., Yang, G., Tew, D., Smith, W. W. (2005). 4-Aryl-1, 2, 3-triazole: a novel template for a reversible methionine aminopeptidase 2 inhibitor, optimized to inhibit angiogenesis in vivo. Journal of Medicinal Chemistry, 48(18), 5644-5647.

Kaur, K., Jain, M., Reddy, R. P., & Jain, R. (2010). Quinolines and structurally related heterocycles as antimalarials. European Journal of Medicinal Chemistry, 45(8), 3245-3264.

Koradi, R., Billeter, M., & Wüthrich, K. (1996). MOLMOL: a program for display and analysis of macromolecular structures. Journal of Molecular Graphics, 14(1), 51-55.

Krishna, R., & Mayer, L. D. (2000). Multidrug resistance (MDR) in cancer: mechanisms, reversal using modulators of MDR and the role of MDR modulators in influencing the pharmacokinetics of anticancer drugs. European Journal of Pharmaceutical Sciences, 11(4), 265-283.

Marino, J. P., Fisher, P. W., Hofmann, G. A., Kirkpatrick, R. B., Janson, C. A., Johnson, R. K., Ryan, M. D. (2007). Highly potent inhibitors of methionine aminopeptidase-2 based on a 1, 2, 4-triazole pharmacophore. Journal of Medicinal Chemistry, 50(16), 3777-3785.

Meunier, B. (2007). Hybrid Molecules with a Dual Mode of Action: Dream or Reality?†. Accounts of Chemical Research, 41(1), 69-77.

Moser, C., Lang, S. A., & Stoeltzing, O. (2009). Heat-shock protein 90 (Hsp90) as a molecular target for therapy of gastrointestinal cancer. Anticancer Research, 29(6), 2031-2042.

Mosmann, T. (1983). Rapid colorimetric assay for cellular growth and survival: application to proliferation and cytotoxicity assays. Journal of Immunological Methods, 65(1), 55-63.

Moustafa, O. S., & Ahmad, R. A. (2003). Synthesis and antimicrobial activity of some new cyanopyridines, isoxazoles, pyrazoles, and pyrimidines bearing sulfonamide moiety. Phosphorus, Sulfur, and Silicon and the Related Elements, 178(3), 475-484.

Nepali, K., Singh, G., Turan, A., Agarwal, A., Sapra, S., Kumar, R., Gupta, M. K. (2011). A rational approach for the design and synthesis of 1-acetyl-3, 5-diaryl-4, 5-dihydro pyrazoles as a new class of potential non-purine xanthine oxidase inhibitors. Bioorganic & Medicinal Chemistry, 19(6), 1950-1958.

Nieth, C., Priebsch, A., Stege, A., & Lage, H. (2003). Modulation of the classical multidrug resistance (MDR) phenotype by RNA interference (RNAi). FEBS letters, 545(2), 144-150.

Pasquier, E., & Kavallaris, M. (2008). Microtubules: a dynamic target in cancer therapy. IUBMB life, 60(3), 165-170.

Patrick, G. L. (2013). An introduction to medicinal chemistry: Oxford university press.

Pienta, K., & Lehr, J. (1993). Inhibition of prostate cancer growth by estramustine and etoposide: evidence for interaction at the nuclear matrix. The Journal of Urology, 149(6), 1622-1625.

Ravelli, R. B., Gigant, B., Curmi, P. A., Jourdain, I., Lachkar, S., Sobel, A., & Knossow, M. (2004). Insight into tubulin regulation from a complex with colchicine and a stathmin-like domain. Nature, 428(6979), 198-202.

Release, S. (2013). 3: Maestro, version 9.6; Schrödinger, LLC: New York, 2013.

Ruan, B.-F., Lu, X., Tang, J.-F., Wei, Y., Wang, X.-L., Zhang, Y.-B., Zhu, H.-L. (2011). Synthesis, biological evaluation, and molecular docking studies of resveratrol derivatives possessing chalcone moiety as potential antitubulin agents. Bioorganic & Medicinal Chemistry, 19(8), 2688-2695.

Saraswathy, M., & Gong, S. (2013). Different strategies to overcome multidrug resistance in cancer. Biotechnology Advances, 31(8), 1397-1407.

Sashidhara, K. V., Kumar, A., Kumar, M., Sarkar, J., & Sinha, S. (2010). Synthesis and in vitro evaluation of novel coumarin–chalcone hybrids as

potential anticancer agents. Bioorganic & Medicinal Chemistry Letters, 20(24), 7205-7211.

Selvakumar, P., Lakshmikuttyamma, A., Dimmock, J. R., & Sharma, R. K. (2006). Methionine aminopeptidase 2 and cancer. Biochimica et Biophysica Acta (BBA)-Reviews on Cancer, 1765(2), 148-154.

Singh, J., Sharma, S., Saxena, A., Nepali, K., & Bedi, P. M. S. (2013). Synthesis of 1, 2, 3-triazole tethered bifunctional hybrids by click chemistry and their cytotoxic studies. Medicinal Chemistry Research, 22(7), 3160-3169.

Sirajuddin, M., Ali, S., & Badshah, A. (2013). DRUG-DNA Interactions and their study by UV-visible, fluorescence spectroscopies and cyclic voltametry. Journal of Photochemistry and Photobiology B: Biology.

Sumantran, V. N. (2011). Cellular chemosensitivity assays: An overview Cancer Cell Culture (pp. 219-236): Springer.

Warshakoon, N. C., Wu, S., Boyer, A., Kawamoto, R., Renock, S., Xu, K., Mekel, M. (2006). Design and synthesis of a series of novel pyrazolopyridines as HIF 1-α prolyl hydroxylase inhibitors. Bioorganic & Medicinal Chemistry Letters, 16(21), 5687-5690.

Xiao, C. F., Tao, L. Y., Sun, H. Y., Wei, W., Chen, Y., Fu, L. W., & Zou, Y. (2010). Design, synthesis and antitumor activity of a series of novel coumarin–stilbenes hybrids, the 3-arylcoumarins. Chinese Chemical Letters, 21(11), 1295-1298.

Zhou, Y., Zhao, Y., O'Boyle, K. M., & Murphy, P. V. (2008). Hybrid angiogenesis inhibitors: synthesis and biological evaluation of bifunctional compounds based on 1-deoxynojirimycin and aryl-1, 2, 3-triazoles. Bioorganic & Medicinal Chemistry Letters, 18(3), 954-958.

Appendix A
(Spectra of representative compounds)

VJ-3

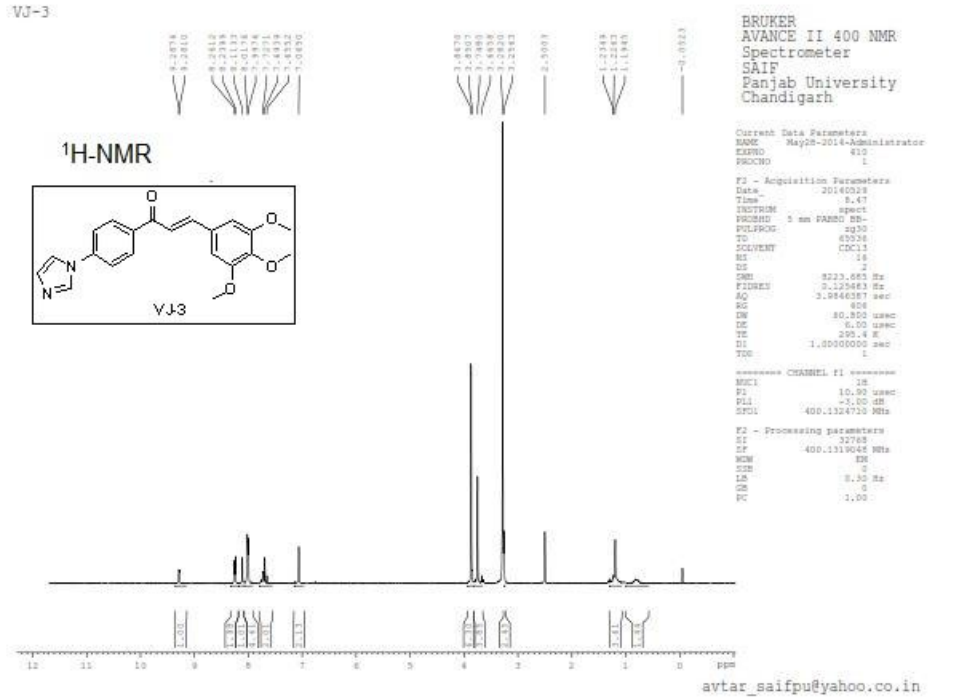
VJ-3
BRUKER
AVANCE II 400 NMR
Spectrometer
SAIF
Panjab University
Chandigarh
^{1}H-NMR
VJ-3
avtar_saifpu@yahoo.co.in

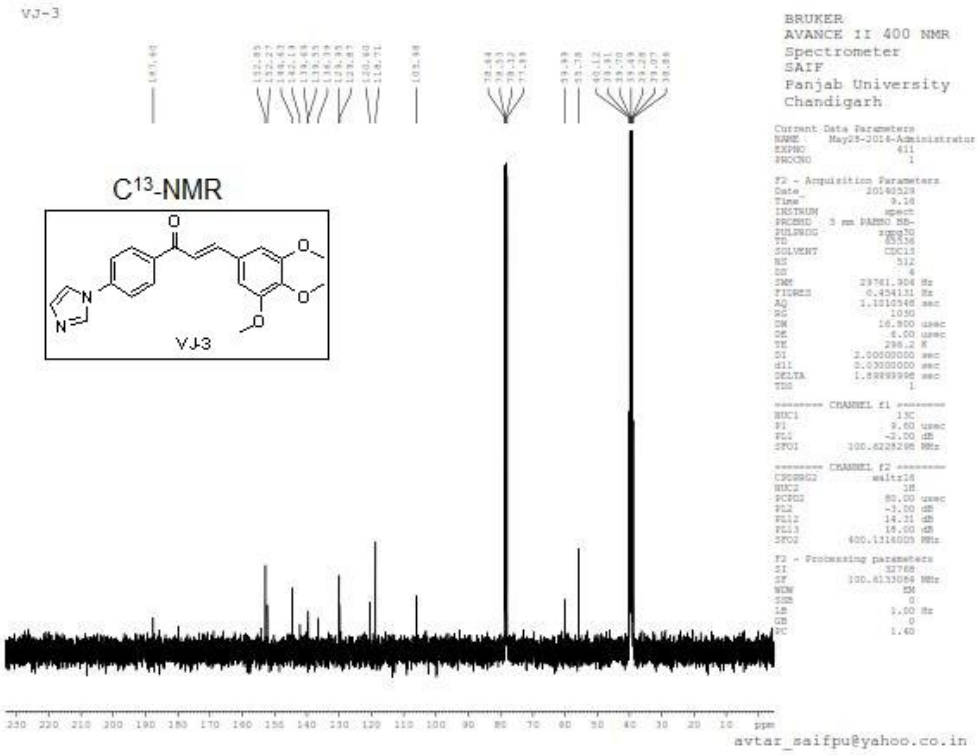
VJ-3
BRUKER
AVANCE II 400 NMR
Spectrometer
SAIF
Panjab University
Chandigarh
C^{13}-NMR
VJ-3
avtar_saifpu@yahoo.co.in

VJ-3

Sample Information

Analyzed by	: Admin
Analyzed	: 3/4/2014 9:46:18 AM
Sample Type	: Unknown
Level #	: 1
Sample Name	: VJ-3
Sample ID	: VJ-3
IS Amount	: [1]=1
Sample Amount	: 1
Dilution Factor	: 1
Vial #	: 15
Injection Volume	: 2.00
Data File	: E:\GCMS Data\RAJ\CBIM-P15.qgd
Org Data File	: E:\GCMS Data\RAJ\CBIM-P15.qgd
Method File	: E:\GCMS METHODS\DI_CUT.qgm
Org Method File	: E:\GCMS METHODS\DI_CUT.qgm
Report File	:
Tuning File	: C:\GCMSsolution\System\Tune1\18-01-2014 HS.qgt
Modified by	: Admin
Modified	: 3/4/2014 11:38:31 AM

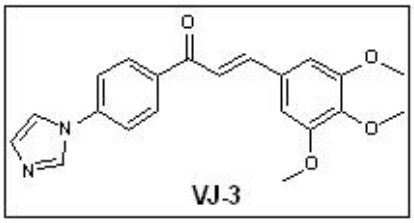

Spectrum

Line#:1 R.Time:6.258(Scan#:512)
MassPeaks:403
RawMode:Averaged 6.250-6.267(511-513) BasePeak:364(15601)
BG Mode:Calc. from Peak Group 1 - Event 1

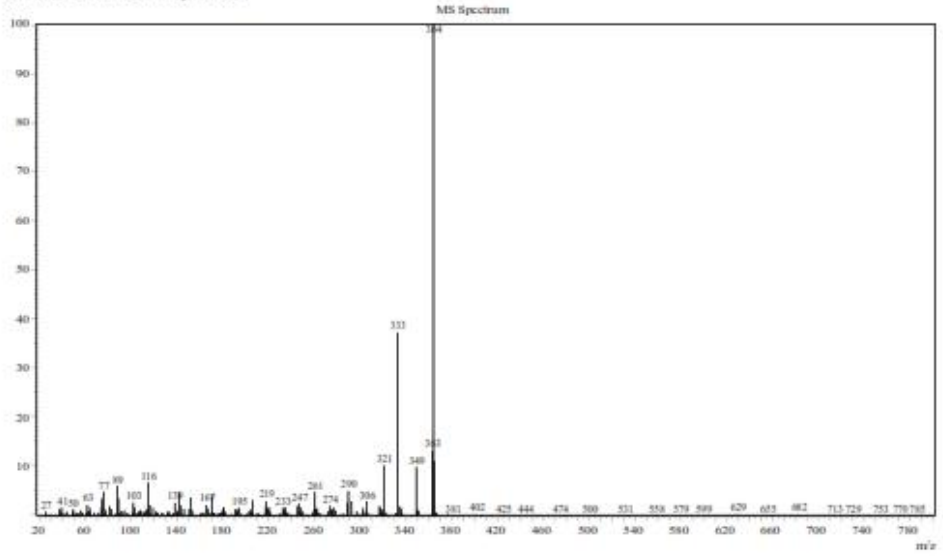

VJ-4

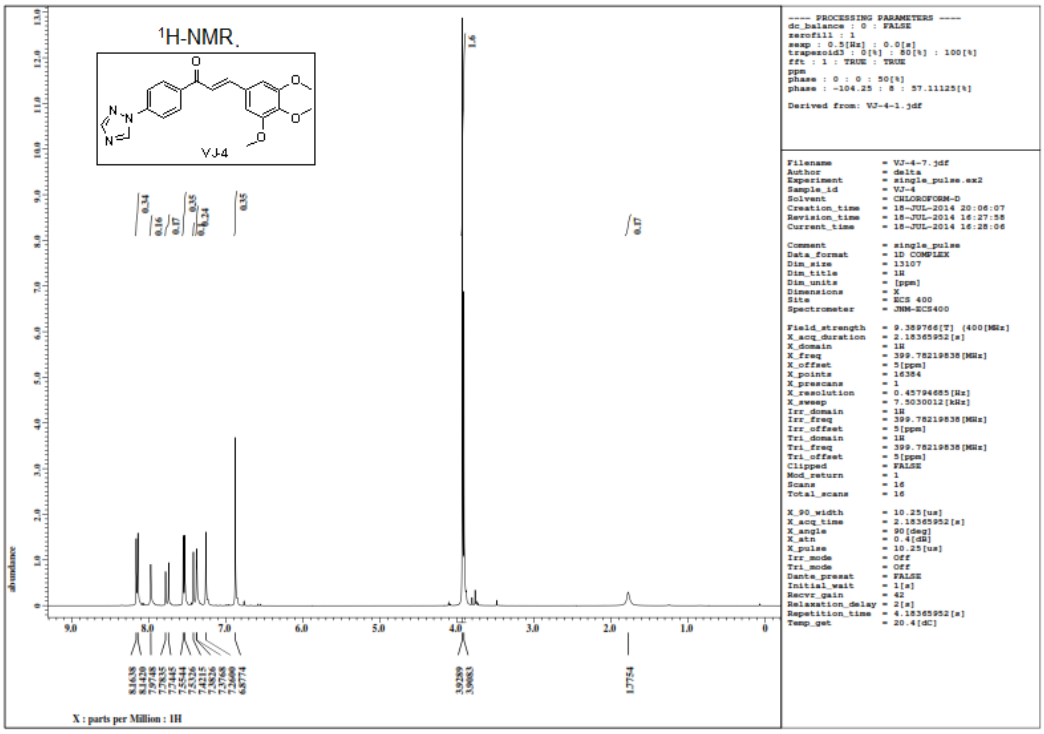
^{1}H-NMR
VJ-4
X : parts per Million : 1H

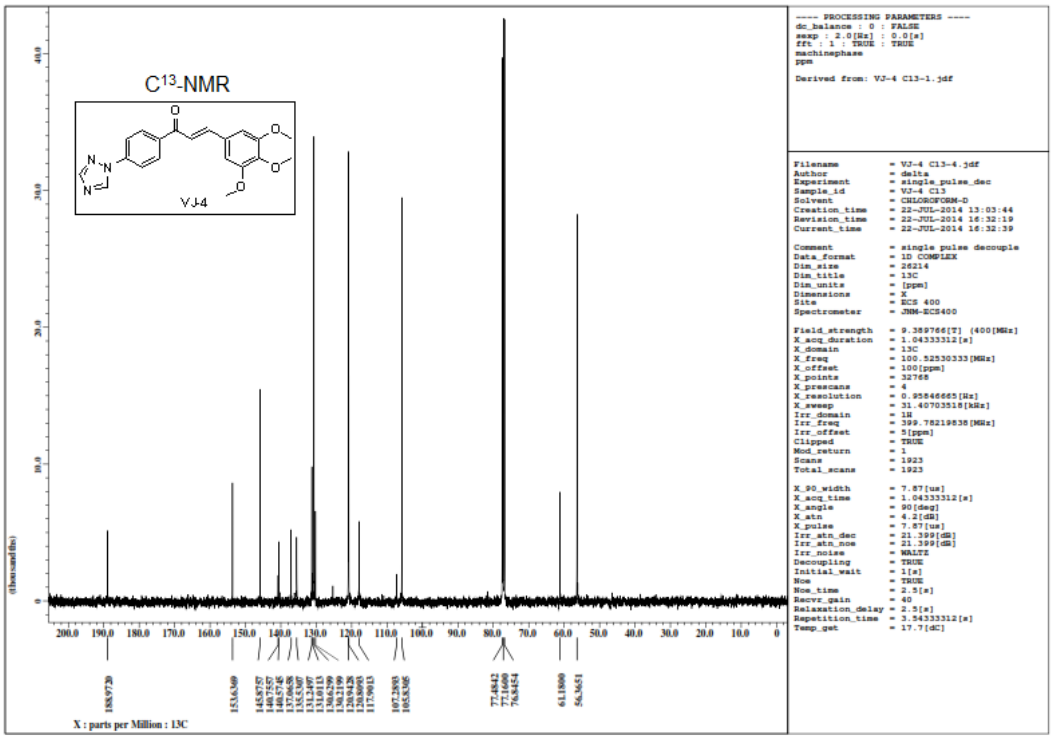
C^{13}-NMR
VJ-4
X : parts per Million : 13C

VJ-2PP2

Sample Information

Analyzed by	: Admin
Analyzed	: 6/3/2014 4:41:08 PM
Sample Type	: Unknown
Level #	: 1
Sample Name	: VJ-2PP2
Sample ID	: VJ-2PP2
IS Amount	: [1]=1
Sample Amount	: 1
Dilution Factor	: 1
Vial #	: 1
Injection Volume	: 1.00
Data File	: E:\GCMS Data\RAJ\PDCBIT-F97.qgd
Org Data File	: E:\GCMS Data\RAJ\PDCBIT-F97.qgd
Method File	: E:\GCMS METHODS\DI_CUP.qgm
Org Method File	: E:\GCMS METHODS\DI_CUP.qgm
Report File	:
Tuning File	: C:\GCMSsolution\System\Tune1\18-01-2014 HS.qgt
Modified by	: Admin
Modified	: 6/4/2014 12:24:09 PM

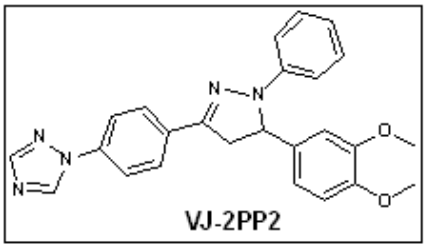

Spectrum

Line#:1 R.Time:5.567(Scan#:429)
MassPeaks:602
RawMode:Averaged 5.558-5.575(428-430) BasePeak:425(59474)
BG Mode:Calc. from Peak Group 1 - Event 1

MS Spectrum

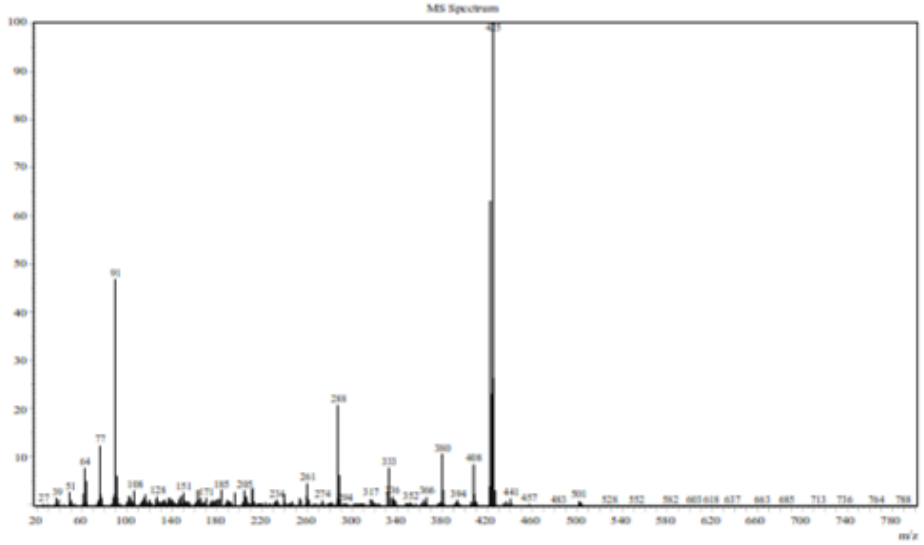

VJ-3PP2

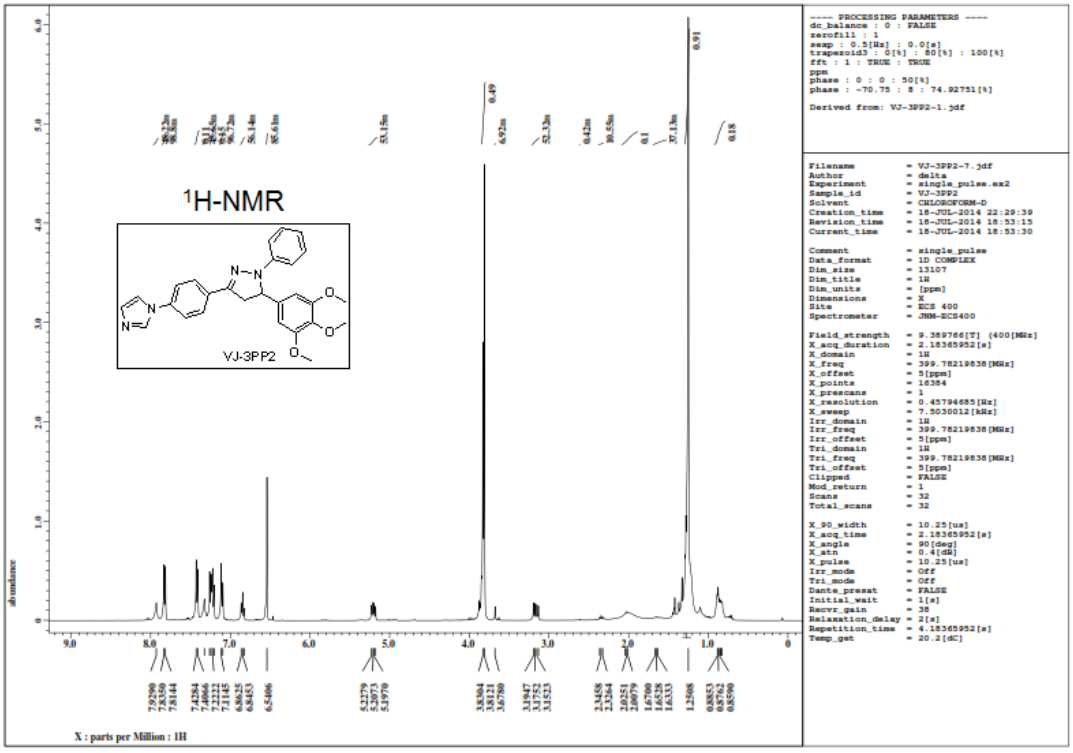
1H-NMR
VJ-3PP2
X : parts per Million : 1H

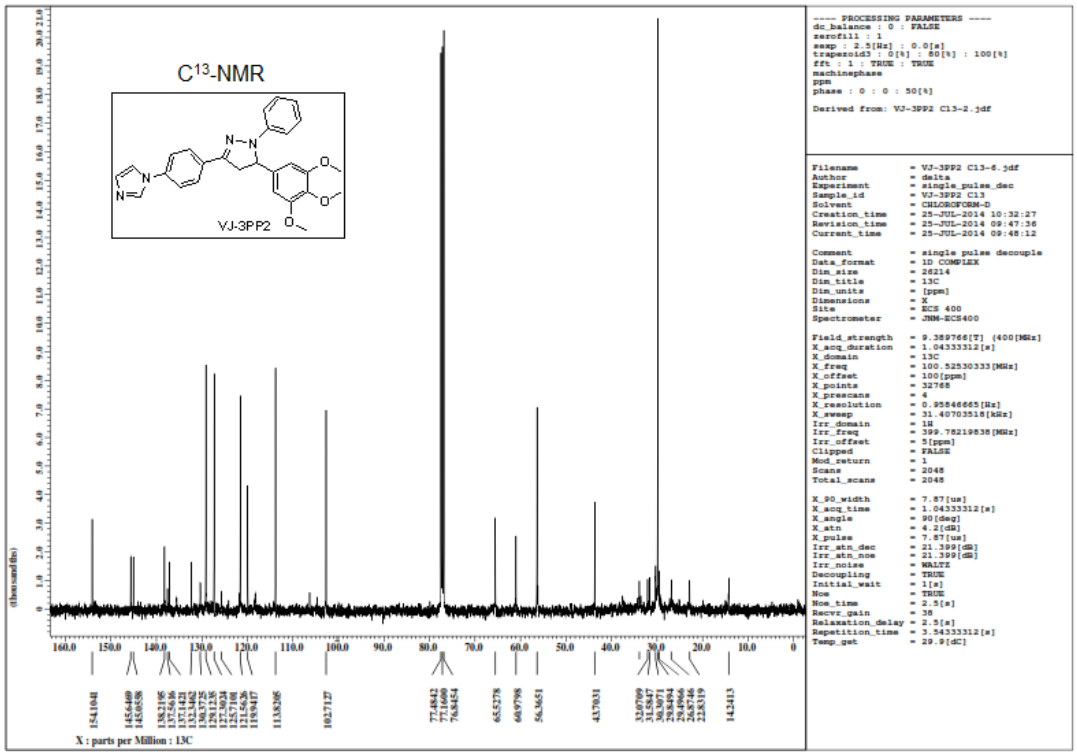
C13-NMR
VJ-3PP2
X : parts per Million : 13C

VJ-3PP2

Sample Information

Analyzed by	: Admin
Analyzed	: 6/9/2014 12:36:20 PM
Sample Type	: Unknown
Level #	: 1
Sample Name	: VJ-3PP2
Sample ID	: VJ-3PP2
IS Amount	: [1]=1
Sample Amount	: 1
Dilution Factor	: 1
Vial #	: 28
Injection Volume	: 5.00
Data File	: E:\GCMS Data\RAJ\PH-105.qgd
Org Data File	: E:\GCMS Data\RAJ\PH-105.qgd
Method File	: E:\GCMS METHODS\DI_CUP.qgm
Org Method File	: E:\GCMS METHODS\DI_CUP.qgm
Report File	:
Tuning File	: C:\GCMSolution\System\Tune\1\18-01-2014 HS.qgt
Modified by	: Admin
Modified	: 6/9/2014 3:20:40 PM

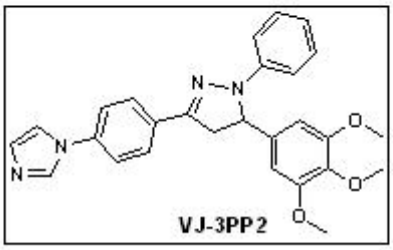

Spectrum

Line#:1 R.Time:5.967(Scan#:477)
MassPeaks:693
RawMode:Averaged 5.958-5.975(476-478) BasePeak:454(45531)
BG Mode:Calc. from Peak Group 1 - Event 1

MS Spectrum

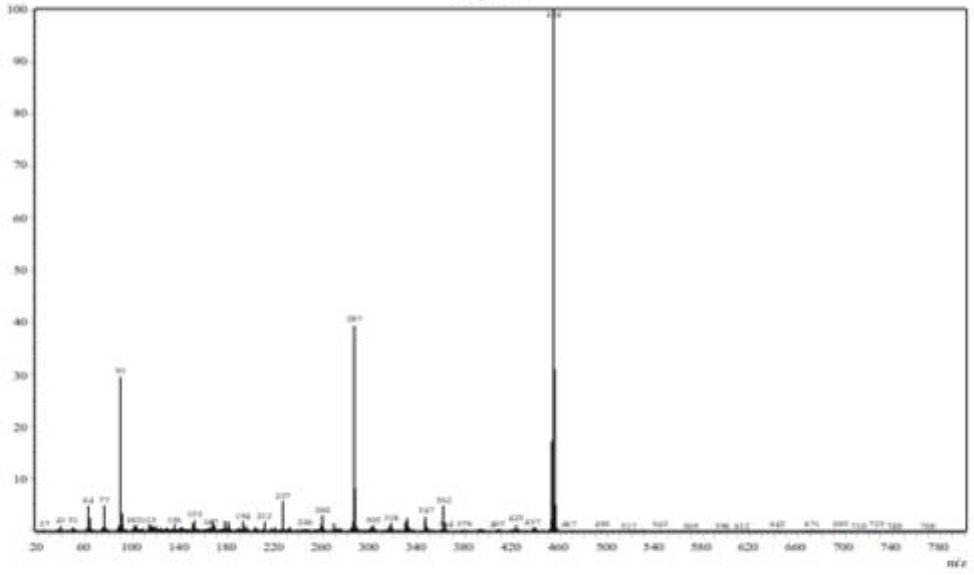

VJ-4PP1

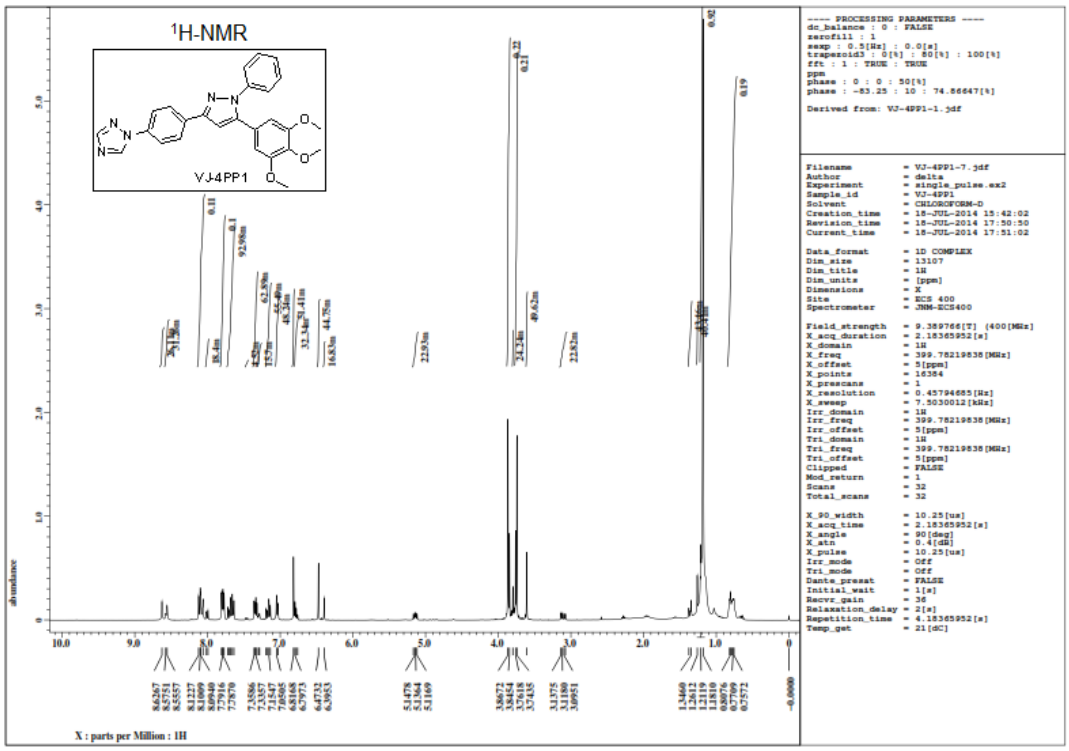
^{1}H-NMR
VJ-4PP1
X : parts per Million : 1H

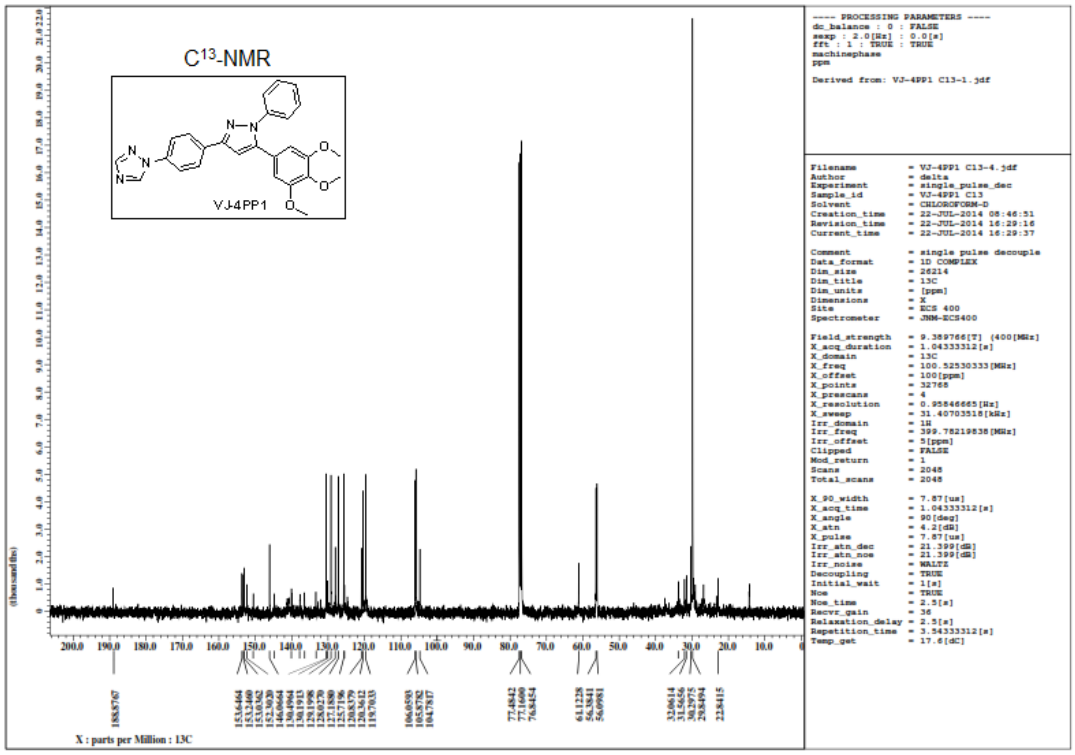
C^{13}-NMR
VJ-4PP1
X : parts per Million : 13C

VJ-4PP1

Sample Information

Analyzed by	: Admin
Analyzed	: 6/9/2014 1:40:55 PM
Sample Type	: Unknown
Level #	: 1
Sample Name	: VJ-4PP1
Sample ID	: VJ-4PP1
IS Amount	: [1]=1
Sample Amount	: 1
Dilution Factor	: 1
Vial #	: 28
Injection Volume	: 5.00
Data File	: E:\GCMS Data\RAJ\PH-103M.qgd
Org Data File	: E:\GCMS Data\RAJ\PH-103M.qgd
Method File	: E:\GCMS METHODS\DI_CUP.qgm
Org Method File	: E:\GCMS METHODS\DI_CUP.qgm
Report File	:
Tuning File	: C:\GCMSsolution\System\Tune\18-01-2014 HS.qgt
Modified by	: Admin
Modified	: 6/9/2014 3:21:15 PM

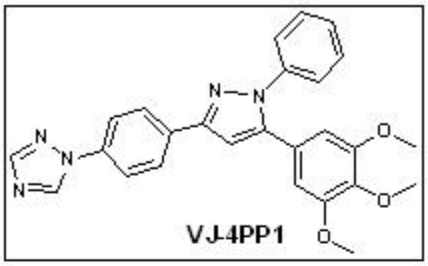

Spectrum

Line#:1 R.Time:5.367(Scan#:405)
MassPeaks:671
RawMode:Averaged 5.358-5.375(404-406) BasePeak:453(28479)
BG Mode:Calc. from Peak Group 1 - Event 1

MS Spectrum

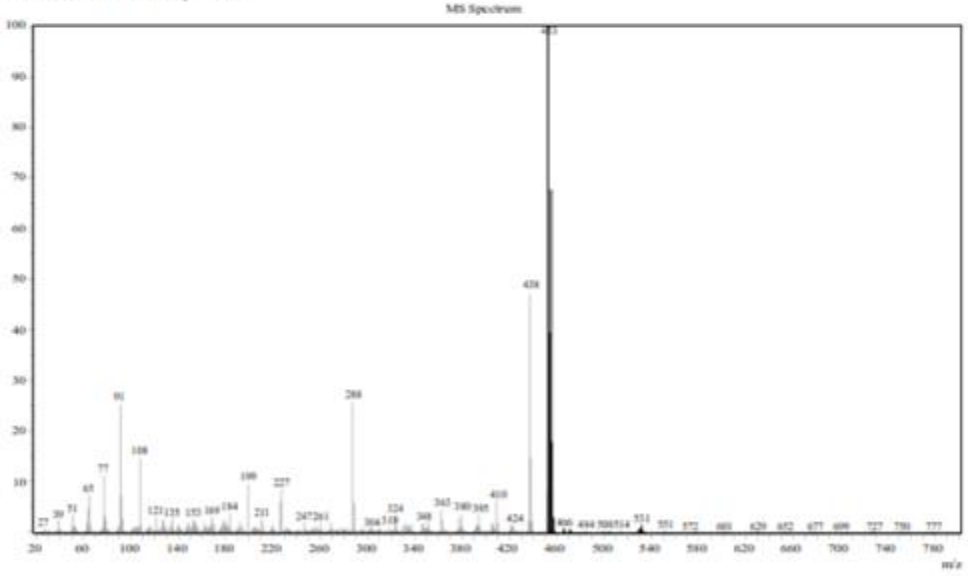

1